CENTRO BRASILEIRO DE PESQUISAS FÍSICAS

Marcelo Amanajás Pires

PHENOMENOLOGICAL CHARACTERIZATION OF BIOLOGICAL COMPLEX SYSTEMS

Rio de de Janeiro - RJ

2021

Marcelo Amanajás Pires

PHENOMENOLOGICAL CHARACTERIZATION OF BIOLOGICAL COMPLEX SYSTEMS

Tese submetida ao Programa de Pós-Graduação em Física do Centro Brasileiro de Pesquisas Físicas para a obtenção do Grau de Doutor em Física.

Orientador: Dr. Sílvio Manuel Duarte Queirós
Coorientador: Dr. Nuno Miguel Melo Crokidakis Peregrino

Rio de de Janeiro - RJ

2021

Acknowledgements

I would like to thank my advisor Professor Sílvio Queirós as well as my co-advisor Professor Nuno Crokidakis for all the orientations and advice during my PhD. I thank CAPES for the fellowship. I also appreciate all the fruitful discussions with my colleagues at both UFF and CBPF. I would like to acknowledge my friends for all the enjoyable moments we had. I also thank my mother and my family for all the support during my scientific journey.

Resumo

Utilizando ferramentas da Física Estatística, investigou-se sistemas complexos relacionados às áreas de Ecologia e Epidemiologia. Especificamente, esta tese focou na fenomenologia emergente a partir de cinco problemas: (i) dinâmica da metapopulação sob o efeito Allee e restrições espaciais; (ii) dinâmica de 2 espécies sob o cenário de uma competição quase neutra dentro de uma estrutura de metapopulação; (iii) dinâmica populacional com perturbações dependentes do tempo com padrões de complexidade distintos; (iv) modelo de 2 populações Susceptível-Infectado-Recuperado-Assintomático-Sintomático-Morto (SIRASD), em que as populações diferem pelo grau de cumprimento das políticas de distanciamento social; (v) dinâmica conjunta opinião-vacinação-epidemias. Em tais problemas, a contribuição desta tese varia de adicionar novos fenômenos a um dado arcabouço teórico (i-v), estabelecer uma nova perspectiva sobre um fenômeno previamente estabelecido (i-v), definir uma nova potencial agenda para futuras investigações empíricas (i-iii), fornecer novas circunstâncias onde fenômenos biológicos contra-intuitivos podem emergir (i,ii,v).

Palavras-chaves: Sistemas biológicos complexos. Simulação de Monte Carlo. Abordagem de campo médio.

Abstract

Employing tools from Statistical Physics, we work on complex systems related to the fields of Ecology and Epidemiology. Specifically, we investigate the emergent phenomenology from five problems: (i) metapopulation dynamics under the Allee effect and spatial restrictions; (ii) 2-species dynamics under the scenario of a quasi-neutral competition within a metapopulation framework; (iii) population dynamics with the Allee Effect and time-dependent perturbations rates with distinct complexity patterns; (iv) 2-population Susceptible-Infected-Recovered-Asymptomatic-Symptomatic-Dead (SIRASD) model, where populations differ by their degree of compliance with social distancing policies; (v) coupled opinion-vaccination-epidemics dynamics in modular networks. In such problems, our contribution ranges from adding a new feature to a theoretical framework (i-v), providing a novel perspective on an established phenomenon (i-v) and setting a new potential agenda for empirical investigations within the approach of Synthetic Biology (i-iii) as well as providing novel circumstances where counter-intuitive biological dynamics can emerge (i,ii,v).

Keywords: Complex Biological systems. Monte Carlo Simulation. Mean-field approach.

Lista de Figuras

Works in Complex Systems

- **M. A. Pires**, et al. "Modeling the functional network of primary intercellular Ca2+ wave propagation in astrocytes and its application to study drug effects." Journal of Theoretical Biology 356 (2014): 201-212. (PIRES; RAISCHEL, et al., 2014)
- **M. A. Pires**, N Crokidakis. "Dynamics of epidemic spreading with vaccination: impact of social pressure and engagement." Physica A 467 (2017): 167-179. (PIRES; CROKIDAKIS, 2017)
- **M. A. Pires**, A. L. Oestereich, N Crokidakis "Sudden transitions in coupled opinion and epidemic dynamics with vaccination." Journal of Statistical Mechanics 2018.5 (2018): 053407. (PIRES; OESTEREICH; CROKIDAKIS, 2018)
- A. L. Oestereich, **M. A. Pires**, N Crokidakis. "Three-state opinion dynamics in modular networks." Physical Review E 100.3 (2019): 032312. (OESTEREICH; PIRES; CROKIDAKIS, 2019)
- **M. A. Pires**, S. M. D. Queirós. "Optimal dispersal in ecological dynamics with Allee effect in metapopulations." PLoS One 14.6 (2019): e0218087. (PIRES; QUEIRÓS, 2019)
- **M. A. Pires**, N Crokidakis, S. M. D. Queirós Randomness in Ecological evolution: the role of complexity on the Allee effect. Authorea preprint. 2020. (PIRES; CROKIDAKIS; QUEIRÓS, 2020)
- A. L. Oestereich, **M. A. Pires**, N Crokidakis, S. M. D. Queirós. "Hysteresis and disorder-induced order in continuous kinetic-like opinion dynamics in complex networks." Chaos, Solitons & Fractals 137 (2020): 109893. (OESTEREICH; PIRES; QUEIRÓS, et al., 2020)
- **M. A. Pires**, et al. "What is the potential for a second peak in the evolution of SARS-CoV-2 in Brazil? Insights from a SIR-ASD model considering the informal economy." Accepted in **International Journal of Modern Physics C** 2021.(PIRES; CROKIDAKIS; CAJUEIRO, et al., 2020).

- **M. A. Pires**, et al. "Modelling behavior changes during the sars-cov-2 spreading: a case study considering the delay in the tests." Research, Society and Development 9.7 (2020): e780975475-e780975475. (PIRES; DIAS, et al., 2020)

- **M. A. Pires**, N Crokidakis, S. M. D. Queirós. "Diffusion plays an unusual role in ecological quasi-neutral competition in metapopulations." Nonlinear Dynamics (2021). (PIRES; CROKIDAKIS; QUEIRÓS, 2021)

- **M. A. Pires**, A. L. Oestereich, N Crokidakis, S. M. D. Queirós. "The anti-vaxx movement and epidemic spreading in the era of social networks: nonmonotonic effects, bistability and network segregation." arXiv preprint arXiv:2101.07869 (2021). (PIRES; OESTEREICH; CROKIDAKIS; QUEIRÓS, 2021)

Works in Quantum Physics

- **M. A. Pires**, G. Di Molfetta, and S. M. D. Queirós. Multiple transitions between normal and hyperballistic diffusion in quantum walks with time-dependent jumps, Scientific Reports 9, 1 (2019). (PIRES; DI MOLFETTA; QUEIRÓS, 2019)

- **M. A. Pires** and S. M. D. Queirós. Quantum walks with sequential aperiodic jumps. Physical Review E 102, 012104 (2020). (PIRES; QUEIRÓS, 2020c)

- **M. A. Pires** and S. M. D. Queirós. "Parrondo's paradox in quantum walks with time-dependent coin operators." Physical Review E 102.4 (2020): 042124. (PIRES; QUEIRÓS, 2020b)

- **M. A. Pires** and S. M. D. Queirós. "Negative correlations can play a positive role in disordered quantum walks." Scientific Reports 11.1 (2021): 1-11. (PIRES; QUEIRÓS, 2020a)

Contents

Introduction

While Physics has a long tradition of using mathematical apparatus, Biology is still moving towards a greater insertion of mathematical tools in many of its subfields. In particular, Ecology and Epidemiology are two subfields of Biology that are receptive to the introduction of mathematical tools(MACKEY; MAINI, 2015).

The first influential applications of mathematics in modern Ecology took place in the early 1900s(MCCANN, 2012). For instance, the predator-prey system of equations, a crucial model in Ecology of competitions, was independently developed by the mathematicians Alfred Lotka in 1925 and Vito Volterra in 1926(MCCANN, 2012; BACAËR, 2011). Levins' work(LEVINS, 1969) is another significant mathematical contribution in modern Ecology where the new concept of metapopulations was explicitly established(HANSKI; GILPIN, 1991).

In turn, mathematical models were established as a solid tool in Epidemiology in the early 1900s(MCCANN, 2012). For instance, in 1911 Ronald Ross introduced a breakthrough idea in Epidemiology. At that time it was commonly accepted that any initial quantity of mosquitoes would lead to a persistence of malaria in a given population (BRAUER; CASTILLO-CHAVEZ; FENG, 2019). Ross developed a flexible compartmental model (ROSS, 1911) that incorporated the human-mosquito interaction. He revealed that decreasing the mosquito density below a threshold would be sufficient

to eradicate malaria. Why the threshold for an epidemic outbreak was missed by many public health and infectious disease experts? The possible reason is that such a threshold cannot be discovered straightforwardly from empirical data; it demands a mathematical model to elucidate its existence(WEISS, 2013). Based on a deterministic epidemic model, Kermack and McKendrick formulated, around 1927, an expression for the final epidemic size, which highlights a threshold for the population density. Above this threshold massive outbreaks can take place, whereas below such threshold the epidemic dies out(KERMACK; MCKENDRICK, 1927).

In this thesis we work on complex biological systems related to Ecology and Epidemiology. Our goal is to investigate the possible emerging scenarios from minimal models. As we will discuss in each part of this thesis, our models can be naturally seasoned with further elements that account for the traits of a given system. It is well-known that the use of minimal models is very helpful in providing an understanding of the cornerstone mechanisms present in tailored models.

This thesis is structured in 5 works that we address in the following way:

- In the chapter 1 we study how dispersal influences ecological dynamics under the Allee effect and spatial restrictions modeled with a k-regular graph. We employ a microscopic minimal model in a metapopulation (without requiring nonlinear birth and death rates).

- In the chapter 2 we investigate the emergent phenomenology from two-species dynamics under the scenario of a quasi-neutral competition within a metapopulation framework using a k-regular graph. We employ stochastic and deterministic approaches, namely spatially-constrained individual-based Monte Carlo simulations and coupled mean-field ODEs.

- In the chapter 3, we aim at shedding light on the question: how extinction is molded by time-dependent perturbations with distinct complexity patterns? To address this issue we employ e-

cological dynamics with the Allee-effect under time-dependent rates with different complexity but the same autocorrelation.

- In the chapter 4 we scrutinize the potential scenarios from a Susceptible-Infected-Recovered-Asymptomatic-Symptomatic-Dead (SIRASD) model.As a novelty we consider populations stratified in groups according to socioeconomic features that are present in emerging and developing countries. As a case study, we consider the case of Brazil. Our results also provide insights for nations where the informal economy has a considerable size.

- In the chapter 5, we study an epidemics spreading under a vaccination campaign with agents in favor and against the vaccine. The chain of contagion is modeled by the SIRS with the additional compartment for the Vaccinated agents. The opinion dynamics follow a pairwise model.

The chapters 1-3 have in common the fact of treating ecological problems. Besides these chapters set an agenda for experimental works within the framework of Synthetic biology where bacteria can be programmed to exhibit new behavior. Moreover, chapters 1 and 3 are related in the sense that both are based on Allee-like dynamics. Apart from this, chapter 1 is also related to chapter 2 since both use metapopulations. In turn, chapters 4-5 have in common the treatment of problems of Epidemiology with models that are extensions of the paradigmatic SIR model. While chapter 4 introduces economic-based features in a multigroup epidemic dynamics, chapter 5 introduces opinions dynamics in a community-based vaccination dynamics. By bridging multiple fields, both works are beyond the standard approach that employs only epidemic models.

It is well established that several of the most important milestones in biology reached during the last two centuries were achieved by acknowledging the importance of random dynamics (HEAMS, 2014), thus in all works of this thesis, the randomness was present as a main or an auxiliary ingredient. In chapters 1 and 5 we observe bistability induced by randomness. In chapter 2 we show the

presence of scenarios in which the randomness is crucial for determining the winner species. In chapter 3 we show how randomness jeopardizes the long-run proliferation of organisms. In chapter 4 the random-based approach is employed to test the robustness of the outcomes obtained with the deterministic framework.

All chapters can be seen from the perspective of nonequilibrium statistical physics. Specifically, all models addressed here have a nonequilibrium transition to an absorbing state, where once the dynamics enter such a state it cannot escape anymore. In the ecological problems of chapters 1-3 the absorbing state is usually undesirable, the extinction of species. Whereas in chapters 4-5 the absorbing state is welcome, the eradication of a disease.

In order to accomplish our goals we use computational and mathematical tools. On the computational side we develop codes in C and R to perform extensive Monte carlo simulations. On the mathematical side, we work with three main tools. From one hand we employ networked (coupled) local-mean-field equations that are able to capture global correlations through a network topology. In the second category we employ ordinary differential equation (ODE) to address important issues. When necessary we use agent-based simulations.

Chapter 1

Optimal dispersal in ecological dynamics with Allee effect in metapopulations

In this chapter, we address the question: how dispersal impacts on ecological dynamics under the Allee effect and spatial constraints? To this task we develop an ecological metapopulation dynamics in order to investigate how the threefold interplay between the Allee Effect, dispersal, and spatial restrictions influences the survival probability of a population dynamics. At first sight, it is presumed that dispersal has an advantageous influence on population persistence by weakening the local struggle for resources. However, interestingly, we note that for rigid spatial restrictions there is the appearance of an optimal dispersal rate that supports the highest survival probability. This nonmonotonic relationship between survival and dispersal — which is not very intuitive at first glance — was recently recognized in controlled experiments with engineered bacteria (SMITH et al., 2014). This work is available in Ref.(PIRES; QUEIRÓS, 2019).

INTRODUCTION

Table 1.1 – List of symbols used in this chapter.

Symbol	Meaning
λ	Reproduction rate
α	Death rate
D	Dispersal rate
n_S	Number of sources in the network
L	Number of populations in the metapopulation
N	Number of individuals in the metapopulation

The logistic growth model is one of the most common dynamics of population Biology. Despite its ubiquity across Ecology, there are several instances where it cannot describe properly collective phenomena emerging in sparse populations such as the Allee effect (COURCHAMP; BEREC; GASCOIGNE, 2008a).

The Allee effect is an influential finding named after the ecologist Warder Clyde Allee (ALLEE, 1931) concerning a phenomenon typically manifested by the departure from the standard logistic growth that enhances the susceptibility to extinction of an already vulnerable sparse population. For illustration consider the Fig.1.1. In the logistic model there is a negative correlation between the per capita growth and population size. In the weak Allee effect, the per capita growth is smaller than in the logistic model, but now at low population sizes there is a positive correlation between the per capita growth and the population size. In the strong Allee effect, there is an additional feature: below a threshold the reduced per capita growth rate becomes negative.

The Allee effect can emerge from a variety of mechanisms such as mate limitation, cooperative breeding, cooperative feeding, habitat amelioration (DRAKE; KRAMER, 2011; COURCHAMP; BEREC; GASCOIGNE, 2008a). Empirical support to the Allee Effect can be found in terrestrial arthropods, aquatic invertebrates, mammals, birds, fish, and reptiles (COURCHAMP; BEREC; GASCOIGNE, 2008a; KRAMER et al., 2009). In addition, thanks to

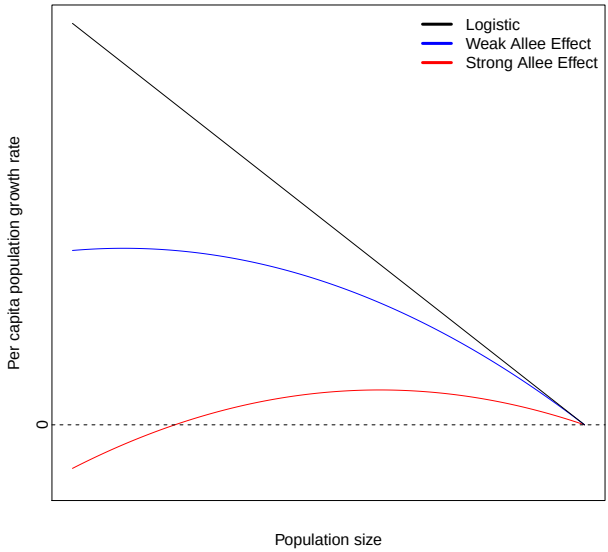

Figure 1.1 – Per capita population growth rate against population size for the Logistic model, weak Allee effect and strong Allee effect.

Synthetic Biology it is possible to observe the Allee effect in programmed bacteria (SMITH et al., 2014).

Besides ecology, conservation biology (COURCHAMP; BEREC; GASCOIGNE, 2008a) and invasion biology (TAYLOR; HASTINGS, 2005), there is a growing number of studies addressing the importance of the Allee effect in other subjects such as epidemiology (REGOES; EBERT; BONHOEFFER, 2002; DEREDEC; COURCHAMP, 2006; HILKER; LANGLAIS; MALCHOW, 2009) and cancer biology (KOROLEV; XAVIER; GORE, 2014; SEWALT et al., 2016) among others. Explicitly, in Ref. (KOROLEV; XAVIER; GORE, 2014) the authors suggest the manifestation of the Allee effect as the tumor growth threshold may be explored in therapeutics.

For long the Allee effect was mostly studied at the popula-

tion scale, but in Ref. (AMARASEKARE, 1998) it was shown its relevance at the metapopulation level as well. Afterwards, it was effectively demonstrated the Allee effect at the metapopulation level can come up from the Allee effect at the local population level (ZHOU; WANG, 2004, 2006).

Focusing on the theoretical approach to the problem, several models — spanning from phenomenological to purely microscopic proposals — have been able to reproduce the Allee effect and to explore its dynamical outcomes (BOUKAL; BEREC, 2002; BEREC, 2008; TAYLOR; HASTINGS, 2005), namely those coping with the interplay between the Allee effect and dispersal. Note that Depending on the primary approach to population dynamics, the concept of dispersal is also known as migration or dispersal. Let us mention a few examples: on the one hand, one can find works showing a positive association between migration and the number of invaded patches (ACKLEH; ALLEN; CARTER, 2007); the invasion diagram presented in Ref. (KEITT; LEWIS; HOLT, 2001) shows that the propagation failure regime shrinks as the dispersal rate increases.

In Ref. (BRASSIL, 2001), it is asserted that in a simple metapopulation dynamics the larger the migration the larger the mean time to extinction. On the other hand, there are works indicating that the combination of the Allee effect and dispersal produces a negative impact on the population dynamics; that is the case of Ref. (HOPPER; ROUSH, 1993) where the authors claim that the vulnerability to extinction increases with the mean-square displacement. Considering a nonlinear dynamics analysis of the Allee effect, the survival-extinction bifurcation diagram shown in Ref. (HADJI-AVGOUSTI; ICHTIAROGLOU, 2004) reveals that the extinction regime augments directly with the dispersal probability. Complementary, it was also found that a dispersive population under the Allee effect faces a dramatically slowed spreading (VEIT; LEWIS, 1996). Additionally, it was shown in (PETROVSKII; MOROZOV; LI, 2005) that the dispersal does not always enhance regional persistence in a predator-prey system under the Allee effect. Last, the results conveyed in Ref. (ROBINET et al., 2008) indicate that populations with the Allee effect face an inverse relationship between

the settlement probability and the pre-mating dispersal.

Particularly in population ecology, Windus and Jensen (WINDUS; JENSEN, 2007) proposed a minimal model that successfully captures the strong Allee Effect – the focus of this work – by means of a bistable dynamics arising from microscopic rules. Inspired by their model, we develop an ecological metapopulation dynamics in order to explore how the threefold interplay between the Allee Effect, dispersal and spatial constraints impacts on the survival probability of a population dynamics. It is reasonably expected that the dispersal has a beneficial impact on population survival by decreasing the local competition for resources. But interestingly, we observe that for severe spatial constraints there is the emergence of an optimal dispersal rate that promotes the highest survival probability. This nonmonotonic relation between survival and dispersal — which is not very intuitive at first glance — was recently observed in controlled experiments with engineered bacteria (SMITH et al., 2014).

MODEL AND MONTE CARLO SIMULATION

Consider a metapopulation (HANSKI; GILPIN, 1991; HANSKI, 1998) with L subpopulations composed of agents that are able to move, die or reproduce. As usual in metapopulation dynamics (HANSKI; GILPIN, 1991), we assume a well-mixed subpopulation, i.e., inside each subpopulation all individuals have the possibility to interact with each other. [1] The mobility is implemented as a random walk between the neighbor subpopulations and it occurs with probability D for each agent. At a given time step, if the dispersal event is not chosen (probability $1-D$) then one of the two events is chosen (WINDUS; JENSEN, 2007): death of an agent with probability α or reproduction with probability λ when two agents meet.

At this point, some remarks are worth making: first, heed that D controls the time scale between migration or death/reproduction; second, it is clear that we make no extra assumptions on the probabilities α or λ; Moreover, there is no local condensation of the

[1] In Statistical Physics parlance that is to say that our local dynamics exhibits a mean-field character.

agents because the random walk uniforms the agents distribution among the subpopulations. We would like to stress that our goal is not to model a specific ecological dynamics, but rather to investigate the possible emerging scenarios from this minimal agent-based migration-reproduction-death dynamics.

The Monte Carlo Algorithm

Computationally[2], we use an array with N states divided into the L subpopulations. Each state in the subpopulation u indicates an agent, i_A^u or a vacancy, i_V^u. The time is measured in Monte Carlo Steps (mcs) that consists of a visit to each one of the N states.

Monte Carlo Step:

For each state $i = 1, \ldots, N$:

- First get the subpopulation, say u, of the state i.
- With probability D:
  - **Dispersal:** If the state i indicates an agent, i_A^u, then move it to one of its neighbors w chosen at random: $i_A^u \Rightarrow i_A^w$
- With probability $1 - D$:
  - **Reproduction:** If the state i indicates a vacancy, i_V^u, then pick at random another state j in the same subpopulation u. If this j indicates an agent, j_A^u, then pick at random another state l in the same subpopulation u. If the state l indicates another agent, l_A^u, then transform the vacancy i_V^u into an agent i_A^u with rate λ: $i_V^u + j_A^u + l_A^u \Rightarrow i_A^u + j_A^u + l_A^u$
  - **Death:** If the state i indicates an agent, i_A^u, then transform it into a vacancy with rate α: $i_A^u \Rightarrow i_V^u$

After each Monte Carlo Step we apply a synchronous updating of the states.

[2] Our main code is availabe at (MAP, 2019).

Mathematical approach

Consider that $A_u(t)$ and $V_u(t)$ are the number of agents and vacancies in the subpopulation u at instant t, respectively. We use a ring metapopulation where each node is a subpopulation connected to k neighbor subpopulations. The parameter k controls the magnitude of the spatial constraints. Let $u = 1, \ldots, L$. Considering the well-mixed population (mean-field) at the local scale, the time evolution of the networked system is given by

$$\frac{dV_u}{dt} = (1-D)\Big[\overbrace{-\frac{\lambda V_u A_u^2}{(V_u+A_u)^2}}^{\text{Reproduction}} + \overbrace{\alpha A_u}^{\text{Death}}\Big] \tag{1.1}$$

$$\frac{dA_u}{dt} = (1-D)\Big[\underbrace{\frac{\lambda V_u A_u^2}{(V_u+A_u)^2}}_{\text{Reproduction}} - \underbrace{\alpha A_u}_{\text{Death}}\Big] + D\Big[\underbrace{-A_u}_{\text{Emigration}} + \underbrace{\sum_{z=1}^{L} \frac{1}{k} W_{uz} A_z}_{\text{Immigration}}\Big] \tag{1.2}$$

with W_{uz} being the elements of the adjacency matrix which assumes the value 1 if u and z are connected or 0 otherwise.

Aiming at taking into account both the cases of single and multiple sources of invasion, we shall use an initial condition given by

$$A_u(0) = \begin{cases} \frac{1}{n_s}\frac{N}{L} & u = 1, \ldots, n_s \\ 0 & u = n_s+1, \ldots, L \end{cases} \tag{1.3}$$

where N/L is the initial size of each subpopulation and n_s is the number of initial sources. By default, we use $V_u(0) = N/L - A_u(0)$ as well.

Survival-extinction phase transition

From a preliminary numerical analysis we observed that the steady-state solution satisfies

$$A_u^\infty = \bar{A}, \quad V_u^\infty = \bar{V} \quad \forall u \quad u = 1, 2, \ldots, L \tag{1.4}$$

Using that observation as an ansatz to solving our equations implies

$$N = \sum_{u=1}^{L} (A_u + V_u) = L(\bar{A} + \bar{V}) \Rightarrow \bar{V} = N/L - \bar{A} \tag{1.5}$$

$$\frac{d\bar{A}}{dt} = (1-D)\left[\frac{\lambda(N/L-\bar{A})\bar{A}^2}{(N/L)^2} - \alpha\bar{A}\right] + D\left[-\bar{A} + \frac{1}{k}\left(k\bar{A}\right)\right] = 0 \tag{1.6}$$

From Eq. (1.6) we can obtain three solutions to $\bar{A}$. The stability analysis yields a qualitative picture of the steady-state:

$$A_u^\infty = \begin{cases} \frac{N}{2L}\left(1 + \sqrt{1-4\frac{\alpha}{\lambda}}\right) & A_u(t=0) \geq A_c^o \text{ and } \alpha \leq \lambda/4 \\ 0 & \text{otherwise} \end{cases} \tag{1.7}$$

Where A_c^o is the threshold initial population size required for the local persistence:

$$A_c^o = \frac{N}{2L}\left(1 - \sqrt{1-4\frac{\alpha}{\lambda}}\right) \tag{1.8}$$

Equations (1.7)-(1.8) do not explicitly take into account the dispersal parameter D, but they allow us to get an insight into the nature of the survival-extinction phase transition: they show that the subpopulation faces a discontinuous transition at the critical point $\alpha_c = \lambda/4$. As in the long-term, the mobility spreads the absence of local correlations to the whole metapopulation, then the global dynamics undergoes an abrupt phase transition as well; we numerically confirm in the next section.

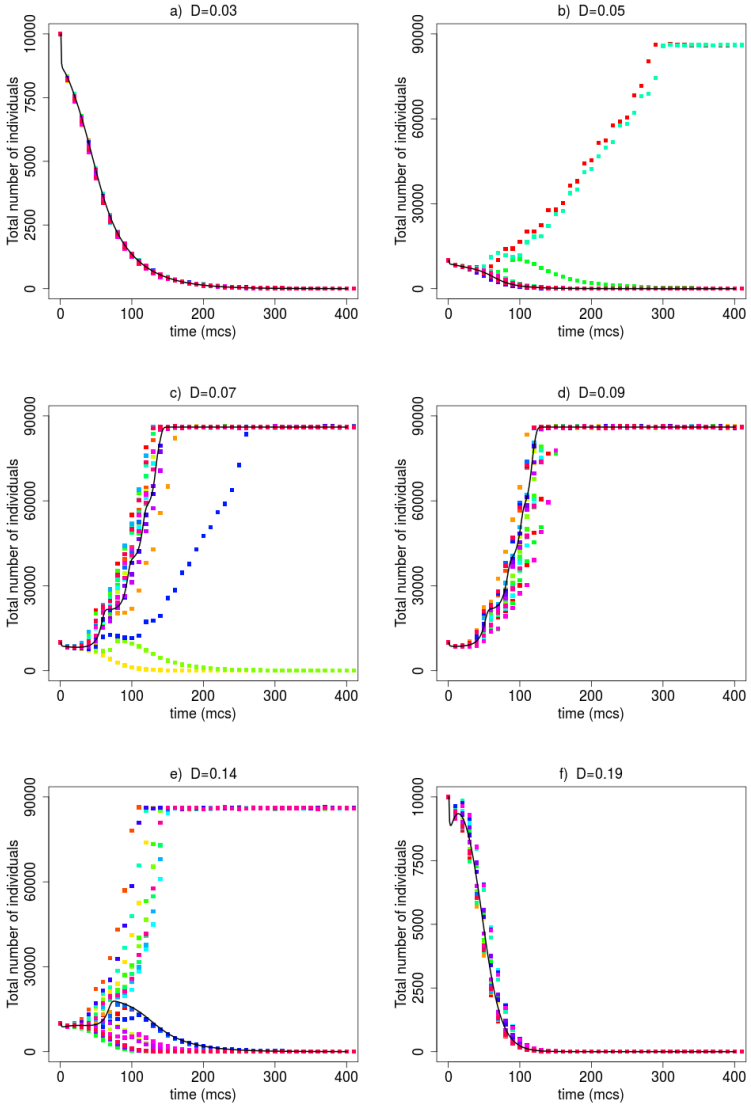

Figure 1.2 – Total number of agents vs time (in mcs) for $D = \{0.03, 0.05, 0.07, 0.09, 0.14, 0.19\}$ with $L = 10$, $N = 10^4 L$, $n_s = 1$. Each color corresponds to one sample. The symbols were obtained from Monte Carlo simulations and the lines from Eqs. (1.1)-(1.2).

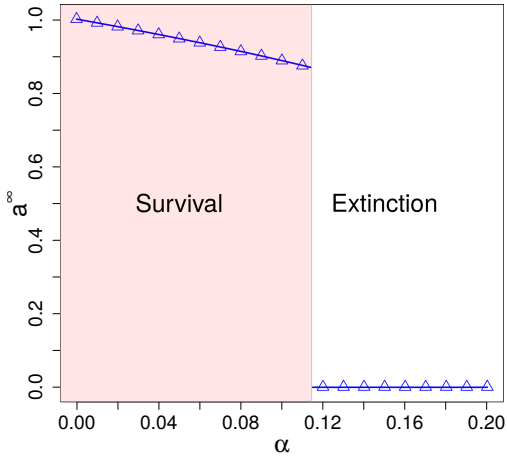

Figure 1.3 – Stationary density of agents a^{∞} vs mortality rate α with $D = 0.2$, $k = 2$, $L = 10$, $N = 10^4 L$, $n_s = 1$. The symbols come from the Monte Carlo Simulations and the lines come from the numerical integration of Eqs. (1.1)-(1.2).

RESULTS AND DISCUSSION

In this section, we present our results for metapopulations of sizes $10 \leq L \leq 50$ and increasing k, but all of the results remain valid for larger networks as we checked using Monte Carlo Simulation and our coupled differential equations (1)-(2), which represent the limit of very large systems. For the sake of simplicity and without losing generality for our results we fix $\lambda = 1$.

Fig.1.2 shows the time series of the total number of agents in the metapopulation for different dispersal rates. The temporal evolutions for $D = \{0.03, 0.09, 0.019\}$ display a single stable (steady) state, but the cases with $D = \{0.05, 0.07, 0.014\}$ exhibit bistable solutions. This rich dynamics is the outcome of competition between the reproducibility and mortality. It is worth stressing the role of randomness — governed by our probability parameters — in revealing that bistability. A clear outcome of the combination of randomness and bistability is the existence of ecological scenarios in which extinction can take place without apparent reason, even in the presence of

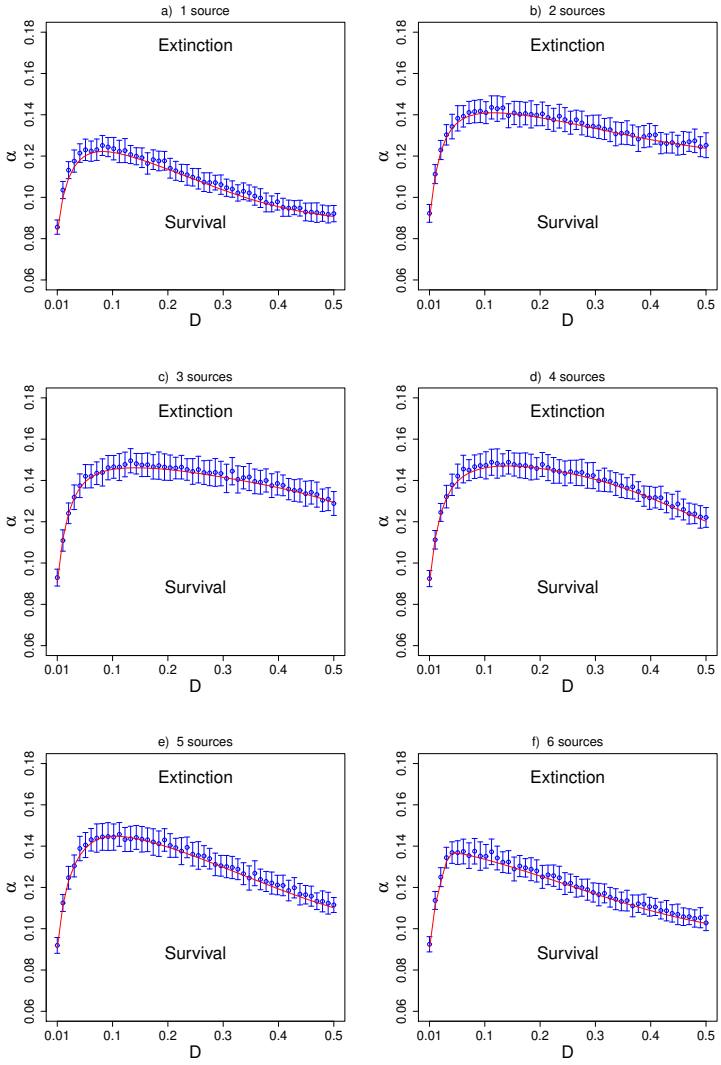

Figure 1.4 – Phase diagram α v D for $n_s = 1, 2, \ldots, 6$ sources, $L = 10$, $N = 10^4 L$. The point $D = 0$ is excluded from the diagram since it refers to isolated populations with threshold $\alpha_c = \lambda/4 = 0.25$. In all the cases $n_0 = \frac{10^4}{n_s}$, where n_0 is the initial subpopulation size. The lines are obtained from Eqs. (1.1)-(1.2).

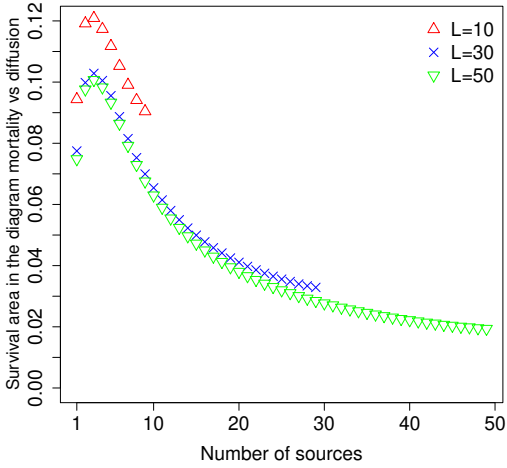

Figure 1.5 – Survival area in the phase diagram $\alpha \times D$ versus the number of sources n_s for $0 < D < 1$. The case $D = 1$ is excluded because it implies no reproduction/death. The case $D = 0$ is excluded because it implies no migration between the patches. In all cases we keep the initial subpopulation size fixed $n_0 = \frac{10^4}{n_s}$ and we use $N = 10^4 L$.

abundant resources. Last, a scenario marked by two well-separated stochastically-induced steady-states is a hallmark of a sudden phase transition as anticipated in the previous section. Such discontinuous transition is confirmed in Fig. 1.3 where we show the density of individuals, which is our order parameter, displays a pronounced jump for a critical mortality rate α_c. To fully grasp the idea behind the survival-extinction transition in Fig. 1.3, consider the ecological scenarios with $\alpha = \{0.04, 0.08, 0.12\}$. If the environmental conditions rise the mortality from $\alpha = 0.04$ to $\alpha = 0.08$, the total density of individuals undergoes just a slight drop (which may cause a false impression of resilience). However, if the mortality increase from point $\alpha = 0.08$ to $\alpha = 0.12$, there is tremendous dynamical response in the population density namely the mass extinction. That is, the same amount of rising in mortality rate can spark either a small or drastic

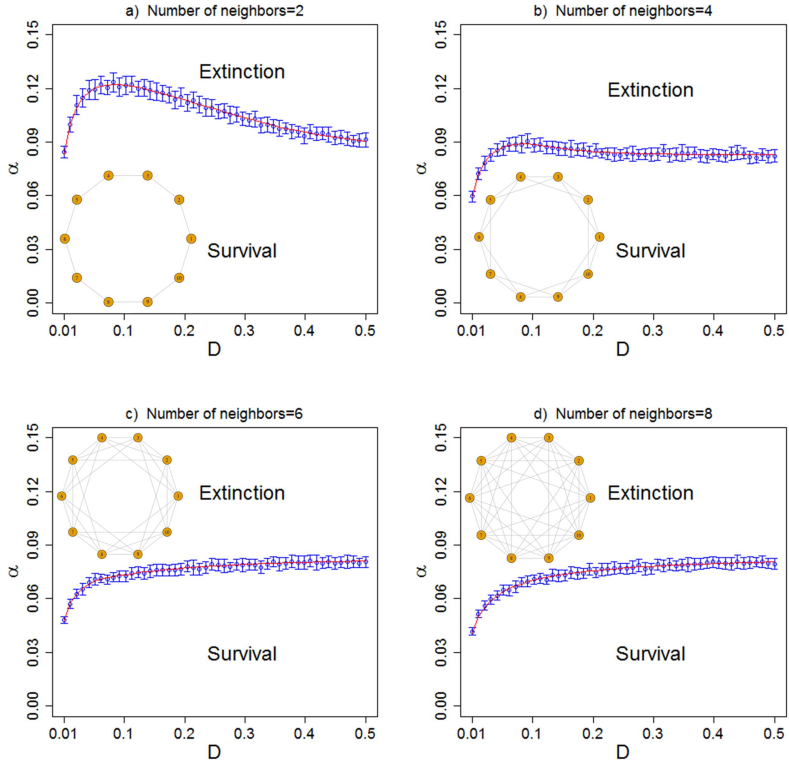

Figure 1.6 – Phase diagram α vs D for networks with increasing number of neighbors $k = 2, 4, 6, 8$ (decreasing spatial constraints). The theoretical lines (red) comes from numerical integration of Eqs. (1.1)-(1.2).

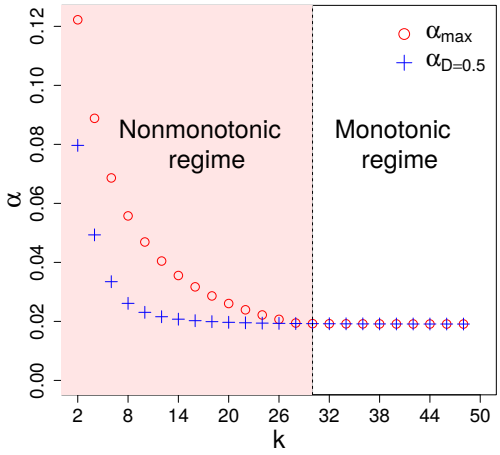

Figure 1.7 – Regime diagram of the dependence between threshold mortality α_c vs dispersal rate D for $L = 50$. The vertical line that separates the two regimes is $k_{threshold} = 30$. For $k < k_{threshold}$: $\alpha_{max} > \alpha_{D=0.5}$ then $\alpha_c \times D$ displays a nonmonotonic dependence. For $k \geq k_{threshold}$: $\alpha_{max} = \alpha_{D=0.5}$ then $\alpha_c \times D$ exhibits a monotonic dependence.

decline in the population. In other words, the population can behave either in a robust or fragile manner to environmental perturbations depending on the proximity to the threshold point. This feature is a remarkable fingerprint of discontinuous phase transition. It is worthwhile to mention that abrupt phase transitions are not an odd phenomenon in biological dynamics.

Up to now, we have not distinguish between the role of D and that of n_s on the threshold $\alpha_c(D)$. In order to separate out each contribution we call attention to Fig. 1.4 disentangles the role played by the interplay between the D and n_s. To estimate the thresholds we have employed an iterative procedure quite similar to that described in section 2.1 of Ref. (WINDUS; JENSEN, 2007): (i) first we set an initial guess for the threshold $\alpha_c{}'$, then the dynamics starts; (ii) if a given sample enters in the extinction state we decrease $\alpha_c{}'$ by a given amount $d\alpha$; (iii) if a given sample has a long-term persistent population, then we increase $\alpha_c{}'$ by a given amount $d\alpha$. In the Fig. 1.4 we see that this iterative procedure provides a rea-

sonable good estimation of the threshold that agrees very well with the theoretical threshold obtained from Eqs. (1.1)-(1.2). Also note that there is an optimal dispersal rate that allows the population to have comparatively high threshold mortality rates α_c. The number of sources do not change the nonmonotonic dependence of α vs D, but it changes the magnitude of this dependence.

Interestingly, Fig.1.5 shows there exists an optimal number of sources that promotes the largest survival area in the diagram α vs $D > 0$, as antecipated in Fig. 1.4; that is to say, the survival probability is maximised for an intermediate number of sources, wherefrom we understand that in populations subjected to the Allee Effect it is best to spare the population in many sources, but not too much. Similar results were found in Ref. (ZHOU; WANG, 2006) where the authors came up with an integrated model that displays an Allee-like effect at the metapopulation level, which is the outcome of imposing the Allee effect at the local population level. That is in contrast with our work because we use a microscopic model with no extra assumption on the birth and death rates.

The survival-extinction phase diagram in Fig. 1.6 shows that a decrease in the severity of the spatial constraints — i.e., an increase of k — leads to a decreasing in the threshold mortality $\alpha_c(D)$ for all k. That is to say, the population becomes more vulnerable to extinction when there are more open paths to emigrate. This result is supported by Ref. (ACKLEH; ALLEN; CARTER, 2007) where it was found that *"with fewer connections, the probability of invasion is greater"*. Furthermore, we observe the emergence of two regimes: α_c increases nonmonotonically with D for severe spatial constraints ($k = 2, 4$), but it increases monotonically with D for loose spatial constraints ($k = 6, 8$). Although we used a simplified minimal network it already shows the importance of spatial constraints in changing the qualitative behavior of the system. At last, Fig. 1.7 summarises our results for different magnitudes of spatial constraints k. Clearly there is a threshold for k, above which there is a monotononic dependence between α_c and D.

What is the underlying mechanism behind the qualitative

change presented in Fig.1.6-1.7? When the geometric constraints are very severe, we have a nonmonotonic regime caused by the source-sink dynamics between the donor subpopulation and its surroundings. For small dispersal, the source cannot provide enough individuals to produce a sustainable colony in the first-neighbors that in turn acts as a drain from the donor subpopulation. For intermediate dispersal the first neighbors receive enough individuals to bear sufficient reproduction to overcome the Allee Effect. However, if the dispersal is further augmented, then the first neighbors receive as many individuals as they lose for the next-nearest neighbors, which yields an insufficient net reproduction to foster long-term survival. Alternatively, in the monotonic regime the of loose spatial constraints allows the emergence of multiple secondary sources that feed one another in a way that by boosting the dispersal one enhances the net reproduction to overcome the Allee effect.

From the empirical side, the specific work of Smith et al (SMITH et al., 2014) supports our finding of the optimal dispersal. Therein, they engineered *E. coli* colonies aiming at displaying the strong Allee effect and found that dispersal acts as a double-edged sword. In other words, intermediate dispersal rates favours bacterial spreading whereas both low and high dispersal rates inhibits the spreading. Additionally, they present empirical evidence for another interesting result present in Fig.1.6-1.7: increasing connectivity can increase the vulnerability to extinction.

FINAL REMARKS

We studied ecological dynamics under the Allee effect and spatial constraints. Employing numerical and analytical tools we have shown that the survival-extinction boundary has a nonmonotonic behavior for severe spatial constraints and but a monotonic behavior for loose spatial constraints. The verification of this qualitative change in the dependence of the mortality threshold as a function of the dispersal highlights the importance of the threefold interplay between the Allee Effect, dispersal and geometric constraints for the persistence of populations.

Besides the experimental work of Ref. (SMITH et al., 2014), there are previous theoretical models pointing to our conclusions over the likely existence of an intermediate mobility rate that optimises the survival probability. Explicitly, Ref. (YANG et al., 2017) found a *"nonmonotonic dependence of the critical Allee thresholds on the migration rate"* by imposing the Allee Effect at the microscopic scale considering a nonlinear per capita birth rate $rn_i/C + rn_ic/C^2$ per capita death rate $rn_i^2/C + rc/C$.[3] In addition, we can also refer to Ref. (SOUTH; KENWARD, 2001) in which it was used an individual two-gender population on a hexagonal grid where the juveniles disperse away from their natal territory with dispersal distances distributed as a negative exponential. In that case, the population growth was highest for an optimal distance of the dispersal. Yet, both works did not observe the fact that the magnitude of the spatial constraints can change qualitatively the survival-extinction boundary from a nonmonotonic to a monotonic dependence.

In a broader view, there are other biological systems that exhibit nonmonotonic effects of dispersal such as epidemic spreading (SOUTH; KENWARD, 2001), birth-death-competition dynamics with migration (LAMPERT; HASTINGS, 2013), evolutionary dynamics with the Allee effect and sex-biased dispersal (SHAW; KOKKO, 2015), logistic growth dynamics in metapopulations with heterogeneous carrying capacities (KHASIN et al., 2012), metapopulation genetics dynamics with balancing selection (LOMBARDO; GAMBASSI; DALL'ASTA, 2014), two-type (mutants, strains, or species) population dynamics under the Allee effect (KOROLEV, 2015), and range expansion of a genetically diverse population where individuals may invest its limited resources partly in motility and partly in reproduction (REITER; RULANDS; FREY, 2014). As we adopted a minimal ecological model, it is possible to bring forth different extensions of the present work in order to fit for the traits of the problems we have just mentioned.

[3] n_i stands for the number of individuals on habitat patch i, C is the carrying capacity, c is an Allee threshold

Chapter 2

Dispersal plays an unusual role in ecological quasi-neutral competition in metapopulations

In this chapter, we investigate the phenomenology emerging from a 2-species dynamics under the scenario of a quasi-neutral competition within a metapopulation framework. We employ stochastic and deterministic approaches, namely spatially-constrained individual-based Monte Carlo simulations and coupled mean-field ODEs. Our results show the multifold interplay between competition, birth-death dynamics and spatial constraints induces a nonmonotonic relation between the ecological majority-minority switching and the diffusion between patches. This work is available in Ref.(PIRES; CROKIDAKIS; QUEIRÓS, 2021).

INTRODUCTION

Table 2.1 – List of symbols used in this chapter.

Symbol	Meaning
λ	Reproduction rate
α	Death rate
r	Ratio between faster (F) and slower species (S)
D	Dispersal rate
f_{Fo}	Initial density of species F
f_{So}	Initial density of species S
n_S	Number of sources in the network
N	Number of individuals in the metapopulation
L	Number of populations in the metapopulation

The battle for resources plays a significant role in the dynamics of competitive ecosystems. For a long time, the outcome of such a dispute was directly associated with the set of birth/death ratios of the contending species, λ_i/α_i. However, that scenario has been challenged by ecological models seasoned with other factors such as mobility, which proved themselves capable of leading to a priori upset results. The impact of those different contributions to competitive dynamics is especially interesting when one is dealing with quasi-neutral instances, for which the specific values of the birth, λ_i, and death, α_i, rate of species i yields the same ratio λ_i/α_i for all i. As we explore herein later on, besides the standard deterministic approach to an ecosystem, the problem has been analyzed from a stochastic perspective by means of a series of techniques systematically applied at the population scale.

In the present work, we tackle the problem of understanding the role played by patch diffusion — which we use as a quantitative proxy for mobility — in quasi-neutral competition within the metapopulation framework. Ecologically, a metapopulation — i.e., a population of populations — corresponds to a group of local connected populations of a species, the size of which changes in time due to microscopic factors such as the birth, death and migration of the individuals as well as mesoscopic events affecting the

local populations contained within the metapopulation, namely emergence and dissolution. We have considered a survey at this scale because a small local population can imperil the species (e.g., by reducing mating) (THOMPSON, 2016). Besides being empirically observed (SWEANOR; LOGAN; HORNOCKER, 2001; BORTHAGARAY et al., 2015; FOBERT; TREML; SWEARER, 2019), metapopulation approaches have set forth important results regarding ecological landscape dynamics in either homogeneous (JOHST; BRANDL; EBER, 2002; VUILLEUMIER; POSSINGHAM, 2006; COLOMBO; ANTENEODO, 2015) or heterogeneous populations (NAGATANI; ICHINOSE, 0019; JÚNIOR; F.FERREIRA; OLIVEIRA, 2014; JUHER; RIPOLL; SALDAÑA, 2009). Our results show that the interplay between quasi-neutral competition between two species with different biological clocks, spatial constraints and diffusion in metapopulation is complex. Indeed, we verified that large mobility between different patches can have the same impact as no migration between patches. In addition, depending on the level of mobility, being biologically slower can be actually an advantage. The ecological majority-minority switching exhibits a nonmonotonic relation with the diffusion between patches.

LITERATURE REVIEW

The effects of diffusion were studied in many works in recent years: In (SMITH et al., 2014) it was studied the Allee effect in bacteria populations and was showed that it led to a biphasic dependence of bacterial spread on the dispersal rate: spread is promoted for intermediate dispersal rates but inhibited at low or high dispersal rates. Correlated to such experimental work, the authors in (PIRES; QUEIRÓS, 2019) explored theoretically the threefold interplay among the Allee Effect, dispersal, and spatial constraints. They showed that the survival-extinction boundary undergoes a novel transition of monotonicity in the way that for the nonmonotonic regime there is an optimal dispersal rate that maximizes the survival probability. Diffusion of populations can also relate to the emergence of Parrondo's paradox instances for which the combination of two losing (extinction) strategies – diffusion and inefficient α –

combined yield a winning (preservation) situation (TAN; CHEONG, 2019; TAN; KOH, et al., 2020).

Considering competition between two distinct species, Pigolotti and Benzi showed that an effective selective advantage emerges when the two competing species diffuse at different rates (PIGOLOTTI; BENZI, 2014). In reaction/kinetic systems, diffusion can lead to distinct scenarios in reaction/kinetic system: it destroys the stability of possible equilibrium, leading to the formation of characteristic patterns; drive an otherwise persistent competing species to extinction (SU; ZOU, 2019). Some paradoxical situations can emerge in the competition between species as well. For instance, for a sizable range of asymmetries in the growth and competition rates, it was discussed that the numerically disadvantaged species according to the deterministic rate equations survive much longer (GABEL; MEERSON; REDNER, 2013). In d-dimensional spatial structures, the survival of the scarcer in space is verified for situations in which the more competitive species is closer to the threshold for extinction than is the less competitive species when considered in isolation (DOS SANTOS; DICKMAN, 2013).

Another recent work studied the competition between fast- and slow-diffusing species, considering non-homogeneous environments (PIGOLOTTI; BENZI, 2016). The authors considered the case in which non-homogeneity in the nutrients is contrasted with a fluid flow concentrating individuals around a velocity sink. In such a case, diffusing faster constitutes an advantage as faster individuals can colonize more easily upstream regions, from which they can invade. It was also argued that in time-independent environments it is always convenient to diffuse less (PIGOLOTTI; BENZI, 2016; HASTINGS, 1983; DOCKERY et al., 1998); particularly, the authors in Ref. (PIGOLOTTI; BENZI, 2016) suggested that deterministic models can miss a crucial ingredient to determine the best dispersal strategy.

Considering two species that differ only in the rates of their biological clocks, the authors in (OLIVEIRA; DICKMAN, 2017) showed that the slower species can enjoy an advantage in stationary

population density for reproduction rates close to (but greater than) a critical value, and large initial population densities. Alternatively, it was shown (CHEONG; TAN; LING, 2018) that switching-rule approaches relying upon biological clocks provide an efficient mechanism by which species might undergo behavioral nomadic-colonial alternation that allows them to develop well. For a recent review about the slower is faster effect, considering pedestrian dynamics, vehicle traffic, traffic light control, logistics, public transport, social dynamics, ecological systems, and others, see (GERSHENSON; HELBING, 2015).

MODEL

Consider a metapopulation with L subpopulations composed of agents that are able to move, die, and reproduce. As usual in metapopulation dynamics, we consider well-mixed subpopulations so that the individuals inside each of them can interact with one another, or in Statistical Physics parlance, we employ a local dynamics that has a mean-field character. The mobility is implemented as a random walk between the neighbor subpopulations and it occurs with probability D for each agent.

At each time step, if the dispersal event is not chosen with probability $1-D$, then we implement the events related to the quasi-neutral competition (OLIVEIRA; DICKMAN, 2017) between species F and S inside each subpopulation:

$$F + V \Rightarrow 2F \quad \text{with rate } \lambda_F \tag{2.1}$$

$$F \Rightarrow V \quad \text{with rate } \alpha_F \tag{2.2}$$

$$S + V \Rightarrow 2S \quad \text{with rate } \lambda_S \tag{2.3}$$

$$S \Rightarrow V \quad \text{with rate } \alpha_S, \tag{2.4}$$

where F (S) stands to faster (slower) species and V for a vacancy.

In order to allow a comparison between the biological clock of the two species we introduce a relative birth ratio so that

$$\lambda_S = r\lambda_F, \qquad \alpha_S = r\alpha_F; \tag{2.5}$$

explicitly we have the following relations:

$$\begin{cases} \lambda_S = r\lambda_F & r < 1 \text{ disadvantage of S: smaller birth rate,} \\ \alpha_S = r\alpha_F & r < 1 \text{ advantage of S: smaller death rate.} \end{cases}$$

To computationally implement the set of microscopic relations Eqs. (1)-(4), we consider an array with N states divided into the L subpopulations. In this case, we assume periodic boundary conditions. Each state in subpopulation u indicates an agent $\{i_F^u, i_S^u\}$ or a vacancy, i_V^u. Our time unit is a Monte Carlo step (mcs) that consists of a visit to each one of the N states.

For each state $i = 1, \ldots, N$:

- First we get the subpopulation, say u, of the state i.
- With probability D:
  - **Dispersal :**
    $i_F^u \Rightarrow i_F^w$. (event 1F)
    $i_S^u \Rightarrow i_S^w$. (event 1S)
- and with probability $1 - D$:
  - **Reproduction:**
    rate λ_F: $i_V^u + j_F^u \Rightarrow i_F^u + j_F^u$. (event 2F)
    rate λ_S: $i_V^u + j_S^u \Rightarrow i_S^u + j_S^u$. (event 2S)
  - **Death:**
    rate α_F: $i_F^u \Rightarrow i_V^u$. (event 3F)
    rate α_S: $i_S^u \Rightarrow i_V^u$. (event 3S)

The details of our computational approach can be found at the URL: https://github.com/PiresMA/diffusion_2cp.

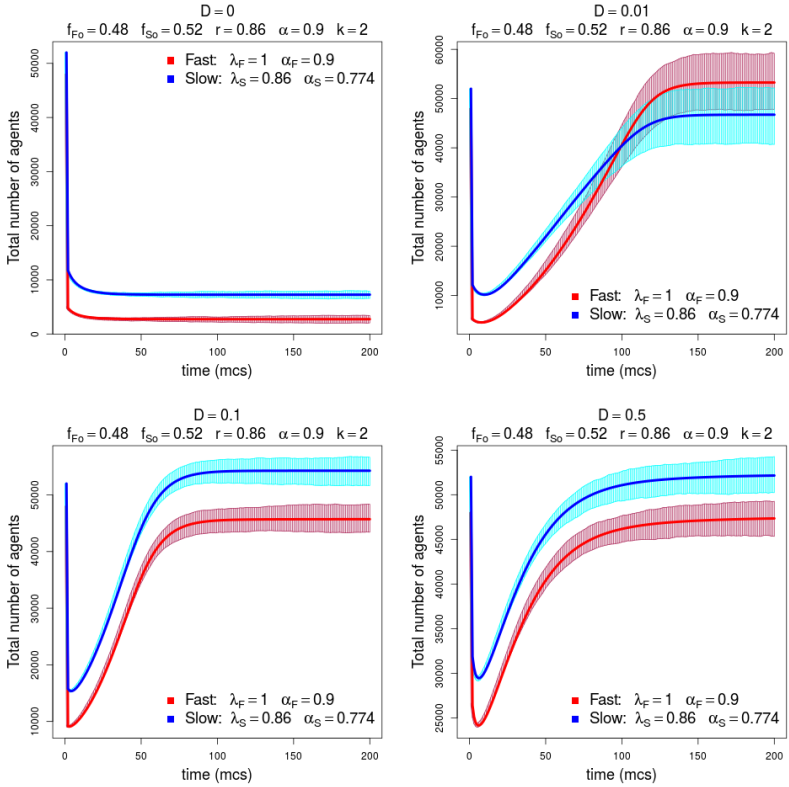

Figure 2.1 – (scenario I) Time series for the total number of individuals F and S. Shaded area comes from Monte Carlo simulation (mean±standard deviation). The theoretical lines comes from the numerical solution of Eqs. (2.6)-(2.8). To summarize: $D = 0$, winner: S; $D = 0.01$, winner: F; $D = 0.1$, winner: S; $D = 0.5$, winner: S.

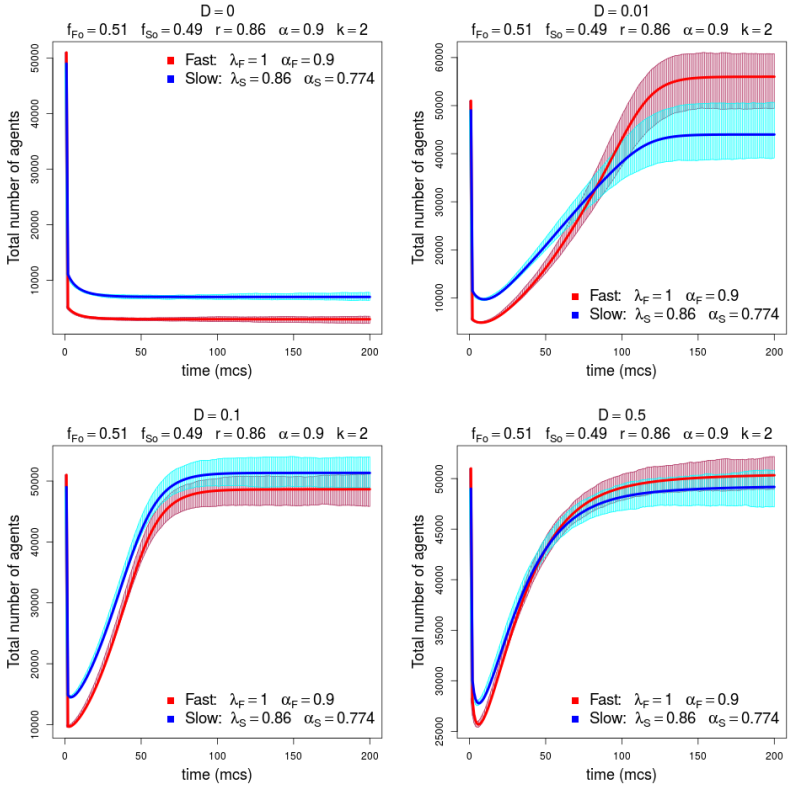

Figure 2.2 – (scenario II) Time series for the total number of individuals F and S. Shaded area comes from Monte Carlo simulation (mean±standard deviation). The theoretical lines comes from Eqs. (2.6)-(2.8). To summarize: $D = 0$, winner: S; $D = 0.01$, winner: F; $D = 0.1$, winner: S; $D = 0.5$, winner: F.

RESULTS

Applying a previous bottom-up mathematical framework (PIRES; QUEIRÓS, 2019) to the set of rules described above we arrive at

$$\frac{dV_u}{dt} = (1-D)\Big[-\overbrace{\frac{\lambda V_u(F_u + r\,S_u)}{V_u+F_u+S_u}}^{\text{Reproduction}} + \overbrace{\alpha(F_u + r\,S_u)}^{\text{Death}}\Big] \tag{2.6}$$

$$\frac{dF_u}{dt} = (1-D)\Big[\underbrace{\frac{\lambda V_u F_u}{V_u+F_u+S_u}}_{\text{Reproduction}} - \underbrace{\alpha F_u}_{\text{Death}}\Big] + D\Big[\underbrace{-F_u}_{\text{Emigration}} + \underbrace{\sum_{z=1}^{L}\frac{1}{k}W_{uz}F_z}_{\text{Immigration}}\Big] \tag{2.7}$$

$$\frac{dS_u}{dt} = (1-D)\Big[\underbrace{\frac{r\lambda V_u S_u}{V_u+Fu+S_u}}_{\text{Reproduction}} - \underbrace{r\alpha S_u}_{\text{Death}}\Big] D\Big[\underbrace{-S_u}_{\text{Emigration}} + \underbrace{\sum_{z=1}^{L}\frac{1}{k}W_{uz}S_z}_{\text{Immigration}}\Big], \tag{2.8}$$

where W_{uz} is the adjacency matrix which assumes values 1 if u and z are connected or 0 otherwise. We work with a circular/ring metapopulation wherein each location/region contains a population that is coupled to k neighbor populations. The parameter k is the connectivity of each population, i.e., it regulates the strength of the spatial constraints. We use an initial condition given by

$$F_u(0) = \frac{f_{Fo}}{n_s}\frac{N}{L} \qquad u = 1,\ldots,n_s \tag{2.9}$$

$$S_u(0) = \frac{f_{So}}{n_s}\frac{N}{L} \qquad u = 1,\ldots,n_s \tag{2.10}$$

with f_{Fo}, f_{So} being the modulating factors that account for the fraction of individuals at the subpopulations, N/L is the initial size of each subpopulation and n_s is the number of initial sources. Additionally, we use $V_u(0) = N/L - F_u(0) - S_u(0)$. As we have a plethora of parameters we set $f_{So} = 1 - f_{Fo}$ as well as $n_s = 1$ (all the agents are located initially in one source). Besides, without losing generality we have also set $\lambda = 1$.

We implement our spatially-constrained Monte Carlo algorithm in computer simulations considering metapopulations with $N = 10^6$ and $L = 10$. Despite that fact, we assert that all of the our findings remain valid for larger metapopulations since the deterministic coupled mean-field Eqs. (2.6)-(2.8) are valid in the limit of infinite population. This assumption is clearly validated with the results shown in Figs. 2.1-2.2 where we see a good agreement between the numerical solution of the multidimensional ODEs in Eqs. (2.6)-(2.8) and the individual-based Monte Carlo simulations (VINCENOT et al., 2011; GRIMM; RAILSBACK, 2005) with 100 samples in each panel.

In Fig. 2.1-2.2, we present the outcomes for some specific configurations in order to explain in detail the myriad of majority-minority switching in the ecological dynamics. In the subsequent analyses we show the results for more general settings in order to provide an overall perspective about the robustness of the emergent phenomenology.

Focusing solely on Fig. 2.1, we depict the time evolution of the number of individuals F and S for which the initial population of the faster species (initial density $f_{Fo} = 0.48$) is smaller than the slower one (initial density $f_{So} = 0.52$). For $D = 0$, the slower species S becomes dominant at the steady state. For small values of dispersal (such as $D = 0.01$) the initially majority species (S) becomes the minority one at the steady state. Such scenario changes for intermediate values of the dispersal rate ($D = 0.1$), where we see that S recover the majority position. For $D = 0.5$, the dominance of species S becomes greater. From the different panels, it is visible that, as we increase the value of the dispersal parameter D, we first observe

the faster species achieves a larger final (steady state) population, and afterward, the slower species S becomes prevalent.

However, the outcome changes as we pay attention to Fig. 2.2, where the faster species has the initial majority ($f_{Fo} = 0.51$ and $f_{So} = 0.49$). For $D = 0$, the slower species S becomes again the dominant one at the steady state. For $D = 0.01$ the initially prevailing species (F) becomes the minority one in the short run but recovers to become the majority at the steady state. For intermediate values in the mobility ($D = 0.1$) the minority species S becomes the majority. For $D = 0.5$ the dominance of species S is destroyed again. That is, the overall picture now is more diverse than the previous setting in Fig. 2.1.

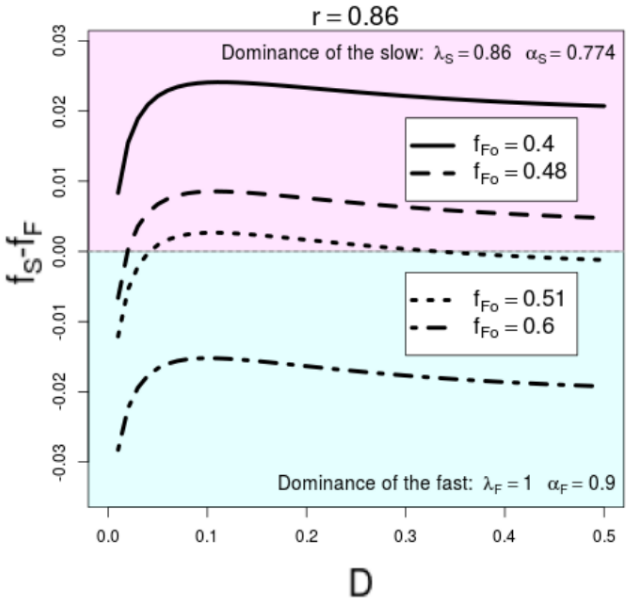

Figure 2.3 – Relative difference in the number of agents $f_S - f_F$ versus the dispersal parameter $0 < D \leq 0.5$. Results are for $r = 0.86$. Dispersal leads to four types of distinct scenarios regarding the dominance of the species F/S.

The dominance of a species can be also represented by the relative difference between the size of the populations at the steady

state, $\Delta_f \equiv f_S - f_F = (N_S - N_F)/N$. For a given value of the asymmetry parameter r we can plot parametric curves for fixed initial conditions in the Δ_f-D plane depicted in Fig. 2.3. In that plot, we verify that taking into consideration the initial condition regarding the initial fraction of each species, there are intuitive curves for which the majority species is the prevalent species in the final (steady) state (e.g., solid and dot-dashed lines) whereas for the dotted line we find a trivial region for large values of the dispersal parameter, $D \gtrsim 0.3$, as well as very limited dispersal parameter $D \lesssim 0.05$ and within those values of D we observe a non-trivial region where in spite of being outnumbered at first by F, the slower species S reach a larger population at last.

Combining Fig. 2.3 and Fig. 2.4, we understand the existence of an optimal value for each curve $f_{Fov} = constant$; that is reminiscent of a competition mechanism between the multifold features of the model. For absent patch diffusion, $D = 0$, the agents interact only inside one patch. For maximal dispersal, the individuals are able to interact with a much larger number of other individuals at the expense of weakening the links that necessarily establish the populations of the metapopulation. Accordingly, there is an optimal value of the dispersal parameter, D^{op}, for each f_{Fov} at which is achieved a balance between finding new individuals whilst preserving the robustness of the metapopulation. Notwithstanding, species F is at its maximal situation, it does not mean it is the prevailing species as in dealing with a similar scenario species S can end up in a situation for which the number of elements in the total population overcomes that F.

We have extended that analysis to other values of the asymmetry parameter r keeping the magnitude of the dispersal rate constant in $D = \{0, 0.01, 0.1, 0.5\}$ in Fig. 2.5. When there is no dispersal in the system, $D = 0$, S is the dominant species, excepting for large values of f_{Fo} and r. However, such scenarios change drastically for all $D > 0$. Specifically, even for the case $D = 0.01$ for which there is very little dispersal, it is already possible to change the outcome regarding the steady-state dominant species. For $r = 0$, the dynamics of S is naturally frozen because $\lambda_S = r\lambda_F = 0$ and $\alpha_S = r\alpha_F = 0$.

The broad panorama from the present panels highlights that the establishment of the final majority depends on an intricate relation between competition, mobility and birth-death dynamics under spatial constraints.

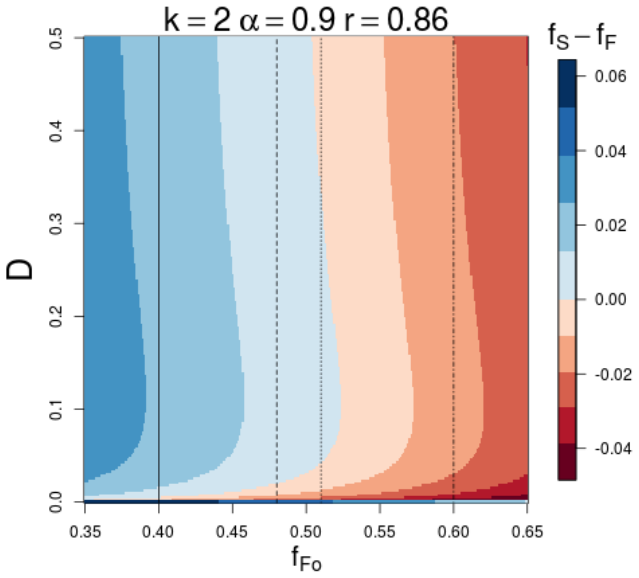

Figure 2.4 – Diagram of the relative difference $f_S - f_F$. The four vertical straight lines in this diagram corresponds to the curves in the Fig.2.3 with $f_{Fo} = \{0.4, 0.48, 0.51, 0.6\}$.

Finally, in the panels exhibited in Fig. 2.6 we analyze how the number of new patches that individuals can move impacts on the mortality-dispersal diagram for the competition between species F/S considering severe ($k = 2$) and loose ($k = 8$) spatial constraints. First, note that for $D = 0$ the slower species (S) becomes dominant for any α. Yet, this picture changes when we have mobility given by $D \neq 0$. For a given α not too high, $\alpha \lesssim 0.2$, S is dominant only if D is high enough. Increasing the number of new patches from $k = 2$ to $k = 8$, by reducing the spatial constraints, the individuals are naturally able to move more which leads to an enhancement of the advantage

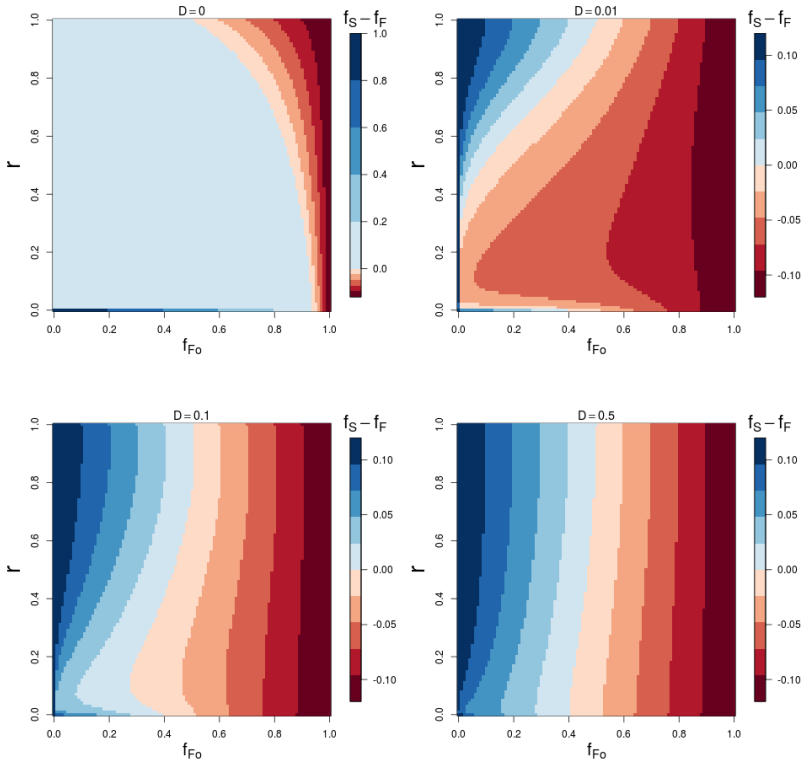

Figure 2.5 – Dependence of the relative difference $f_S - f_F$ in the steady state with r versus f_{Fo}. Diagrams obtained from Eqs. (2.6)-(2.8) with $\alpha = 0.88$, $k = 2$.

of being slow. To explain such results keep in mind that in the long-run the mobility spreads the absence of local correlations to the whole metapopulation and thus the results for high D qualitatively approaches the results for $D = 0$ as k increases.

FINAL REMARKS

In this work, we have used dispersal to study the role played by mobility in quasi-neutral competition within a metapopulation context, which from a physical perspective can be understood as a

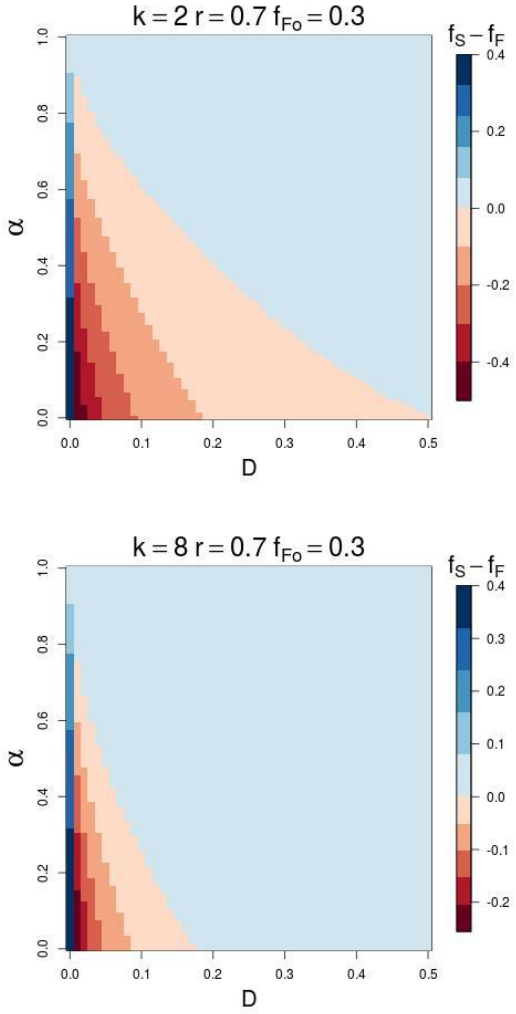

Figure 2.6 – Dominant species in the mortality vs dispersal diagram for strong ($k = 2$) and weak ($k = 8$) spatial constraints.

coarse-grained approach to an ecological system. Considering quasi-neutral competition a metapopulation analysis is worthwhile since in being a population of populations, events that affect local populations, namely the possibility of moving with impact on mating and the structure of network correlations, can put the whole metapopulation structure.

Our theoretical results – obtained from Monte Carlo simulations as well as numerical integration of multidimensional ODEs – show that the multifold interplay between quasi-neutral competition between two species with different biological clocks, spatial constraints, and dispersal in metapopulation is remarkably complex. Nevertheless, it was possible to understand that large mobility between different patches — which at first would benefit mating — can have the same impact as no migration between patches. That being so, for given initial conditions, there is a set of parameters that optimize the population imbalance, which can be favorable to the slower species. In other words, depending on the level of mobility, being biologically slower can be actually an advantage. The take-home message from our work is that the ecological majority-minority switching for quasi-neutral competition in metapopulations exhibits a nonmonotonic relation with the diffusion between patches. This phenomenon is highly counter-intuitive, but it could be further studied resorting to experimental setups within Synthetic Biology where bacteria can be programmed to exhibit new behavior (SMITH et al., 2014; DING; WU; TAN, 2014; WANG et al., 2016; PADILLA-VACA; ANAYA-VELÁZQUEZ; FRANCO, 2015). From a broader point of view, the present contribution adds an interesting and new building block to the list of counter-intuitive ecological dynamics (SHAW; KOKKO, 2015; LOMBARDO; GAMBASSI; DALL'ASTA, 2014; KHASIN et al., 2012; KOROLEV, 2015; ABBOTT, 2011; DUNCAN; GONZALEZ; KALTZ, 2015; CHEONG; KOH; JONES, 2019; DOAK et al., 2008). It is worthwhile to note that minority-majority inversions have also been observed in social systems (CROKIDAKIS; OLIVEIRA, 2014).

Some points were not addressed in our work, like the impact of the presence of a topology or time-dependent rates in the results.

In future works, it would be interesting to generalize our model to incorporate time-dependent dispersal rates as well as networks with more sophisticated topologies than those used in this manuscript.

Chapter 3

Ecology with the Allee effect: impact of nonlinear correlations

In this chapter, we consider ecological Allee-like dynamics under perturbations with random and nonrandom temporal arrangements but the same *linear* autocorrelation pattern. We show that populations are more vulnerable to extinction under perturbations with nonlinear correlations. Accordingly, this result provides an insight toward the disentangling the distinction between linear and nonlinear correlation in extinction dynamics which, in turn, allows comprehending *how* randomness jeopardises the long-run proliferation of organisms. This work is available in Ref.(PIRES; CROKIDAKIS; QUEIRÓS, 2020).

INTRODUCTION

Table 3.1 – List of symbols used in this chapter.

Symbol	Meaning
λ	Reproduction rate
α	Death rate
$p(t)$	Proportion of individuals in the population
f_{ext}	Fraction of populations undergoing extinction
ACF	Autocorrelation function
LZC	Lempel-Ziv complexity

The study of Ecological problems – namely, population dynamics – can be easily placed at the spotlight of Complexity. Besides the interaction between the biotic and abiotic elements, it is possible to find several layers of further interactions and dependencies that impact in the evolution of the system. With that respect, extinction is still the subject of great academic debate and in the spotlight of opinion public and mass media because of the rising interest in environmental preservation and conservation. Several ecological mechanisms of extinction were discussed in Ref. (BEISSINGER, 2000), like distinct rates of population increase (e.g., fecundity, survival rates, generation times), differential vulnerability of lineages to habitat loss, introduction of predators, mobility among other features. Those mechanisms often influence one another and can also affect and be affected by macroscopic measures of the ecosystem like the population size/density. One of those cases is the Allee effect that describes the relation between population measures and the fitness of a species (COURCHAMP; BEREC; GASCOIGNE, 2008b). Moreover, mechanisms as those we have listed are usually translated into parameters when we establish quantitative descriptions of Ecology. However, quantities like survival, fecundity, etc., are not fixed in time and generically subjected to randomness.

Mathematically, randomness can assume alternative origins implying in different dynamical and statistical features, namely correlation and dependence. In this manuscript, we aim at shedding light on the effects created by different non-linear properties of the

randomness of the 'parameters' of a standard Allee effect dynamical model.

LITERATURE REVIEW

From molecular biology (WOLFRAM, 2002; LONGO; MONTÉVIL, 2012) (eg, cell mitosis, morphogenesis) to collective behaviour (CAVAGNA et al., 2013), passing by evolution (WAGNER, 2012; ROSA; VILLEGAS, 2019), randomness – including disorder – has shown to be a key ingredient in Biology (MERLIN, 2009; SPAGNOLO; VALENTI; FIASCONARO, 2004).

Understanding the ecological mechanisms that lead to the extinction of a species is thus fundamental to conserve it. The impact of the different sources of ecological evolution – particularly those we have made mention to – have been consistently surveyed in the literature. Considering the ancestry issue it was observed different lineages are threatened by distinct mechanisms of extinction, and unrelated ecological factors predispose taxa to different sources of extinction risk (OWENS; BENNETT, 2000). In Ref. (O'GRADY et al., 2004), the authors pointed that population size and trend in population size were clearly the best predictors of extinction risk. Mathematical and computational models were widely proposed to explain the phenomenon of extinction (FORGERINI; CROKIDAKIS, 2014; CARLSON et al., 2018; DRAKE, 2014).

At the level of the resources in ecological systems, it is possible to find randomness and stochasticity as well. Namely, simple models incorporating the key features of time-dependent resources and specific descriptions of survivorship for consumer species show the importance of the time dependence of available resources and the role that allochthonous inputs play on the temporal and spatial abundances of species (HASTINGS, 2012; TULJAPURKAR, 1990).

Extinction is a major ecological event. Because it corresponds to the termination of a species, extinction can be understood within a Physics framework as a phase transition event with the emergence of an absorbing state. The Contact Process (CP) is the paradigmatic model for phase transitions into absorbing states

(MARRO; DICKMAN, 2005). In the CP, temporal disorder can be introduced by allowing the control parameter to be time dependent. For example, the authors in (FIORE; OLIVEIRA; HOYOS, 2018) showed that in contrast to spatial disorder, uncorrelated temporal disorder does not forbid the existence of discontinuous absorbing phase transitions, and it can also turn a discontinuous transition into a continuous one when disorder is sufficiently strong, even for low-dimensional systems (OLIVEIRA; FIORE, 2016). Also considering the CP, the authors in (BARGHATHI; VOJTA; HOYOS, 2016; VOJTA; HOYOS, 2015) considered the temporal disorder as an external environmental noise. The results suggest that the temporal disorder gives rise to an exotic critical point, where the average density and survival probability decay only logarithmically with time. In nonequilibrium magnetic models, temporal disorder acting as a time-dependent magnetic field leads to rich critical phenomena, with the occurrence of dynamical tricritical points (CROKIDAKIS, 2010; YÜKSEL et al., 2012).

An Ecosystem has been regarded as the quintessential complex systems since the interactions between its components can feed back to impact such interactions by means of the macroscopic state that gets established (LEVIN, 1998). Accordingly, considering tools like agent-based or cellular automata models, a new understanding arises of ecosystems as wholes that emerge in novel ways from possibly simple, mechanical rules governing interactions among their parts (PROCTOR; LARSON, 2005).

Finding robust methods for quantifying spatio-temporal signals in the presence of noise, nonstationarity and short data series is an active area of research in many disciplines. For ecosystem applications, we would expect these methods to detect pattern transitions (i.e., sequences of stable, periodic, quasi-periodic, chaotic, or random trends) as well as where and when they occur (PROULX, 2007).

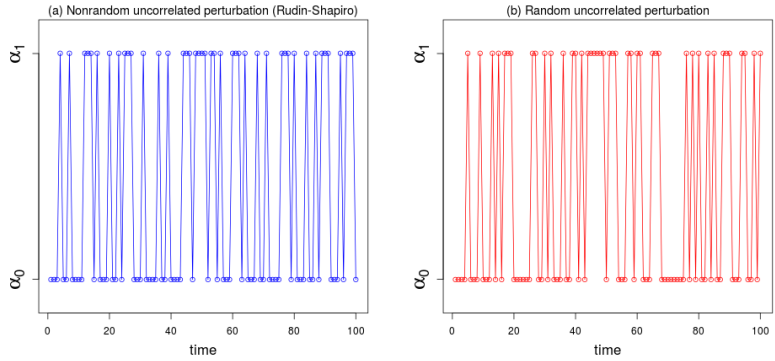

Figure 3.1 – Time-dependent death rate $\alpha(t) = \{\alpha_0, \alpha_1\}$ considering the protocols: (a) nonrandom and (b) random. Both time series have the same mean value $\bar{\alpha}$, since the case (b) is just a shuffle of the case (a).

MODEL

Extinction dynamics

We consider an ecological dynamics for the proportion of individuals in a given population, $p(t)$, that takes into account the Allee effect by means of the minimal ODE (WINDUS; JENSEN, 2007)

$$\frac{dp(t)}{dt} = \lambda[1-p(t)]p^2(t) - \alpha(t)\,p(t). \tag{3.1}$$

The first term on the right hand side is related to reproduction occurring at rate λ and the second term is related to death rate $\alpha(t)$. While in Ref. (WINDUS; JENSEN, 2007) the death rate is a constant, here we consider that it is time-dependent.

The reproduction-death dynamics described by Eq. (3.1) also includes the Allee effect (ALLEE, 1931; DRAKE; KRAMER, 2011) that is an important class of density-dependent phenomenon which has been widely observed in nature (KRAMER et al., 2009). Apart from Ecology, the Allee effect is also important in several research areas such as conservation biology (COURCHAMP; BEREC;

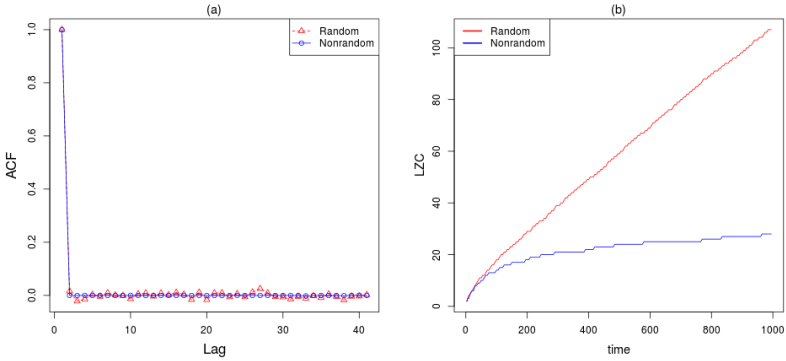

Figure 3.2 – Main properties of the time-dependent binary sequences used for $\alpha(t) = \{\alpha_0, \alpha_1\}$. (a) Autocorrelation (ACF) versus lags. (b) Lempel-Ziv complexity (LZC) over time. The LZC is able to detect hidden patterns that are not recognized by the ACF.

GASCOIGNE, 2008b), invasion biology (TAYLOR; HASTINGS, 2005) as well as biofilm formation (GOSWAMI; BHATTACHARYYA; TRIBEDI, 2017; JORNET, 2020), epidemiology (REGOES; EBERT; BONHOEFFER, 2002; HILKER; LANGLAIS; MALCHOW, 2009; DEREDEC; COURCHAMP, 2006) and cancer biology (KOROLEV; XAVIER; GORE, 2014; SEWALT et al., 2016; JOHNSON, K. E. et al., 2019; NEUFELD et al., 2017). Such variety of domains wherein the Allee effect plays a role highlights the significance and broad interest of our work.

An initial insight into Eq. (3.1) is obtained from the steady-state solution for the case with constant death rate $\alpha(t) = a$

$$P^{\infty} = \begin{cases} \frac{1}{2} + \frac{1}{2}\sqrt{1 - 4\frac{a}{\lambda}} & P_o \geq P_c^o \text{ and } a \leq \frac{\lambda}{4} \\ 0 & \text{otherwise} \end{cases} \tag{3.2}$$

where P_c^o is the initial density required for the long-run survival,

$$P_c^o = \frac{1}{2}\left(1 - \sqrt{1 - 4\frac{a}{\lambda}}\right). \tag{3.3}$$

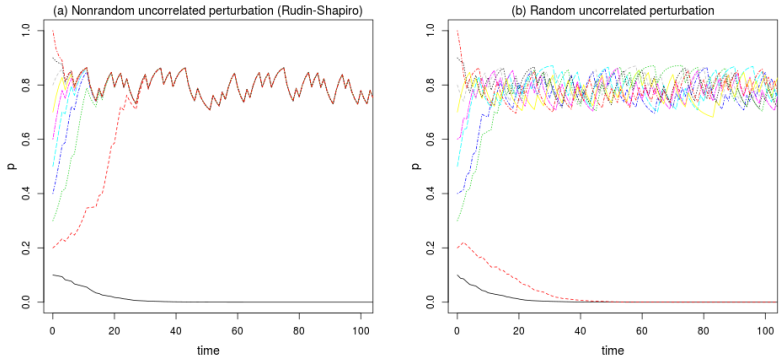

Figure 3.3 – Time series for the population fraction considering (a) nonrandom and (b) random perturbations. Each curve is obtained with increasing initial population densities $P_0 = \{0.1, 0.2, \ldots, 1\}$. Parameters: $\lambda = 0.9$ and $\alpha_0 = 0.2$.

From Eq. (3.2), we see that the time-independent model with $\alpha(t) = a$ presents a discontinuous absorbing transition(MARRO; DICKMAN, 2005; HENKEL et al., 2008; PIRES; OESTEREICH; CROKIDAKIS, 2018). Equation (3.3) yields the Allee threshold, ie, the population fraction below which extinction is the eventual scenario. Thus, the bistable nature incorporated in Eq. (3.1) is the mechanism responsible for the Allee effect. Frameworks more general than Eq. (3.1) could be considered (BEREC, 2008), but we are interested in a fundamental question: What makes the pure randomness increase the vulnerability of populations?

Protocol for $\alpha(t)$

As we aim at studying the possible effects of randomness on the dynamics of Eq. (3.1), we assume the simplest of the instances where α alternates between α_0 and α_1. In order to assess the role of non-linearities in that process we assume that $\alpha(t)$ sequences are given by either purely or Rudin-Shapiro protocols. In such binary arrays we map $0 \to \alpha_0$ and $1 \to \alpha_1$. In all the cases, we start from 0, subsequently we apply one of the following rules:

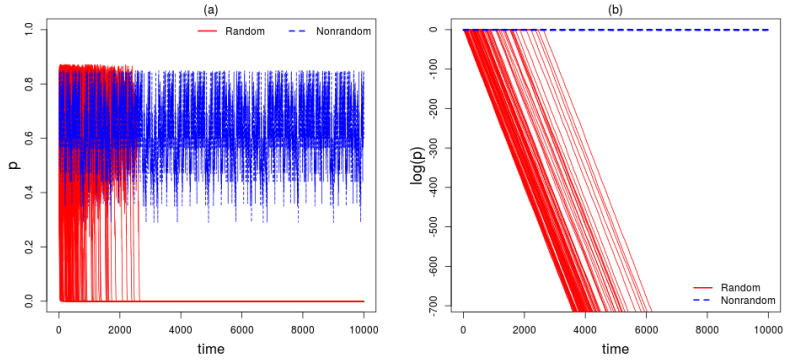

Figure 3.4 – Time series for the population fraction considering non-random and random perturbations. (a) Linear scale and (b) Semi-log scale. We use 100 samples for the protocol with randomness. Parameters: $P_0 = 0.5$, $\lambda = 0.9$, $\alpha_0 = 0.1$ and $\alpha_1 = 0.3$.

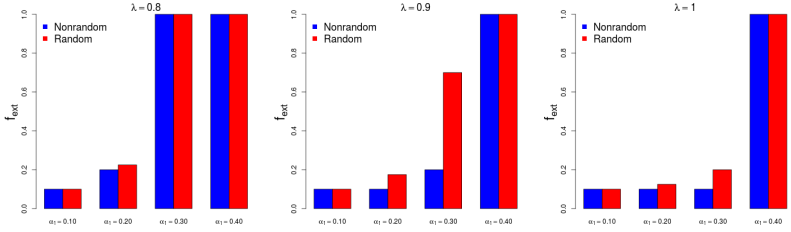

Figure 3.5 – Barplot with the fraction of populations undergoing extinction, f_{ext}, among the total of time series obtained with $P_0 = \{0.1, 0.2, \ldots, 1\}$. For all panels, we have $\alpha_0 = 0.1$.

- Rudin-Shapiro: first, we generate a sequence with four letters by means of the substitution rule $A \to AB$, $B \to AC$, $C \to DB$ and $D \to DC$. Then we set $A = B \to 0$ and $C = D \to 1$;
- Random: we first generate a sequence with the Rudin-Shapiro protocol until $t_{\max}$, then we shuffle it. This procedure is done to make a fair comparison between such sequences.

For further details on the Rudin-Shapiro (RS) sequences we point the reader to Refs. (BARBER, 2008; DAL NEGRO; BORISKINA, 2012). From such references, we see that aperiodic series have been used for a long time in Physics, but these sequences remain underemployed in Ecology. At this point we stress that we do not claim that RS sequences model a realistic system in Ecology. Rather, we show that the pure RS and the randomly rearranged RS sequences work as an insightful theoretical platform that enables to disentangle the distinction between linear and nonlinear correlation in extinction dynamics.

RESULTS AND DISCUSSION

In this section, we show our results obtained by solving the ODE in Eq. (3.1), where we employ the *solveivp* of python. Concretely, we apply the *RK45* routine that performs the Runge-Kutta method of order 5(4). Thus, the time evolution takes place with a 4-order accurate control of errors and 5-order accurate formula for steps. In such procedure, we set the time increment with maximum value $dt_{max} = 0.1$ and between each interval $[i, i+1[$ we keep the same $\alpha(i)$, where $i = 0, 1, 2, \ldots, t_{max}$.

Before delving into the analysis of the population dynamics per se, let us discuss the properties of $\alpha(t)$. In Fig. 3.1 we illustrate the setups for $\alpha(t)$ and in Fig. 3.2 we evaluate the architectural characteristics of the sequences we use for each protocol. Firstly, we compute the autocorrelation function (ACF) considering several lags. In Fig. 3.2 (a) we see that the overall behavior of the nonrandom RS array presents values for the ACF that resembles the ACF values for the random series, although with weak fluctuations.

Additionally, we quantify the Lempel-Ziv complexity (LZC) of the sequences we use. The LZC is is a nonlinear measure that provides information about the abundance of nonidentical patterns in an array when examined from t_0 to $t_{\max}$ (LEMPEL; ZIV, 1976; KASPAR; SCHUSTER, 1987). In this sense, the minimum and maximum values for the LZC are obtained for the periodic and random sequences, respectively. Although the Rudin-Shapiro chain has a lin-

ear correlation pattern comparable to random series [Fig.3.2(a)], its LZC presents considerable differences [Fig.3.2(b)]. In this work, the LZC is used as a measure of nonlinear correlations.

In Fig. 3.3, we observe how the bistability embedded in Eq. (3.1) is impacted by the presence or not of randomness in $\alpha(t)$. On the one hand, if the initial density P_o is high enough, the population survives regardless of the type of perturbation. On the other hand, if the initial density P_o is too low, the extinction takes place independently of the kind of perturbation. Between both cases, it is clear the ecological outcome depends on how the perturbation is temporally arranged. In such setting ($P_o = 0.2$) the time evolution leads to extinct state for the random protocol, whereas it leads to a survival state for the nonrandom protocol. If $\alpha(t)$ exhibits the same autocorrelation pattern and the same mean $\bar{\alpha}$, why do the random and nonrandom protocols lead to different outcomes? The answer in our controlled computational experiment relies on the nonlinear correlations incorporated in $\alpha(t)$, as shown in Fig. 3.2 (b). Thus, the dynamics of a species on the verge of extinction is strongly influenced by the nonlinear correlation of time-dependent perturbation. This is an important finding because at present there several species at risk of extinction (PIMM; RAVEN, 2000; IUCN, 2020).

In Fig. 3.4, we see the long-run scenarios arising from the random and nonrandom setups considering a fixed initial condition $P_o = 0.5$. Both time evolutions are marked by fluctuations that are driven by the switches between $\{\alpha_0, \alpha_1\}$. We emphasize that all the curves (blue or red) are obtained considering sequences that display null Pearson's correlation and have the same mean $\bar{\alpha}$. Despite that the nonrandom perturbation promotes a long-run survival of the population, however the presence of randomness compromise the population persistence. That is, the Rudin-Shapiro protocol for time-dependent perturbations in $\alpha(t)$ is less prone to induce a transition to an absorbing state. This adds new understanding of the field of nonequilibrium absorbing-state phase transitions (MARRO; DICKMAN, 2005; HENKEL et al., 2008; PIRES; OESTEREICH; CROKIDAKIS, 2018).

In Fig. 3.5, we see how the outcomes regarding fraction of extinction f_{ext} are affected by different values for the reproduction rate as well as the death rate α_1. We note an agreement between the long-run scenarios for some combinations of parameters meaning that in such cases the underlying birth-death dynamics is more important than the type of patterns in $\alpha(t)$. For other cases, we see a disagreement between f_{ext}, meaning that for such settings the temporal arrangement of the patterns in the perturbation $\alpha(t)$ plays an important role on the final ecological outcome. Thus, it is clear a competition between dynamics (reproduction and death) and structure of $\alpha(t)$.

Taking a broad view of the information conveyed in Figs. 3.1 - 3.5, we note that the random and nonrandom perturbations can lead to different scenarios depending on the balance between the birth-death dynamics and the disposition of the patterns in $\alpha(t)$. When the imbalance between structure and dynamics sets the arrangement of patterns as a relevant feature, we see that the ACF fails to provide an explanation for the fate of extinction in the random perturbation, whereas the LZC allows us to explain the distinct emergent phenomenon observed in the time evolution of the population. In such cases, the mass extinction events are triggered by cumulative effects arising from hidden patterns in $\alpha(t)$ that are detected by a quantifier of nonlinear correlations. Mathematically, this can be traced back to the fact that the time series can be embedded with nonlinear dependencies that are not recognized by a single measure (see e.g. Ref. (QUEIRÓS, 2009)).

While we could have employed an agent-based simulation (VINCENOT et al., 2011; GRIMM; RAILSBACK, 2005; PIRES; QUEIRÓS, 2019), in this work we have used a mean-field approach because we avoid the presence of multiple sources of randomness. With a single source of randomness we can make controlled computational experiments. Equation (3.1) – valid in the limit of infinitely large population size – enables us to understand how large populations respond to random and nonrandom perturbations. In relation to that, we note in Figs. 3.3 - 3.5 that uncorrelated sequences do not necessarily endanger the sustainability of a population, but non-trivial and

hidden patterns – produced by randomness – are the great villain of population survival in our controlled setup.

Previously, it was shown (OLIVEIRA; FIORE, 2016) that temporal randomly distributed disorder does not destroy the bistable nature of dynamics described by models similar to Eq. (3.1). Our results exhibited in Figures 3.3 and 3.5 expand such claim regarding the robustness of the bistability for the realm of nonrandom aperiodic disorder incorporated as a time-dependent perturbation.

FINAL REMARKS

The minimal and universal set of ingredients embedded in Eq. (3.1) puts us in a position to provide fundamental comprehension on how the notion of chance shapes the ecology of extinctions (BEISSINGER, 2000; EHRLICH; EHRLICH, 1981; SIMBERLOFF, 1993). Specifically, we show that a measure of nonlinear correlations, rather than the standard Pearson correlation coefficient, is able to properly explain the fate of extinction for Allee-like dynamics under linearly uncorrelated perturbations with random and nonrandom temporal arrangements. Thus, our work opens the door for the possibility of new bridges between the theory of nonlinear correlations and ecological dynamics.

As previously mentioned, the Allee effect has been considered as an important phenomenon in several fields including cancer research (KOROLEV; XAVIER; GORE, 2014; SEWALT et al., 2016; JOHNSON, K. E. et al., 2019; NEUFELD et al., 2017). For instance, in Ref. (KOROLEV; XAVIER; GORE, 2014) it was proposed that the presence of the Allee effect in the tumor growth dynamics may offer a window for therapeutics. In that sense, the results shown herein can provide insights into this kind of dynamics since they show *how* randomness becomes a threat for the long-run proliferation of organisms. Effects of diffusion were analyzed in the context of models similar to Eq. (3.1) with temporal disorder (SOLANO; OLIVEIRA; FIORE, 2016). Such temporal disorder was considered as a time-dependent diffusion rate D(t). The results suggest a strong effect of such time dependence on the phase diagrams of the CP.

It can be interesting to also consider diffusion in our model with a time-dependent rate D(t), and analyze the impact of such disorder in the extinction patterns.

From an experimental point of view, the few number of parameters in our proposal – basically related to reproduction and death – is an advantage in terms of the build-to-understand approach in Synthetic Biology (SMITH et al., 2014; DING; WU; TAN, 2014; WANG et al., 2016; PADILLA-VACA; ANAYA-VELÁZQUEZ; FRANCO, 2015). For instance, we mention that in such a field bacteria can be engineered to display the Allee effect (SMITH et al., 2014) as well other new behaviors (DING; WU; TAN, 2014; WANG et al., 2016; PADILLA-VACA; ANAYA-VELÁZQUEZ; FRANCO, 2015). In other words, our take-home message that nonlinear correlations jeopardizes population survival can be biologically programmed within the current technology.

We have adopted a widespread and practical measure of nonlinear correlations that is based on the number of unlike patterns (LEMPEL; ZIV, 1976; KASPAR; SCHUSTER, 1987). By using the paradigmatic Rudin-Shapiro sequence and its shuffled version we have disentangled how linear and nonlinear correlations impact extinction dynamics. In future works, it would be interesting to engineer new sequences for $\alpha(t)$ that capture nuances of complexity, per se (LLOYD, 2001).

Chapter 4

On the potential for a second peak in the evolution of SARS-CoV-2 in emerging and developing economies

In this chapter, we investigate the potential scenarios from a Susceptible-Infected-Recovered-Asymptomatic-Symptomatic-Dead (SIRASD) model. As a novelty we consider populations that differ in their degree of compliance with social distancing policies following economic attributes that are observed in emerging and developing countries. Considering epidemiological parameters estimated from data of the propagation of SARS-CoV-2 in Brazil – where there is a significant stake of the population making their living in the informal economy and thus prone to not follow self-isolation – we assert that if the confinement measures are lifted too soon, namely as much as one week of consecutive declining numbers of new cases, it is very likely the appearance of a second peak. Our approach should be valid for any country where the number of people involved in the informal economy is a large proportion of the total labor force.

This work is available in Ref.(PIRES; CROKIDAKIS; CAJUEIRO, et al., 2020).

INTRODUCTION

Table 4.1 – List of symbols used in this chapter. See Fig.4.1.

Symbol	Meaning
ϕ_u	Noncompliance degree of the group $u = \{1, 2\}$
p	Proportion of individuals who develop symptoms
q	Probability of an individual dying from infection
β_A	Transmissibility rate of the asymptomatic cases
β_I	Transmissibility rate of the symptomatic cases
g_A	Recovery rate of the asymptomatic cases
g_I	Recovery rate of the symptomatic cases

Despite existing some differences among the countries public health policies, the vast majority of them have tried to reduce the growth rate of the COVID-19 pandemic by implementing policies of social distancing (ADAM, 2020) aiming at preventing mayhem of the health-care systems, the so-called "flattening of the curve". A series of models have been brought forth to the specific study of the evolution of COVID-19 through the world. Initially, some of those works focused on its calibration in order to estimate typical parameters of the disease, like infection rates, epidemic doubling times among others (CROKIDAKIS, 2020b; LI et al., 2020; MUNIZ-RODRIGUEZ et al., 2020; LIU et al., 2020; ZHAO; LIN, et al., 2020; LAI et al., 2020; ZHOU; LIU, et al., 2020; PEDERSEN; MENEGHINI, 2020a; TSALLIS; TIRNAKLI, 2020; ROCHA FILHO et al., 2020; WEBER; IANELLI; GONCALVES, 2020). After these preliminary studies, many authors considered the effect of several types of non-pharmaceutical interventions (CROKIDAKIS, 2020a; BASTOS; CAJUEIRO, 2020; DE FALCO et al., 2020; PELLIS et al., 2020; MANCHEIN et al., 2020; MAIER; BROCKMANN, 2020; VASCONCELOS et al., 2020; FAGGIAN; URBANI; ZANOTTO, 2020; FERGUSON et al., 2020; KRAEMER et al., 2020; BIN et al., 2020; BISWAS; KHALEQUE; SEN, 2020; ARENAS et al.,

2020).

A study analyzed the impacts of mobility lockdown in Italy due to the fast spreading of COVID-19 (BONACCORSI et al., 2020) in which the authors identified two ways through which mobility restrictions affect the population. They verified that the impact of lockdown is stronger in municipalities with higher fiscal capacity, and also that mobility restrictions are stronger in municipalities for which inequality is higher and where individuals have lower income per capita, causing a segregation effect. In Ref. (BONACCORSI et al., 2020), the authors also discussed about the income distribution, that plays an important role: municipalities where inequality is greater have experienced a stronger increase in mobility and their citizens are more at risk. Finally, they concluded that the results suggest the necessity of asymmetric fiscal measures. In other words, according to that work, central governments should implement financial transfer mechanisms to people, companies and local government in the form of living allowances, no-interest loans and treasury transfers to compensate the loss of tax income to allow each case to cope with the current scenario. As also stated in Ref. (BONACCORSI et al., 2020), the absence of targeted lines of intervention during the lockdown would induce a further increase in poverty and inequality.

Another work deals with wealth distributions under the spread of infectious diseases (DIMARCO et al., 2020). Considering the coupling of a compartmental epidemic dynamics with a kinetic model of wealth exchange, the authors found that that the spread of the disease seriously affects the distribution of wealth. Indeed, the evolution of disease together with the dynamics of wealth exchange changes the wealth distributions from a bimodal form to a fat-tailed one (DIMARCO et al., 2020). Still talking about the economic implications of mobility restrictions, it was reported the decline of Gross Domestic Product in China (HUANG et al., 2020).

In this chapter, we discuss the effectiveness of social distance policies in developing and emerging countries where the share of informal employment is very high. Although it is not always true that there is a relationship between informal employment and poverty,

we may find a clear positive relationship among them. It is worth mentioning that in developing and emerging countries the share of informal employment in total employment ranges from 50% to more than 98%(ORGANIZATION, 2018). In this context, we investigate emerging scenarios for a generalized SIR-like model taking into account a heterogeneous propensity of individuals to comply with the self-isolation policies.

MODEL

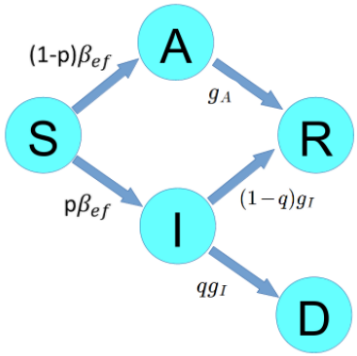

Figure 4.1 – Susceptible - Infected - Recovered - Asymptomatic - Symptomatic - Dead (SIRASD) compartmental model.

We divide the population into two types of individuals:

- Type 1: the group that has the option of self-isolation. This group represents a fraction f_1 of the full population.
- Type 2: low income workers in the gig economy and informal sectors. This group represents a fraction $f_2 = 1 - f_1$ of the full population.

Let ϕ_u be the noncompliance degree of the group $u (u = \{1,2\})$ concerning governmental containment policies. Thus $1 - \phi_u$ is the degree of engagement with self-isolation advice.

For the COVID-19 there are both asymptomatic and symp-

tomatic cases. Thereby we consider a framework close to Ref. (BASTOS; CAJUEIRO, 2020) (and references therein), ie, we use a SIR-ASD (Susceptible-Infected-Recovered-Asymptomatic-Symptomatic-Dead) model where here extend it for the inclusion of two groups.

To explain in detail our model consider two individuals $\{i, j\}$ belonging to the groups $\{u, z\}$, respectively. Then

- If i is in the state S and if j is infected in the state $X = \{A \text{ or } I\}$ then a transmission event occurs in which i enters in the state I with rate $p\phi_z\phi_u\beta_X$ or enters in the state A with rate $(1-p)\phi_z\phi_u\beta_X$, where p is the proportion of individuals who develop symptoms.
- If i is in the state A then it enters in the state R with rate g_A.
- If i is in the state I then it enters in the state D with rate qg_I, otherwise it enters in the state R with rate $(1-q)g_I$. In such case, q is the probability of an individual in the class I dying from infection before recovering.

  It is important to stress that $D(t)$ informs how many individuals who tested positive for COVID-19 were declared dead at date t.

An illustration of the transition between the compartments is shown in Fig.4.1. From the above-stated rules the set of coupled ODEs that govern the system considering the mean-field assumption. Explicitly, we arrive at:

$$\frac{dS_u}{dt} = -\frac{S_u}{N}\sum_{z=1}^{2}\phi_u\phi_z(\beta_I I_z + \beta_A A_z), \tag{4.1}$$

$$\frac{dA_u}{dt} = \frac{S_u}{N}(1-p)\sum_{z=1}^{2}\phi_u\phi_z(\beta_I I_z + \beta_A A_z) - g_A A_u, \tag{4.2}$$

$$\frac{dI_u}{dt} = \frac{S_u}{N}p\sum_{z=1}^{2}\phi_u\phi_z(\beta_I I_z + \beta_A A_z) - g_I I_u, \tag{4.3}$$

$$\frac{dR_u}{dt} = (1-q)g_I I_u + g_A A_u, \tag{4.4}$$

$$\frac{dD_u}{dt} = q g_I I_u, \tag{4.5}$$

where $N = \sum_{u=1}^{2}(S_u + A_u + I_u + R_u)$. From the aforementioned equations we define the effective transmission rate,

$$\beta_{ef}^{u} = \sum_{z=1}^{2} \phi_u \phi_z (\beta_I \frac{I_z}{N} + \beta_A \frac{A_z}{N}) \ , \tag{4.6}$$

where the terms $\phi_u \phi_z$ show that the interaction can involve individuals within the same group (intragroup interaction: $\phi_1\phi_1$, $\phi_2\phi_2$) or between different groups (intergroup interaction: $\phi_1\phi_2$, $\phi_2\phi_1$).

We intend to model scenarios that arise, as above-mentioned, in emerging and developing economies, where the number of individuals in the informal economy is a large stake of the total labor force. In order to provide convincing numerical arguments, our model uses epidemiological parameters that come directly or indirectly from Ref. (BASTOS; CAJUEIRO, 2020), that were estimated from the COVID-19 pandemics that has taken place in Brazil: $\beta_A = 0.458$, $\beta_I = 0.455$, $g_A = 0.144$, $p = 0.624$, $q = 0.029$, $g_I = 0.149$ and $\phi_u = 0.799$. For further comments on q, g_I and ϕ_u see our supplementary material. Here we consider $N = 210147125$ as the total population (similar to Brazil). We consider an initial condition as $I_1(t_0) = 1$ and $A_1(t_0) = 0.5$ for the group 1. For the group 2 we set $I_2(t_0) = A_2(t_0) = 0$.

RESULTS

In this section we present the results solving our coupled ODEs using the *solveivp* of python. Specifically, we use the *RK45* method that implements an explicit Runge-Kutta method of order 5(4). Such procedure manages the error considering an accuracy of the 4-order and it employs a 5-order accurate formula to take the steps.

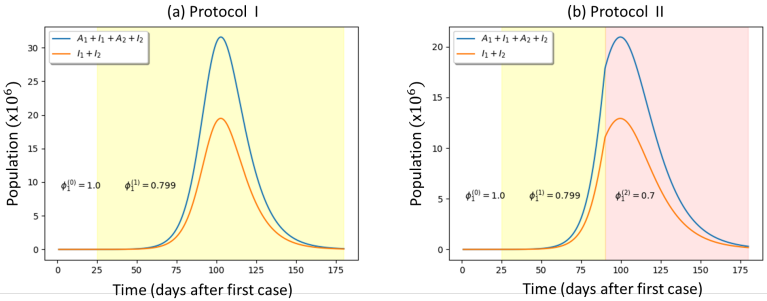

Figure 4.2 – Time series for the number of individuals in the class $\sum_i I_i$ as well as $\sum_i (A_i + I_i)$ considering: (a) protocol I (b) protocol II. In the protocol II we apply $\phi = 0.799 \rightarrow \phi = 0.7$ on day $t^{(2)}_{policy} = 90$ after the first case (red shaded region).

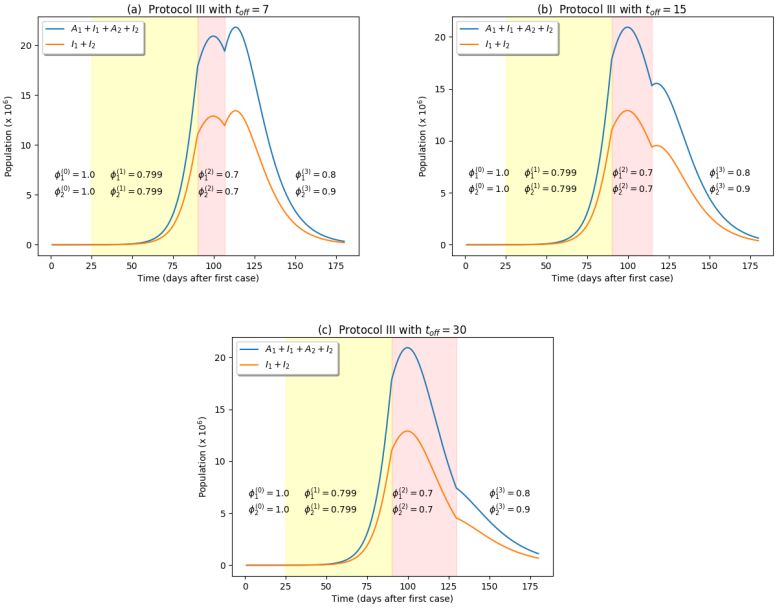

Figure 4.3 – Time series for the number of individuals in the class $\sum_i I_i$ as well as $\sum_i (A_i + I_i)$ considering: (a) $t_{OFF} = 7$, (b) $t_{OFF} = 15$ and (c) $t_{OFF} = 30$. The first white, yellow and red shaded areas are explained in the previous Figure. The last white region represents the case with soft self-isolation rules.

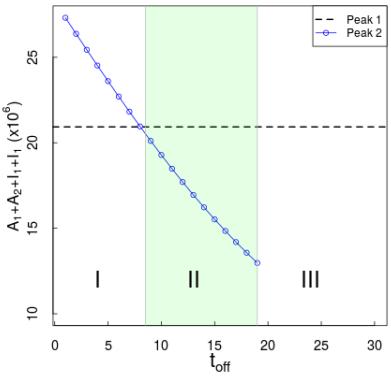

Figure 4.4 – Dependence of the peak size of $\sum_i (A_i + I_i)$ with t_{OFF}. Parameters: $t_{max} = 365$, $f_1 = 0.6$, $\phi_1^{(2)} = \phi_2^{(2)} = 0.7$, $\phi_1^{(3)} = 0.8$ and $\phi_2^{(3)} = 0.9$. Regime I: the second peak is larger than the first one. Regime II: the secondary peak is smaller than the first one. Regime III: absence of a second peak. Each of these regimes is illustrated in Fig. 4.3.

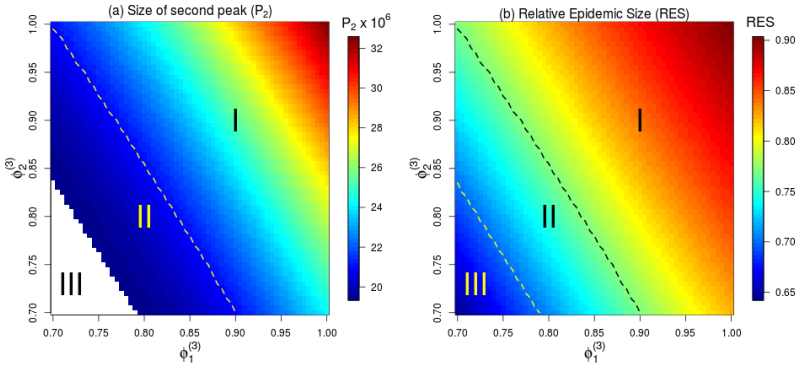

Figure 4.5 – Diagrams $\phi_1^{(3)}$ vs $\phi_2^{(3)}$ for: (a) P_2 and (b) RES. Results obtained for $t_{max} = 365$ days, $t_{OFF} = 7$, $f_1 = 0.6$ and $f_2 = 0.4$. The regimes I,II and III are explained in the Fig.4.4. P_2 is computed considering both symptomatic and asymptomatic individuals, ie $A_1 + A_2 + I_1 + I_2$.

It is important to mention that second waves of infections can be observed measuring distinct quantities, like the new daily cases or the number of active cases in a given day (LEUNG et al., 2020; CASTRO, 2020; PEDRO et al., 2020; FARANDA; ALBERTI, 2020; VAID et al., 2020; XU; LI, 2020; NETO et al., 2020; SINGH; MOHAPATRA, 2020; MENON et al., 2020; GHANBARI, 2020). In this work, we choose to exhibit the number of active cases in a given day.

Apart from the number of individuals in each class, there is a second quantity of interest, namely the Relative Epidemic Size (RES) that is computed from t_0 to t

$$RES = \sum_{z=1}^{2} \frac{S_z(t_0) - S_z(t)}{N} \ . \tag{4.7}$$

In order to better grasp our full protocol lets first consider the case with $f_1 = 1$. Let u be the index of group u. We consider $\phi_u = \phi_u^{(0)} = 1$ during the initial stage of the epidemic spreading because the level of self-isolation is almost null. We shall assume $\phi_u^{(0)} \to \phi_u^{(1)} = 0.799$ on day $t_{policy}^{(1)} = 25$ after the beginning of the epidemic spreading. With this procedure (we call it protocol I) we obtain the time series shown in Fig.4.2(a) that recover the results presented in Ref. (BASTOS; CAJUEIRO, 2020) considering the scenarios with the current confinement rules imposed by the government for an indefinite time. Taking into consideration that the value of the total population is 210 million people, the peaks in the panels are between 9% and 14% for Infected+Asymptomatic cases and circa 5% for the Infected cases alone. In spite of the subnotification issues that have been reported (VOLPATTO et al., 2020; PAIXÃO et al., 2020; CORONAVIRUS BRAZIL, 2020), these figures are compatible with the fraction of infected people computed in other countries close to 10% as well (FLAXMAN et al., 2020).

Consider the protocol II shown in Fig.4.2(b). During the explosive growth of the epidemic, the isolation policy is improved by better surveillance. Explicitly, we decrease the noncompliance degree from $\phi_u^{(1)} = 0.799$ to $\phi_u = \phi_u^{(2)}$ on day $t_{policy}^{(2)} = 90$ after the first case

at day t_0. Henceforth we set $\phi_u^{(2)} = 0.7$, but the nature of our results does not change qualitatively for other values, as discussed in the supplementary material. In Fig. 4.2(b), we see that such strengthening of the confinement restrictions leads to a substantial decrease in the number of symptomatic and asymptomatic individuals.

The self-isolation measures are permanent in the protocols I and II. However, after the epidemic growing phase, there might be political and economic pressure to ease strict confinement rules. In that sense, lets us move to the protocol III with temporary self-isolation guidelines. Explicitly,

- After each time step (day) we monitor $\delta I(t) = \sum_z (I_z(t) - I_z(t-1))$.
- At t_0 we set $t_{decrease} = 0$. For each $dI(t) < 0$ we increase $t_{decrease}$ in one unit.
- If $t_{decrease} = t_{OFF}$ we set $\phi_u = \phi_u^{(3)}$. That is if $dI(t) < 0$ during t_{OFF} consecutive days, the social distancing rules are relaxed.

As one can see in the above items, the method we consider is applicable after the number of active cases has reached a peak. Figure 4.3 exhibits the time series for the number of individuals infected considering $f_1 = 0.6$ and $f_2 = 0.4$. We have made this choice due to a recent poll in Brazil made by the Brazilian Institute of Geography and Statistics (IBGE), that stated 39.9% of the population works in the informal economy (BRAZILIAN INSTITUTE OF GEOGRAPHY AND STATISTICS - IBGE, 2020), which leads to $f_2 = 0.4$. However, we considered other values of f_1 and f_2 in the supplementary material. The self-isolation measures are lifted t_{OFF} days after the peak. At that moment, the degree of noncompliance is increased to $\phi_1^{(3)} = 0.8$ and $\phi_2^{(3)} = 0.9$ (last white regions in Fig. 4.3). If the interruption of the confinement rules takes place one week after the peak, $t_{OFF} = 7$, we see that the second outbreak is larger than the first one. This scenario is different for $t_{OFF} = 15$, where the secondary peak is smaller than the first one. If $t_{OFF} = 30$ days, then there is no rising of the secondary peak even though there is a rise in the person-to-person contagion.

Figure 4.4 shows how the time for interruption of the confinement rules impacts the epidemic spreading behavior. The peak size is computed taking into account both symptomatic and asymptomatic individuals $A_1 + A_2 + I_1 + I_2$. Specifically, there are three main outcomes. Easing the mobility restrictions too soon triggers an abrupt rise of the new cases that leads to a pronounced second peak that is worse than the first one. This is the regime I. In regime II, the secondary chain of contagion also leads to a new noticeable outbreak but now with magnitude smaller than the first one. In regime III, there is no second local maximum. Then, we highlight that there are two thresholds: (i) for prevention of a second large-scale epidemic outbreak; (ii) for prevention of a second small-scale outbreak.

Figure 4.5 disentangles the role played by the degree of non-compliance $\phi_u^{(3)}$ of each group u. When the confinement guidelines are lifted too early ($t_{OFF} = 7$) the majority of the combinations of $\phi_1^{(3)}$ vs $\phi_2^{(3)}$ leads to the regime I where the second outbreak is more aggressive than the first one. In this setting, the relative epidemic size (RES) can achieve about 90% of the population in the long-run (1 year in such figure). For combinations of moderated values of $\phi_1^{(3)}$ vs $\phi_2^{(3)}$, there is a substantial region in regime II where RES is mostly between 70%-80% of the population. The non-negligible presence of the regime III indicates that the prevention of a secondary epidemic outbreak can be achieved if the engagement of the population with the stay-at-home guidelines does not decrease too much.

Let us now turn our attention to the main results depicted in Figs.4.6-4.7 for $f_1 = \{0.6, ..., 1\}$ and $t_{OFF} = \{7, 15, 30\}$. In panels (a-c) each barplot or boxplot is obtained considering grids with $61x61$ combinations of $\phi_1^{(3)} \times \phi_2^{(3)} \in [\phi_1^{(2)}, 1] \times [\phi_2^{(2)}, 1]$ where $\phi_1^{(2)} = \phi_2^{(2)} = 0.7$. Thus, all the panels (a-c) totalize $3 * 5 * 61 * 61 = 55815$ different projections. The panels (d-f) show the results for the those combinations satisfying $\phi_2^{(3)} \geq \phi_1^{(3)}$. In the boxplot the gray shaded box goes from the first quartile to the third quartile and the horizontal line inside the box is the median.

Figure 4.6 shows the barplots for the proportion of each

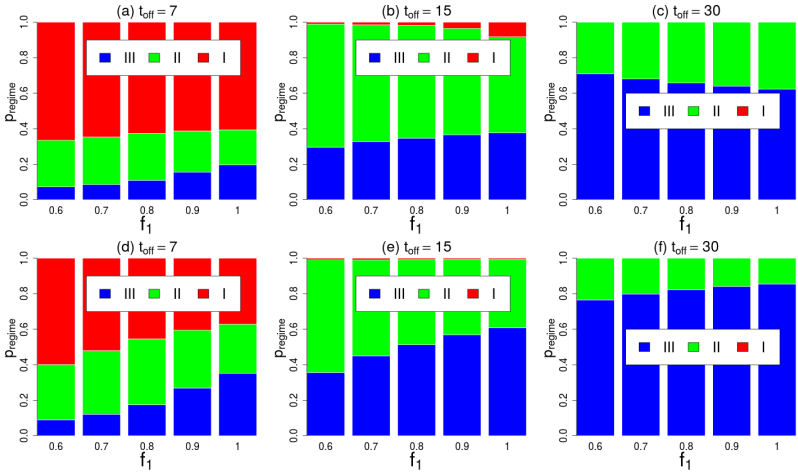

Figure 4.6 – Barplot with the proportion of each regime p_{regime} in diagrams similar to the shown in Fig.4.5. (Top) All $61x61$ combinations of $\phi_1^{(3)} \times \phi_2^{(3)} \in [0.7, 1] \times [0.7, 1]$. (Bottom) Combinations satisfying $\phi_2^{(3)} \geq \phi_1^{(3)}$. Regime I: the second peak is larger than the first one. Regime II: the secondary peak is smaller than the first one. Regime III: absence of a second peak. Outcomes for: (a,d) $t_{OFF} = 7$, (b,e) $t_{OFF} = 15$ and (c,f) $t_{OFF} = 30$.

regime p_{regime} for several f_1 and t_{OFF}. In the setting with $t_{OFF} = 7$ and $f_1 = 0.6$, the overwhelming majority of configurations lead to the establishment of the regime I, as previously observed. But, this advantage of the regime I decrease as f_2 decreases (by increasing f_1). In the setting with $t_{OFF} = 15$ all the scenarios exhibit a smaller proportion for the regime I in comparison with corresponding scenarios for $t_{OFF} = 7$. However, there is a dual effect of rising f_1. On the one hand, it increases the proportion of configurations associated with the regime III. On the other hand, it also increases the possibilities for the emergence of regime I. In the setting with $t_{OFF} = 30$ we also see a double-edged sword: (a) the percentage of regime I is null and all the percentage of the regime III is higher than the corresponding to the cases $t_{OFF} = \{7, 15\}$; (b) an increase of f_1 increases the relative advantage of regime II. These nonmono-

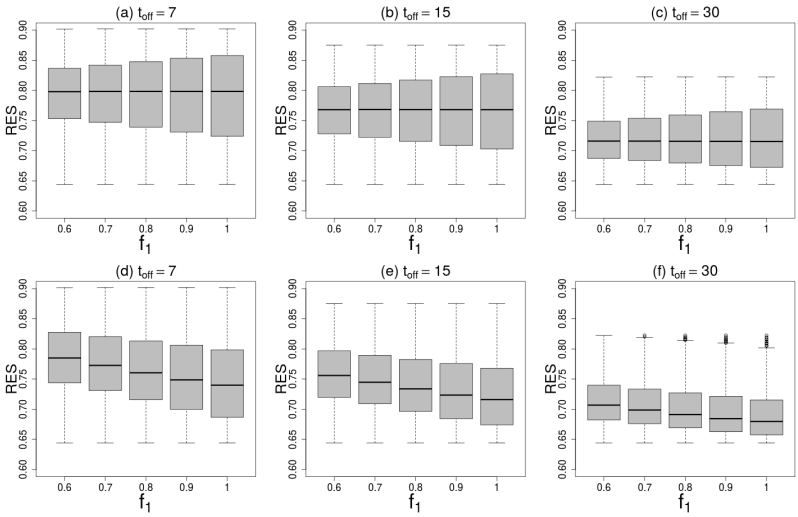

Figure 4.7 – Boxplot with the range of values exhibited by RES in diagrams similar to the shown in Fig.4.5. (Top) All $61x61$ combinations of $\phi_1^{(3)} \times \phi_2^{(3)} \in [0.7, 1] \times [0.7, 1]$. (Bottom) Combinations satisfying $\phi_2^{(3)} \geq \phi_1^{(3)}$. Results for: (a,d) $t_{OFF} = 7$, (b,e) $t_{OFF} = 15$ and (c,f) $t_{OFF} = 30$.

tonic effects arise because some combinations $\phi_1^{(3)} \times \phi_2^{(3)}$ favor the regime I and other combinations favor the regime III as depicted in Figure 4.5. Such mechanism is corroborated with the panels (d-f) where we see that the combinations satisfying $\phi_2^{(3)} \geq \phi_1^{(3)}$ leads to a monotonic behavior of p_{regime} vs f_1 for all $t_{OFF} = \{7, 15, 30\}$.

Figure 4.7 shows the boxplots for RES considering decreasing values of $f_2 = 1 - f_1$ as well for increasing values of t_{OFF}. Such results show that an increment in t_{OFF} leads to an overall decrease in the relative epidemic size (RES). But a detailed analysis in each panel shows that an increase in f_1 produces an increase in the interquartile range of values for RES (gray area). This indicates the presence of a twofold effect since RES can achieve smaller values as f_1 increases, but it also leads to the possibility for RES reaching higher values. Again such twofold effect arises because some combinations $\phi_1^{(3)} \times \phi_2^{(3)}$ are responsive for an increase in RES and other

combinations promote a decrease in RES as unveiled in Figure 4.5. This is confirmed with the panels (d-f) where the combinations satisfying $\phi_2^{(3)} \geq \phi_1^{(3)}$ leads to a decrease in RES as f_1 increases for all $t_{OFF} = \{7, 15, 30\}$.

DISCUSSION

The findings in Figs. 4.6-4.7 are our main results. Such figures show that, for our parameters, it is very likely the emergence of a second peak (regimes I+II) if the preventive measures are lifted too soon. Even more alarming, there is a non-negligible risk for the magnitude of such second peak be higher than the first one (regime I). Apart from this, we note that for a given t_{OFF} there is the possibility for a twofold effect in which an intervention designed to hamper the epidemic spreading can backfire. However, in such a situation the establishment of positive or negative outcomes depends on the combinations of $\phi_1^{(3)}$ vs $\phi_2^{(3)}$ as indicated in Fig.4.5. Such findings highlight that it is significant to have a substantial alignment between different interventions designed to decrease the degree of non-compliance as well as to support the fraction of the population that cannot afford for the self-isolation even after the first peak of spreading. Moreover, complementary studies using different parameters we could verify that the present model is also capable of reproducing different situations of separated peaks as found in several U.S.A. cities during the Spanish flu pandemics(BOOTSMA; FERGUSON, 2007; HATCHETT; MECHER; LIPSITCH, 2007). Therein, it is possible to assess the impact of different public health measures in the number and evolution of fatalities, with some cities basically exhibiting a single peak (an indicator of proper policies) and other cities with significant second peaks. Importantly, some of the cities showing two peaks were cities that have not had good governance and provided adequate responses to the COVID-19 pandemics. In other words, although we have adjusted our model to the present COVID-19 case, our model is likely to be relevant, in theoretical viewpoint, in the analysis of other situations, namely the computational forward testing of public health policies.

Other correlated works considering COVID-19 spreading have also shown the possibility of a second epidemic peak. In Ref. (ROGERS, 2020), it is shown – with variants of the SIR model – the potential of the second peak of infections for the UK. In Ref. (HOERTEL et al., 2020), the authors calibrated a stochastic agent-based model from data in France and they projected that it would be unlikely to prevent the second chain of contagions once quarantine is lifted. A second chain of spreading was also predicted – using a generalization of the SIR model – as a potential outcome for Italy after the relaxation of the mobility restrictions (PEDERSEN; MENEGHINI, 2020b). A recent work considering the case of Brazil in a group-free Susceptible-Exposed-Infected-Recovered-Dead model presented some time series suggesting that the social isolation must hold until the end of 2020 in order to diminish the chance of the second peak (CINTRA; NUNES, 2020). Effectively, the conclusion of all those works is that the safer situation is to hold the isolation for as long as possible in order to decrease the magnitude of the second peak. For further discussion see our supplementary material.

LIMITATIONS

We consider that as the epidemic starts to climb sharply there will be an increased pressure to decrease the degree of non-compliance (red shaded region in Fig.4.3). At this point we still assumed the same level of compliance of both groups because of the current implementation of income transfer for the group 2 (BRAZILIAN FEDERAL GOVERNMENT, 2020). After the first peak and as soon as the stay-at-home restrictions are suspended we set different levels of compliance with the post-quarantine stage for each group (last white region in Fig.4.3).

Besides, our work does not consider explicitly an upper bound for the capacity of the healthcare system. Underreporting is another feature that is not modeled here and we have not considered the clear regional heterogeneity in Brazil as well. In addition, we considered a mean-field-like approach, where each individual can interact will all others. In this case, spatial features were not consid-

ered in the model.

Although our work presents limitations in several dimensions, the qualitative results of our work do not seem to change for several variations of the parameters of our model as we have checked with extensive simulations with deterministic and Monte Carlo simulations.

FINAL REMARKS

Our work has investigated the evolution of COVID-19 pandemics in emerging and developing economies where the informal economy represents a large fraction of the total economy. Although we have used parameters estimated for the Brazilian case to analyze the effectiveness of social distancing policies and to estimate the likelihood of arising a second peak, our results are qualitatively the same for all economies that show these characteristics. We apply a SIRASD model considering a population split into two groups with different behaviors, namely a group that belongs to a class that is able to self-isolate and a group that is formed by low-income workers in the gig economy or informal sectors. While the first group usually belongs to the higher income class or is able to work at home, the second group is usually in a low-income class and supplies services to consumers and businesses, and is not able to provide their services in home office. In this context, the results show that the existence of these two types of social behaviors strongly affects the dynamics and possibility of a second peak in the evolution of COVID-19. Based on these results, it is possible to understand that in order to master the evolution of the disease, low-income people — who largely make their living on informality — must adhere to self-isolation as pointed by public health authorities worldwide. In order to solve the dilemma choosing between i) going out to get few earnings and risk being infected or ii) stay home and face starvation in favor of the latter, the present results signal it is pivotal the design of income transfer policies that pay for these people to stay at home at least 30 days after of the first peak.

Chapter 5

Coupled opinion and epidemic dynamics with vaccination in modular networks

In this chapter, we study an epidemic spreading under a vaccination campaign in community-based populations with individuals in favor and against the vaccine. Our results show that such coupled dynamics exhibit a myriad of phenomena such as nonequilibrium transitions accompanied by bistability. Besides we observe the emergence of an optimal modularity where the community structure can favor the negative opinions about vaccination but counterintuitively hinders - rather than enhance - the global disease spreading. Thus, our results point out that vaccination campaigns should avoid policies that end up segregating excessively anti-vaccine groups. This work is available in Ref.(PIRES; OESTEREICH; CROKIDAKIS; QUEIRÓS, 2021).

INTRODUCTION

Table 5.1 – List of symbols used in this chapter. See Fig.4.1.

Symbol	Meaning
λ	Transmissibility rate
g_i	Vaccination rate of agent i
ϕ	Resusceptibility rate
α	Recovery rate
μ	Community interconnectivity

One of the greatest expectations of today is precisely the new vaccine to contain the spread of SARS-CoV-2. While vaccination has been started in some countries for specific groups, there is also growing concerns about the presence of groups opposed to vaccines. Indeed, it is possible to find several anti-vaccine movement around the world (JOHNSON, Neil F et al., 2020), despite the success of the mass vaccination (KEELING et al., 2013). In population terms, if a large proportion of citizens choose not to be vaccinated, the consequences can be disastrous, as happened in Rio de Janeiro in 1904 with the vaccine revolt (NEEDELL, 1987) and more recently in France in 2010 where the French government required 90 million doses of the H1N1 vaccine, but only about 6 million people decided to get vaccinated (GALAM, 2010).

The interplay between the spreading of opinion — particularly the diffusion of 'anti-vaxxers' ideas — and the dissemination of a contagious disease is a natural focus of attention for policymakers. Since the online discussions dominate the social interactions in our modern world, the propagation of such anti-vaccine opinions is growing fast. The authors in (JOHNSON, Neil F et al., 2020) recently pointed that if the current trends continue, anti-vaccine views will dominate online discussion in 10 years. The importance of anti-vaccine movement is fundamental for the evolution of COVID-19 outbreaks. Indeed, the authors in (BUONOMO, 2020) called attention to the fact that it is a key point to qualitatively assess how the administration of a vaccine could affect the COVID-19 outbreak, taking into account of the behavioral changes of individuals in response to the information available on the status of the disease in the community. According to a study published in August 2020, nearly

one in four adults would not get a vaccine for COVID-19 (BOYON; SILVERSTEIN, 2020) and in some countries, more than half of the population would not get it, including Poland and France (CURIEL; RAMÍREZ, 2020). In September 2020, it was verified that only 42 percent of Americans said *yes* to receiving a future COVID-19 vaccine, across all political sides. It means that even in a best-case scenario where a future high performing vaccine is 95% effective in an individual, it would only impact 42x95$\approx$ 40% of the population, which is way below predicted thresholds for herd immunity (JOHNSON, N F et al., 2020).

Complex networks are natural tools to study processes that take place in society. The impact of network modularity in general spreading processes have been investigated in recent years. Since the work of Ref. (NEMATZADEH; FERRARA, et al., 2014), a series of works were published regarding the subject of optimal network modularity; therein, the authors showed that modular structure may have counterintuitive effects on information diffusion. Indeed, it was discussed that the presence of strong communities in modular networks can facilitate global diffusion by enhancing local, intracommunity spreading.

Still in relation to modular networks, it was recently found that an optimal community structure that maximizes spreading dynamics which can pave the way to rich phase diagrams with exhibiting first-order phase transitions (SU; WANG, et al., 2018). Within the same context, the authors in (WU et al., 2016) discussed about the impact social reinforcement in information diffusion. They also found optimal multi-community network modularity for information diffusion, i.e., depending on the range of the parameters the multi-community structure can facilitate information diffusion instead of hindering it.

The authors in (CUI et al., 2018) studied the importance of close and ordinary social contacts in promoting large-scale contagion and found an optimal fraction of ordinary contacts for outbreak at a global scale. With respect to correlations in complex networks, it was found that constraining the mean degree and the fraction of

initially informed nodes, the optimal structure can be assortative (modular), core-periphery, or even disassortative (CURATO; LILLO, 2016). Other recent works leading with optimal modularity in networks can be found in (NEMATZADEH; RODRIGUEZ, et al., 2018; PENG et al., 2020).

In a recent work (VALDEZ; BRAUNSTEIN; HAVLIN, 2020), it was proposed a model of disease spreading in a structural modular complex network and studied how the number of bridge nodes n that connect communities affects disease spread. It was verified that near the critical point as n increases, the disease reaches most of the communities, but each community has only a small fraction of recovered nodes.

Disease information can spark strong emotions like fear — or even panic — that would affect behaviour during an epidemic. The authors in (BI et al., 2019) considered an agent-based model that assumes that agents can obtain a complete picture of the epidemic via information from local daily contacts or global news coverage. Those results helped conclude that such model can be used to mimic real-world epidemic situations and explain disease transmission, behavior changes, and distribution of prevalence panic. Game theory was also considered to reproduce the decision-making process of individuals during the evolution of a disease. In (ZHAO; KUANG, et al., 2018) a spatial evolutionary game was coupled to a SIR model, and the results showed that protective behaviors decrease the numbers of infected individuals and delay the peak time of infection. The study also concluded that increased numbers of risk-averse individuals and preemptive actions can more effectively mitigate disease transmission; however, changes in human behavior require a high social cost (such as avoidance of crowded places leading to absences in schools, workplaces, or other public places).

Recently, the anti-vaccine sentiment was treated as a cultural pathogen. The authors in (MEHTA; ROSENBERG, 2020) modeled it as a 'infection' dynamics. The authors showed that interventions to increase vaccination can potentially target any of three types of transitions - decreasing sentiment transmission to unde-

cided individuals, increasing pro-vaccine decisions among undecided individuals, or increasing sentiment switching among anti-vaccine individuals.

Models of opinion dynamics were applied in the context of opinions about vaccination (pro versus anti-vaccine) without coupling an epidemic process (GALAM, 2010). Later, kinetic opinion dynamics were coupled to classical epidemic models in order to study the feedback among risk perception, opinions about vaccination, and the disease spreading. In (PIRES; CROKIDAKIS, 2017) it was found that the engagement of the pro-vaccine individuals can be crucial for stopping the epidemic spreading. On the other hand, the work (PIRES; OESTEREICH; CROKIDAKIS, 2018) found counterintuitive outcomes like the fact that an increment in the initial fraction of the population that is pro-vaccine can lead to smaller epidemic outbreaks in the short term, but it also contributes to the survival of the chain of infections in the long term.

Coupled behavior-change and infection in a structured population characterized by homophily and outgroup aversion (SMALDINO; JONES, 2020). It was found that homophily can either increase or decrease the final size of the epidemic depending on its relative strength in the two groups. In addition, homophily and outgroup aversion can also produce a 'second wave' in the first group that follows the peak of the epidemic in the second group.

MODEL

Opinion dynamics

Based on (PIRES; OESTEREICH; CROKIDAKIS, 2018) (and the original model (LALLOUACHE et al., 2010)), we consider an agent-based dynamics in which the opinion about vaccination, $o_i \in [-1,1]$, of each agent, i, evolves with

$$o_i(t+1) = o_i(t) + \epsilon o_j(t) + w I_{neig(i)}(t) \tag{5.1}$$

A negative (positive) values of o_i represents an individual i supporting anti-vaccine (pro-vaccine) opinion. Eq. (5.1) takes into account

that the agent's opinion $o_i(t+1)$ depends on multiples factors: (i) his previous opinion $o_i(t)$; (ii) a peer pressure exerted by a randomly selected neighbor j, modulated by a heterogeneity ϵ which is randomly distributed; (iii) the proportion of infected neighbors $I_{neig(i)}(t)$ modulated by a risk perception parameter w.

The opinion dynamics regarding the vaccination campaign is coupled with the epidemic dynamics, due to the factor $I_{neig(i)}(t)$ in Eq. (5.1). The microscopic details of the disease dynamics and the evolution of the epidemic compartments will be discussed in the next subsection. In Fig.5.1 we present an overview of our model.

Epidemics-vaccination dynamics

Based on (PIRES; CROKIDAKIS, 2017; PIRES; OESTEREICH; CROKIDAKIS, 2018) (and references therein), we define the transitions among the epidemic compartments as follows:

- $S \xrightarrow{g_i} R$: a Susceptible agent i becomes Vaccinated with probability g_i;
- $S \xrightarrow{(1-g_i)\lambda} I$: a Susceptible agent i becomes Infected with probability $(1-g_i)\lambda$ if he is in contact with an Infected agent;
- $I \xrightarrow{\alpha} S$: an Infected agent i recovers and becomes susceptible again with probability α;
- $R \xrightarrow{\phi} S$: a immune agent i becomes Susceptible again with the resusceptibility probability ϕ. Based on (ZENG; CHEN, 2005; RAO; MANDAL; KANG, 2019; MONEIM; GREENHALGH, 2005; LAHROUZ et al., 2012; DOUTOR et al., 2016) we assume that Vaccinated and Recovered agents are in the same compartment.

The vaccination probability g_i of an agent i is proportional to his opinion about vaccination $-1 \leq o_i \leq 1$:

$$g_i(t) = \frac{1+o_i(t)}{2} \in [0,1] \tag{5.2}$$

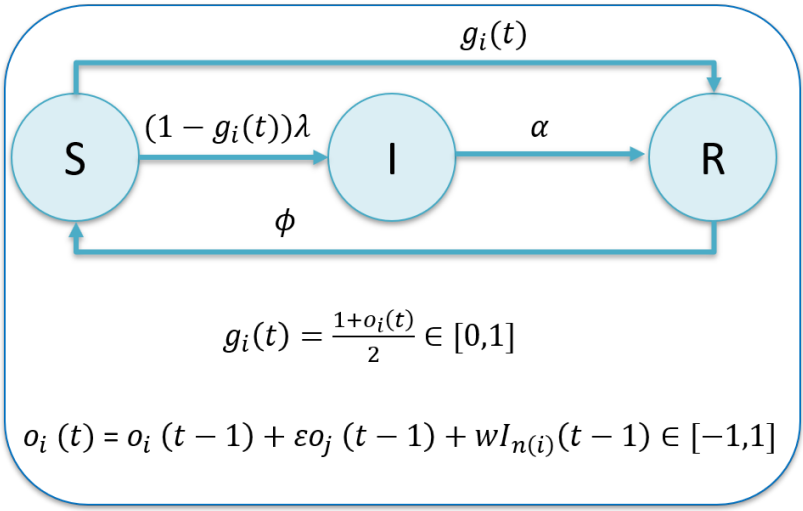

Figure 5.1 – Sketch of our coupled model with epidemic and opinion dynamics about vaccination.

Community structure

Based on (OESTEREICH; PIRES; CROKIDAKIS, 2019) and related literature, we start by picking the first $N_1 = N/2$ of the N nodes and attaching them to community 1, and assigning the other $N_2 = N - N_1$ nodes to community 2. We then proceed to randomly assigning $(1-\mu)M$ connections randomly among pairs of nodes from the same community and μM connections are randomly distributed among pairs of nodes that belong to distinct community.

The parameter μ regulates the community strength: large values of μ means more ties between the two communities consequently a weaker community organization. See Fig.1 5.2.

Initial condition

We consider that the community 1 holds a positive view about vaccination, whereas the community 2 holds a negative opinion about the vaccine. We also assume that the chain of infections starts in the community 2 because this case is more important since

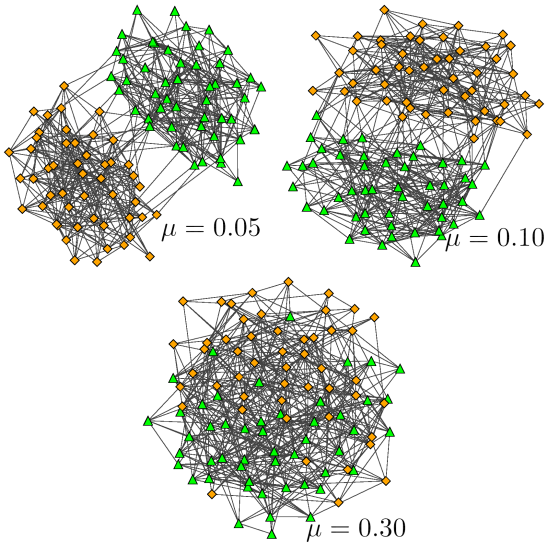

Figure 5.2 – Examples of modular networks with $N = 100$, $\langle k \rangle = 10$ for different values of μ. In these examples we can see the strengthening of the community structure for lower values of μ.

$o_i < 0$ leads to a low propensity for the agents to get vaccinated. If the epidemic would start in the community 1, the positive opinions $o_i > 0$ would induce a relatively high probability for an agent to get vaccinated which ends up disrupting the chain of contagions.

Let $U(a,b)$ be a single random value from a uniform distribution in the range $[a,b]$.

At $t = 0$ we set:

- For i in $0 \ldots N/2-1$: (community 1: $o_i > 0$; 0% infected)
  - $o_i \sim U(0,1)$
  - status(i) = S
- For i in $N/2 \ldots N-1$: (community 2: $o_i < 0$; 1% of infected)
  - $o_i \sim U(-1,0)$
  - status(i) = S with probability 0.99

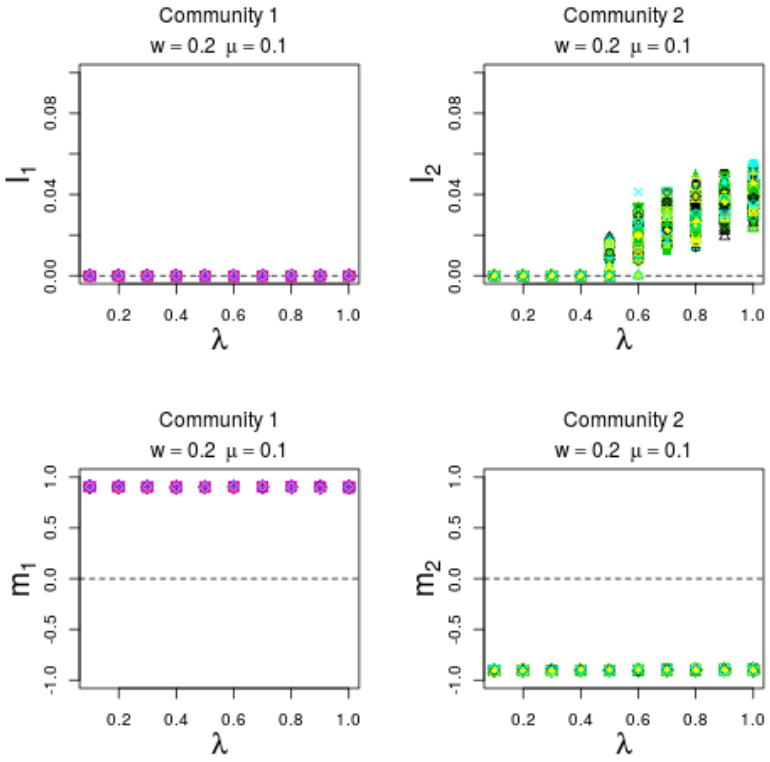

Figure 5.3 – Steady-state for the spreading measure I_i and collective opinion m_i for each community $i = \{1, 2\}$. Symbols are the steady-state outcome for each sample. Results for $\mu = 0.1$.

– status(i) = I with probability 0.01

RESULTS AND DISCUSSION

In this section we present our results come from Monte Carlo simulations of networks with $N = 10^4$ nodes. In all simulations we set $\alpha = 0.1$ and $\phi = 0.01$, without losing generality. In Figs.5.3-5.6 we show I_u that is the steady-state density of infected agents in the community u. We also show m_u that is the stationary opinion in the

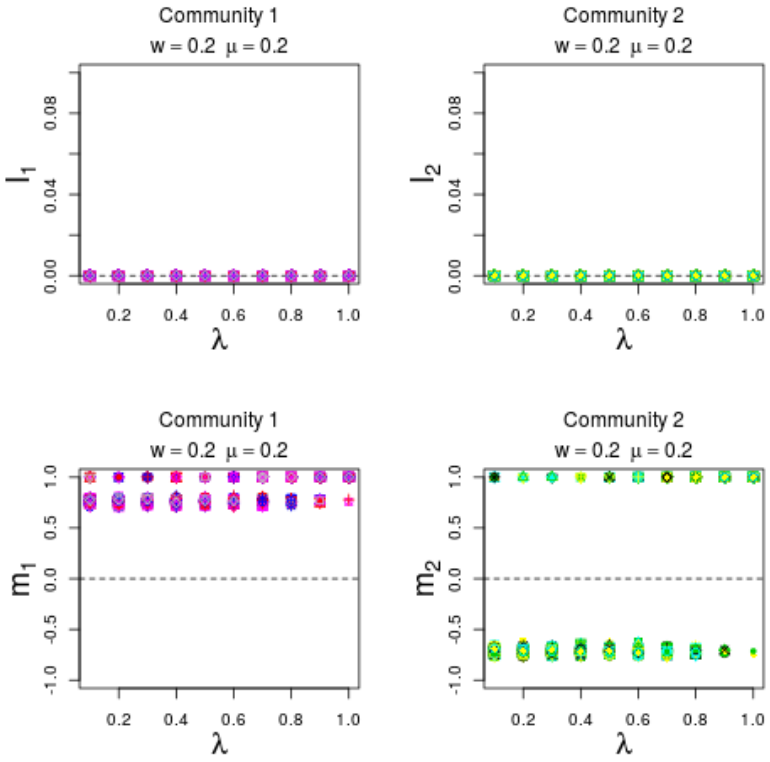

Figure 5.4 – Steady-state for the spreading measure I_i and collective opinion m_i for each community $i = \{1, 2\}$. Symbols are the steady-state outcome for each sample. Results for $\mu = 0.2$.

community u. In turn, I_{tot} and m_{tot} refer to the global proportion of infected individuals and global mean opinion.

The outcomes in Fig.5.3 show that in the community 2 (seed community) there is a transition from the absorbing phase (extinction of the epidemic) to the epidemic survival phase. In the community 1 there is no survival of the chain of infections in the long term. In this setting with $\mu = 0.1$ (weak modular structure) the seed community remains with the negative opinion about vaccination which weakens the vaccination campaign and thus facilitates the local per-

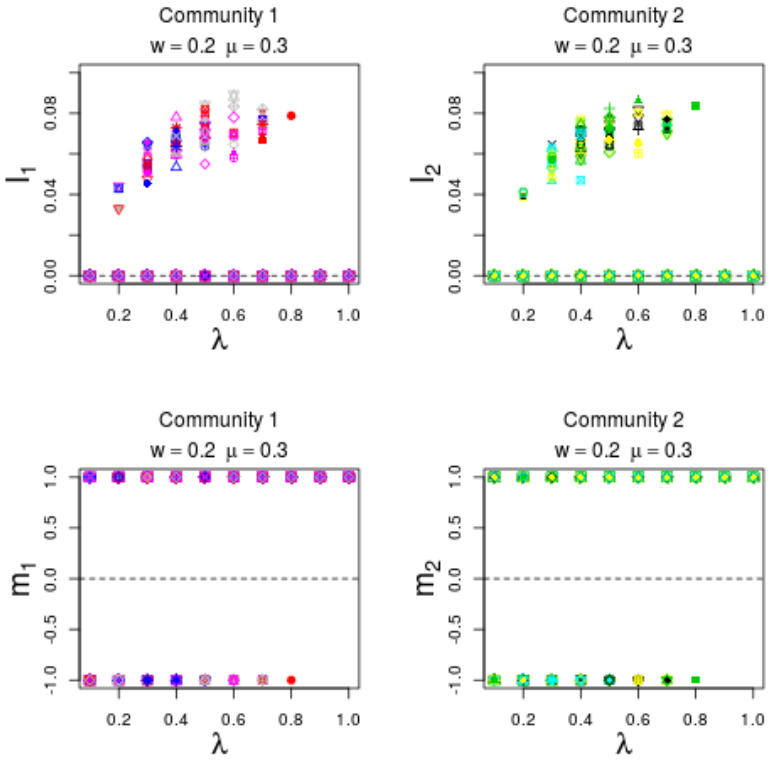

Figure 5.5 – Steady-state for the spreading measure I_i and collective opinion m_i for each community $i = \{1, 2\}$. Symbols are the steady-state outcome for each sample. Results for $\mu = 0.3$.

manence of the disease. Similarly, there is a persistence of the initial opinion in community 1, which in this case is pro-vaccine and therefore favors the vaccine uptake that makes the epidemic spreading unsustainable. This means that a low number of inter-community ties hinders the change in the community stance about vaccination, thus creating a strong distinction in epidemic spread between both communities. Community 1 being unfavorable to epidemic spreading since $m_1 > 0$, and community 2 being favorable since $m_2 < 0$.

In Fig.5.4 it is notable that an intermediate community

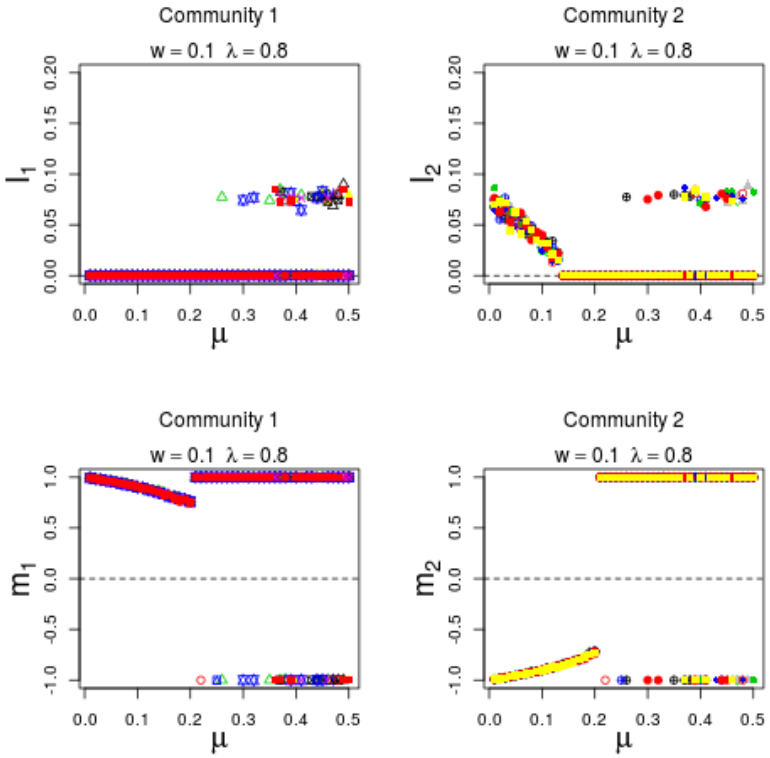

Figure 5.6 – Steady-state for the spreading measure I_i and collective opinion m_i for each community $i = \{1, 2\}$. Symbols are the steady-state outcome for each sample. Results for $w = 0.1$ and $\lambda = 0.8$.

strength leads to the elimination of the epidemic transmission in both communities even when there is a dominance of the negative opinion about vaccination in community 2. The epidemic contagion spreading is halted in community 2, even thou the agents have a negative opinion about the vaccination, due to the intermediate number of bridges, $\mu = 0.2$, to the other community. These bridges are just strong enough to drain the infected agents of community 2, but not strong enough to change its average opinion.

In Fig.5.5, with $\mu = 0.3$ there is a high number of inter-

community links. This additional connectivity between communities weakens the initial epidemic spreading in community 2, but it is sufficient to introduce the possibility of a community wide opinion change in community 1. The opinion change in community 1 facilitates the epidemic spreading in that community. This effect is limited, because we can see that for high infection probabilities $\lambda > 0.8$ the epidemic spread vanishes. So, we have a counterintuitive effect, because for a higher transmissibility the epidemic spread vanishes. The reason behind this is the risk perception, wI in Eq.5.1, which promotes vaccination, so a higher transmissibility leads to a bigger outbreak that in turn leads to better opinions about vaccination which ends up stopping the epidemic outbreak.

In Fig.5.6 is evident the emergence of an intermediate range of μ that blocks the local and global epidemic spreading. Regarding the opinion dynamics, an initial increase in μ leads to a decrease in m_1 and an increase in m_2, that is the collective opinions tend to be less extremist for an initial rise in the amount of inter-communities routes. Then a further increase in μ promotes a sudden rise in m_1 and m_2 which means a speed up in the switch of opinions in the community 2. A further rise in μ leads to a biestable behavior in both communities.

While in Figs.5.3-5.4 there is a single stable steady-state (either extinction or persistence), Figs.5.5 display bistable solutions depending on the randomness 'embebed' in the dynamics. Moreover, the outcomes in Figs.5.3 suggest that the absorbing-active epidemic transition is continuous for strong communities (such as $\mu = 0.1$) whereas the results shown in Figs.5.5 signalize that this extinction-persistence epidemic transition is discontinuous for weak communities (such as $\mu = 0.3$). Therefore, the structural factors present in the modular networks can induce the emergence of bistability in the epidemic-vaccination-opinion dynamics as well as a change in the nature of the absorbing-active transitions.

An overall look into Figs.5.3-5.6 reveals that a sudden transition can emerge from structural factors (increasing μ) or epidemiological factors (increasing λ). The transitions from the Disease-Free

phase to the active phase and vice-versa (epidemic resurgence) highlight the nonmonotonic behavior of the full dynamics with the transmissibility λ.

Comparing with other works, we see that while in (NEMATZADEH; FERRARA, et al., 2014) there is an optimal modularity for enhancing information spreading, here there is an optimal modularity for hindering epidemic spreading.

FINAL REMARKS

In (SALATHÉ; BONHOEFFER, 2008) was shown with a binary opinion dynamics that the spread of opinions against vaccination is one of the potential responsible for the large outbreaks of vaccine-preventable diseases in many high-income countries. Here we show with continuous opinion dynamics coupled to a networked SIRSV model that the spectrum of scenarios arising from the competition of pro vs anti vaccine views during an epidemic spreading is highly complex.

The several outcomes shown in Figs.5.3-5.6 point out that our model produces a diverse phenomenology where the social and biological scenarios exhibit a nonmonotonic dependence with spreading rate λ. From the perspective of the dynamical systems, our results provide a new mechanism for bistability in a biological-social setting. From a practical point of view, our work offers new perspectives for the development of novel strategies for halting epidemic spreading based on tuning the modularity to an optimal degree.

Some pro-vaccine strategies can have as side effects the segregation between individuals with conflicting views about the vaccines. In this regard, it was shown recently (BIZZARRI; PANEBIANCO; PIN, 2020) that segregation of anti-vaxxers can potentially extend the duration of an epidemic spreading. In (SAAD-ROY et al., 2020) was found that an increase in the contact between vaccine refusers and the rest of the society can lead to a scenario where vaccination alone may not be able to prevent an outbreak. Here we show that too much or too low segregation of anti-vaxxers favors the chain of contagion, but an intermediate level of segregation disfavor the

epidemic spreading. Therefore, our results indicate that vaccination campaigns should avoid strategies that have as a side effect too much segregation of anti-vaccine groups.

Our work produces an intriguing analogy. In a small-world architecture there is an intermediate number of long-range bridges that lead the full network to have unusual properties such as high clustering and low path lengths. Here, a structure with an intermediate number of inter-community ties lead the dynamics in the full network to produce an interesting outcome, namely the suppression of the epidemics. In future works it would be valuable to consider more sophisticated network architectures.

Concluding Remarks

In this thesis we worked in some important problems related to the fields of Ecology and Epidemiology. We employed two tools such as agent-based simulations as well as simple and coupled mean-field equations. We obtain a series of novel results:

- In the chapter 1 we show that the survival-extinction boundary undergoes a monotonicity transition: it has a nonmonotonic behavior for severe spatial constraints, but it has a monotonic behavior for loose spatial restrictions. As a consequence we show the emergence of an optimal diffusion that maximizes the survival probability for metapopulations with weak connectivity (strong spatial restrictions). Besides, this work set an agenda for empirical studies that could be done within the field of Synthetic Biology.

- In the chapter 2 our results point out that the multifold interplay between competition, birth-death dynamics and spatial constraints induces an interesting nonmonotonic relation between the ecological majority-minority switching and the dispersal between patches. This study also set an agenda for works that could be done within the field of Synthetic Biology.

- In the chapter 3 we show that a complexity measure, rather than the standard autocorrelation function, is able to properly explain the fate of extinction and to what extent the threshold

establishing the risk of extinction. Accordingly, these results allows comprehending *how* randomness jeopardises the long-run proliferation of organisms. Moreover, this work can also inspire empirical studies of Synthetic Biology.

- In the chapter 4 we show that the existence of two types of social behaviors strongly affects the dynamics and possibility of a second peak in the evolution of COVID-19. Taking Brazil as a case study our results point out that if the confinement measures are lifted too soon, namely as much as one week of consecutive declining numbers of new cases, it is very likely the appearance of a second peak. This work has the contribution of adding a new feature to the epidemic modelling, namely the stratification in groups according to socioeconomic attributes that are observed in emerging and developing countries

- In the chapter 5 we show that network modularity produces nonmonotonic effects on coupled opinion-vaccination-epidemic dynamics. Moreover, we provide insights into the problem of segregation of anti-vaxxers where we show that vaccination campaigns should avoid strategies that have as a side effect too much segregation of anti-vaccine groups. This work adds a new framework to the field of vaccination dynamics, namely the bridging of multiple fields (epidemic-vaccination-opinion dynamics) within the setup of complex networks. Another contribution of this endeavor is the new mechanism for bistability in a biological system.

In all chapters, we have observed transitions between states. This fact, under the presence of randomness, has important consequences in scenarios closer to a critical point: (i) for chapters 1-3 it unfolds the occurrence of ecological scenarios in which extinction can take place without apparent reason, even in the presence of abundant resources; (ii) for chapters 4-5 it implies that it is possible that the disease spreading can be interrupted without the application of suitable policy interventions, which may lead to misleading for policy-makers.

All in all, this thesis produces a series of contributions in relevant areas of Ecology and Epidemiology. As we have employed minimal models it is natural that there are many extensions of our works. In chapter 1 we have observed that the magnitude of the spatial constraints can change qualitatively the survival-extinction boundary from a nonmonotonic to a monotonic dependence. We have used a k-regular graph, thus it will be worthwhile to consider more sophisticated complex networks (BASCOMPTE, 2007). Similarly, in chapter 2 it will be important to investigate how the underlying connectivity matrix influences the ecological majority-minority switching. In chapter 3 it will be interesting to extend our analyze on *how* randomness/complexity jeopardizes the long-run survival of species for a spatially-constrained environment (DEANGELIS; YUREK, 2017; MERON, 2015). In chapter 4 we have assumed that after recovering from COVID-19 individuals cannot be infected anymore. Thus, this assumption should be relaxed as new evidence shows the possibility of reinfections (SAAD-ROY et al., 2020). Finally, in chapter 5 it will be worthwhile to consider the interplay between several sources of heterogeneity in the agent's bias, namely plurality and polarization (OESTEREICH; PIRES; QUEIRÓS, et al., 2020).

References

ABBOTT, Karen C. A dispersal-induced paradox: synchrony and stability in stochastic metapopulations. **Ecology letters**, Wiley Online Library, v. 14, n. 11, p. 1158–1169, 2011. Citado 1 vez on page 49.

ACKLEH, Azmy S; ALLEN, Linda JS; CARTER, Jacoby. Establishing a beachhead: a stochastic population model with an Allee effect applied to species invasion. **Theoretical Population Biology**, Elsevier, v. 71, n. 3, p. 290–300, 2007. Citado 2 vezes on pages 20, 31.

ADAM, D. The simulations driving the world's response to COVID-19. How epidemiologists rushed to model the coronavirus pandemic? **Nature**, April, 2020. Citado 1 vez on page 65.

ALLEE, WC. Animal aggregations, a study in general sociology.,(The University of Chicago Press: Chicago, IL, USA). Chicago: University of Chicago Press, 1931. Citado 2 vezes on pages 18, 55.

AMARASEKARE, Priyanga. Allee effects in metapopulation dynamics. **The American Naturalist**, The University of Chicago Press, v. 152, n. 2, p. 298–302, 1998. Citado 1 vez on page 20.

ARENAS, Alex et al. A mathematical model for the spatiotemporal epidemic spreading of COVID19. **medRxiv**, Cold Spring Harbor Laboratory Press, 2020. Citado 1 vez on page 65.

BACAËR, Nicolas. Lotka, Volterra and the predator–prey system (1920–1926). In: A short history of mathematical population dynamics. [S.l.]: Springer, 2011. P. 71–76. Citado 1 vez on page 13.

BARBER, Enrique Macia. **Aperiodic structures in condensed matter: fundamentals and applications**. [S.l.]: CRC Press, 2008. Citado 1 vez on page 59.

BARGHATHI, Hatem; VOJTA, Thomas; HOYOS, José A. Contact process with temporal disorder. **Physical Review E**, APS, v. 94, n. 2, p. 022111, 2016. Citado 1 vez on page 54.

BASCOMPTE, Jordi. Networks in ecology. **Basic and Applied Ecology**, Elsevier, v. 8, n. 6, p. 485–490, 2007. Citado 1 vez on page 97.

BASTOS, Saulo B; CAJUEIRO, Daniel O. Modeling and forecasting the early evolution of the Covid-19 pandemic in Brazil. **Scientific Reports**, v. 19457, 2020. Citado 4 vezes on pages 65, 68, 69, 72.

BEISSINGER, Steven R. Ecological mechanisms of extinction. **Proceedings of the National Academy of Sciences**, National Acad Sciences, v. 97, n. 22, p. 11688–11689, 2000. Citado 2 vezes on pages 52, 62.

BEREC, LUDĚK. Models of Allee effects and their implications for population and community dynamics. **Biophysical Reviews and Letters**, World Scientific, v. 3, 01n02, p. 157–181, 2008. Citado 2 vezes on pages 20, 57.

BI, Kaiming et al. Modeling learning and forgetting processes with the corresponding impacts on human behaviors in infectious disease epidemics. **Computers & Industrial Engineering**, Elsevier, v. 129, p. 563–577, 2019. Citado 1 vez on page 83.

BIN, Michelangelo et al. On Fast Multi-Shot COVID-19 Interventions for Post Lock-Down Mitigation. **arXiv preprint arXiv:2003.09930**, 2020. Citado 1 vez on page 65.

BISWAS, Kathakali; KHALEQUE, Abdul; SEN, Parongama. Covid-19 spread: Reproduction of data and prediction using a SIR model on Euclidean network. **arXiv preprint arXiv:2003.07063**, 2020. Citado 1 vez on page 65.

BIZZARRI, Matteo; PANEBIANCO, Fabrizio; PIN, Paolo. Is segregating anti-vaxxers a good idea? **arXiv preprint arXiv:2007.08523**, 2020. Citado 1 vez on page 93.

BONACCORSI, Giovanni et al. Evidence of economic segregation from mobility lockdown during COVID-19 epidemic. **Available at SSRN 3573609**, 2020. Citado 3 vezes on page 66.

BOOTSMA, Martin CJ; FERGUSON, Neil M. The effect of public health measures on the 1918 influenza pandemic in US cities. **Proceedings of the National Academy of Sciences**, National Acad Sciences, v. 104, n. 18, p. 7588–7593, 2007. Citado 1 vez on page 77.

BORTHAGARAY, Ana Inês et al. Effects of Metacommunity Networks on Local Community Structures: From Theoretical Predictions to Empirical Evaluations. In: BELGRANO, Andrea; WOODWARD, Guy; JACOB, Ute (Eds.). **Aquatic Functional Biodiversity**. San Diego: Academic Press, 2015. P. 75. Citado 1 vez on page 36.

BOUKAL, David S; BEREC, Luděk. Single-species models of the Allee effect: extinction boundaries, sex ratios and mate encounters. **Journal of Theoretical Biology**, Elsevier, v. 218, n. 3, p. 375–394, 2002. Citado 1 vez on page 20.

BOYON, Nicolas; SILVERSTEIN, Kate. Three in four adults globally say they would get a vaccine for COVID-19. **Ipsos, News & Pools**, 2020. Citado 1 vez on page 82.

BRASSIL, Chad E. Mean time to extinction of a metapopulation with an Allee effect. **Ecological Modelling**, Elsevier, v. 143, n. 1-2, p. 9–16, 2001. Citado 1 vez on page 20.

BRAUER, Fred; CASTILLO-CHAVEZ, Carlos; FENG, Zhilan. Introduction: A Prelude to Mathematical Epidemiology. In: MATHEMATICAL Models in Epidemiology. [S.l.]: Springer, 2019. P. 3–19. Citado 1 vez on page 13.

BRAZILIAN FEDERAL GOVERNMENT. **Auxílio Emergencial (Coronavírus - COVID 19)**. [S.l.: s.n.], 2020. https://www.gov.br/pt-br/servicos/solicitar-auxilio-emergencial-de-r-600-covid-19. Citado 1 vez on page 78.

BRAZILIAN INSTITUTE OF GEOGRAPHY AND STATISTICS - IBGE. **Quarterly Continuous PNAD, Informality rate**. [S.l.: s.n.], 2020. https://agenciadenoticias.ibge.gov.br/en/agencia-press-room/2185-news-agency/releases-en/27709-quarterly-continuous-pnad-unemployment-grows-in-

12-and-remains-stable-in-15-fus-in-the-1st-quarter-of-2020. Citado 1 vez on page 73.

BUONOMO, Bruno. Effects of information-dependent vaccination behavior on coronavirus outbreak: insights from a SIRI model. **Ricerche di Matematica**, Springer, v. 69, p. 483–499, 2020. Citado 1 vez on page 81.

CARLSON, Colin J et al. Spatial extinction date estimation: a novel method for reconstructing spatiotemporal patterns of extinction and identifying potential zones of rediscovery. **bioRxiv**, Cold Spring Harbor Laboratory, p. 279679, 2018. Citado 1 vez on page 53.

CASTRO, Francisco de. Modelling of the second (and subsequent) waves of the coronavirus epidemic. Spain and Germany as case studies. **medRxiv**, Cold Spring Harbor Laboratory Press, 2020. Citado 1 vez on page 72.

CAVAGNA, Andrea et al. Diffusion of individual birds in starling flocks. **Proceedings of the Royal Society B: Biological Sciences**, The Royal Society, v. 280, n. 1756, p. 20122484, 2013. Citado 1 vez on page 53.

CHEONG, Kang Hao; KOH, Jin Ming; JONES, Michael C. Paradoxical survival: Examining the parrondo effect across biology. **BioEssays**, Wiley Online Library, v. 41, n. 6, p. 1900027, 2019. Citado 1 vez on page 49.

CHEONG, Kang Hao; TAN, Zong Xuan; LING, Yan Hao. A time-based switching scheme for nomadic-colonial alternation under noisy conditions. **Communications in Nonlinear Science and Numerical Simulation**, v. 60, p. 107, 2018. Citado 1 vez on page 38.

CINTRA, Pedro Henrique Pinheiro; NUNES, Felipe Fontinele. Estimative of real number of infections by COVID-19 on Brazil and possible scenarios. **medRxiv**, Cold Spring Harbor Laboratory Press, 2020. Citado 1 vez on page 78.

COLOMBO, Eduardo H.; ANTENEODO, Celia. Metapopulation dynamics in a complex ecological landscape. **Phys. Rev. E**, v. 92, p. 022714, 2015. Citado 1 vez on page 36.

CORONAVIRUS BRAZIL. **Subnotification analysis**. [S.l.: s.n.], 2020. https://ciis.fmrp.usp.br/covid19/analise-subnotificacao/. Citado 1 vez on page 72.

COURCHAMP, Franck; BEREC, Ludek; GASCOIGNE, Joanna. **Allee effects in ecology and conservation**. [S.l.]: Oxford University Press, 2008. Citado 4 vezes on pages 18, 19.

_____._____. [S.l.]: Oxford University Press, 2008. Citado 2 vezes on pages 52, 55.

CROKIDAKIS, Nuno. COVID-19 spreading in Rio de Janeiro, Brazil: do the policies of social isolation really work? **Chaos, Solitons & Fractals**, Elsevier, v. 136, p. 109930, 2020. Citado 1 vez on page 65.

_____. Modeling the early evolution of the COVID-19 in Brazil: results from a Susceptible-Infectious-Quarantined-Recovered (SIQR) model. **International Journal of Modern Physics C**, World Scientific, 2020. Citado 1 vez on page 65.

_____. Nonequilibrium phase transitions and tricriticality in a three-dimensional lattice system with random-field competing kinetics. **Physical Review E**, APS, v. 81, n. 4, p. 041138, 2010. Citado 1 vez on page 54.

CROKIDAKIS, Nuno; OLIVEIRA, Paulo Murilo Castro de. The first shall be last: Selection-driven minority becomes majority. **Physica A: Statistical Mechanics and its Applications**, Elsevier, v. 409, p. 48–52, 2014. Citado 1 vez on page 49.

CUI, Peng-Bi et al. Close and ordinary social contacts: How important are they in promoting large-scale contagion? **Physical Review E**, APS, v. 98, n. 5, p. 052311, 2018. Citado 1 vez on page 82.

CURATO, Gianbiagio; LILLO, Fabrizio. Optimal information diffusion in stochastic block models. **Physical Review E**, APS, v. 94, n. 3, p. 032310, 2016. Citado 1 vez on page 83.

CURIEL, Rafael Prieto; RAMÍREZ, Humberto González. **Vaccination strategies against COVID-19 and the diffusion of anti-vaccination views**. [S.l.: s.n.], 2020. Citado 1 vez on page 82.

DAL NEGRO, Luca; BORISKINA, Svetlana V. Deterministic aperiodic nanostructures for photonics and plasmonics applications. **Laser & Photonics Reviews**, Wiley Online Library, v. 6, n. 2, p. 178–218, 2012. Citado 1 vez on page 59.

DE FALCO, I et al. Coronavirus Covid-19 spreading in Italy: optimizing an epidemiological model with dynamic social distancing through Differential Evolution. **arXiv preprint arXiv:2004.00553**, 2020. Citado 1 vez on page 65.

DEANGELIS, Donald L; YUREK, Simeon. Spatially explicit modeling in ecology: a review. **Ecosystems**, Springer, v. 20, n. 2, p. 284–300, 2017. Citado 1 vez on page 97.

DEREDEC, Anne; COURCHAMP, Franck. Combined impacts of Allee effects and parasitism. **Oikos**, Wiley Online Library, v. 112, n. 3, p. 667–679, 2006. Citado 2 vezes on pages 19, 56.

DIMARCO, G et al. Wealth distribution under the spread of infectious diseases. **arXiv preprint arXiv:2004.13620**, 2020. Citado 2 vezes on page 66.

DING, Yunfeng; WU, Fan; TAN, Cheemeng. Synthetic biology: A bridge between artificial and natural cells. **Life**, Multidisciplinary Digital Publishing Institute, v. 4, n. 4, p. 1092–1116, 2014. Citado 3 vezes on pages 49, 63.

DOAK, Daniel F et al. Understanding and predicting ecological dynamics: are major surprises inevitable. **Ecology**, Wiley Online Library, v. 89, n. 4, p. 952–961, 2008. Citado 1 vez on page 49.

DOCKERY, Jack et al. The evolution of slow dispersal rates: a reaction diffusion model. **Journal of Mathematical Biology**, Springer, v. 37, n. 1, p. 61–83, 1998. Citado 1 vez on page 37.

DOS SANTOS, Renato Vieira; DICKMAN, Ronald. Survival of the scarcer in space. **Journal of Statistical Mechanics: Theory and Experiment**, IOP Publishing, v. 2013, n. 07, p07004, 2013. Citado 1 vez on page 37.

DOUTOR, Paulo et al. Optimal vaccination strategies and rational behaviour in seasonal epidemics. **Journal of mathematical biology**, Springer, v. 73, n. 6-7, p. 1437–1465, 2016. Citado 1 vez on page 85.

DRAKE, JM; KRAMER, AM. Allee effects. **Nat. Educ. Knowl**, v. 3, n. 10, p. 2, 2011. Citado 2 vezes on pages 18, 55.

DRAKE, John M. Tail probabilities of extinction time in a large number of experimental populations. **Ecology**, Wiley Online Library, v. 95, n. 5, p. 1119–1126, 2014. Citado 1 vez on page 53.

DUNCAN, Alison B; GONZALEZ, Andrew; KALTZ, Oliver. Dispersal, environmental forcing, and parasites combine to affect metapopulation synchrony and stability. **Ecology**, Wiley Online Library, v. 96, n. 1, p. 284–290, 2015. Citado 1 vez on page 49.

EHRLICH, Paul; EHRLICH, Anne. **Extinction: the causes and consequences of the disappearance of species**. [S.l.: s.n.], 1981. Citado 1 vez on page 62.

FAGGIAN, Marco; URBANI, Michele; ZANOTTO, Luca. Proximity: a recipe to break the outbreak. **arXiv preprint arXiv:2003.10222**, 2020. Citado 1 vez on page 65.

FARANDA, Davide; ALBERTI, Tommaso. Modelling the second wave of COVID-19 infections in France and Italy via a Stochastic SEIR model. **arXiv preprint arXiv:2006.05081**, 2020. Citado 1 vez on page 72.

FERGUSON, NM et al. Impact of non-pharmaceutical interventions (NPIs) to reduce COVID-19 mortality and healthcare demand. Imperial College COVID-19 Response Team. **Preprint at Spiral https://doi. org/10.25561/77482**, 2020. Citado 1 vez on page 65.

FIORE, Carlos E; OLIVEIRA, MM de; HOYOS, José A. Temporal disorder in discontinuous nonequilibrium phase transitions: General results. **Physical Review E**, APS, v. 98, n. 3, p. 032129, 2018. Citado 1 vez on page 54.

FLAXMAN, Seth et al. Estimating the effects of non-pharmaceutical interventions on COVID-19 in Europe. **Nature**, Nature Publishing Group, v. 584, p. 1–8, 2020. Citado 1 vez on page 72.

FOBERT, Emily K.; TREML, Eric A.; SWEARER, Stephen E. Diffusively coupled Allee effect on heterogeneous and homogeneous graphs. **Proc. R. Soc. B**, v. 286, p. 1104, 2019. Citado 1 vez on page 36.

FORGERINI, Fabricio L; CROKIDAKIS, Nuno. Competition and evolution in restricted space. **Journal of Statistical Mechanics: Theory and Experiment**, IOP Publishing, v. 2014, n. 7, p07016, 2014. Citado 1 vez on page 53.

GABEL, Alan; MEERSON, Baruch; REDNER, S. Survival of the scarcer. **Physical Review E**, APS, v. 87, n. 1, p. 010101, 2013. Citado 1 vez on page 37.

GALAM, Serge. Public debates driven by incomplete scientific data: the cases of evolution theory, global warming and H1N1 pandemic influenza. **Physica A: Statistical Mechanics and its Applications**, Elsevier, v. 389, n. 17, p. 3619–3631, 2010. Citado 2 vezes on pages 81, 84.

GERSHENSON, Carlos; HELBING, Dirk. When slower is faster. **Complexity**, Wiley Online Library, v. 21, n. 2, p. 9–15, 2015. Citado 1 vez on page 38.

GHANBARI, Behzad. On forecasting the spread of the COVID-19 in Iran: The second wave. **Chaos, Solitons & Fractals**, Elsevier, v. 140, p. 110176, 2020. Citado 1 vez on page 72.

GOSWAMI, Madhurankhi; BHATTACHARYYA, Purnita; TRIBEDI, Prosun. Allee effect: The story behind the stabilization or extinction of microbial ecosystem. **Archives of microbiology**, Springer, v. 199, n. 2, p. 185–190, 2017. Citado 1 vez on page 56.

GRIMM, Volker; RAILSBACK, Steven F. **Individual-based modeling and ecology**. [S.l.]: Princeton university press, 2005. v. 8. Citado 2 vezes on pages 43, 61.

HADJIAVGOUSTI, Despina; ICHTIAROGLOU, Simos. Existence of stable localized structures in population dynamics through the Allee effect. **Chaos, Solitons & Fractals**, Elsevier, v. 21, n. 1, p. 119–131, 2004. Citado 1 vez on page 20.

HANSKI, Ilkka. Metapopulation dynamics. **Nature**, Nature Publishing Group, v. 396, n. 6706, p. 41–49, 1998. Citado 1 vez on page 21.

HANSKI, Ilkka; GILPIN, Michael. Metapopulation dynamics: brief history and conceptual domain. **Biological journal of the Linnean Society**, Oxford University Press, v. 42, n. 1-2, p. 3–16, 1991. Citado 3 vezes on pages 13, 21.

HASTINGS, Alan. Can spatial variation alone lead to selection for dispersal? **Theoretical Population Biology**, Elsevier, v. 24, n. 3, p. 244–251, 1983. Citado 1 vez on page 37.

_____. Temporally varying resources amplify the importance of resource input in ecological populations. **Biology Letters**, The Royal Society, v. 8, n. 6, p. 1067, 2012. Citado 1 vez on page 53.

HATCHETT, Richard J; MECHER, Carter E; LIPSITCH, Marc. Public health interventions and epidemic intensity during the 1918 influenza pandemic. **Proceedings of the National Academy of Sciences**, National Acad Sciences, v. 104, n. 18, p. 7582–7587, 2007. Citado 1 vez on page 77.

HEAMS, Thomas. Randomness in biology. **Mathematical Structures in Computer Science**, Cambridge University Press, v. 24, n. 3, 2014. Citado 1 vez on page 15.

HENKEL, Malte et al. **Non-equilibrium phase transitions**. [S.l.]: Springer, 2008. v. 1. Citado 2 vezes on pages 57, 60.

HILKER, Frank M; LANGLAIS, Michel; MALCHOW, Horst. The Allee effect and infectious diseases: extinction, multistability, and the (dis-) appearance of oscillations. **The American Naturalist**, The University of Chicago Press, v. 173, n. 1, p. 72–88, 2009. Citado 2 vezes on pages 19, 56.

HOERTEL, Nicolas et al. Lockdown exit strategies and risk of a second epidemic peak: a stochastic agent-based model of SARS-CoV-2 epidemic in France. **medRxiv**, Cold Spring Harbor Laboratory Press, 2020. Citado 1 vez on page 78.

HOPPER, KEITH R; ROUSH, RICHARD T. Mate finding, dispersal, number released, and the success of biological control introductions. **Ecological entomology**, Wiley Online Library, v. 18, n. 4, p. 321–331, 1993. Citado 1 vez on page 20.

HUANG, Jizhou et al. Quantifying the Economic Impact of COVID-19 in Mainland China Using Human Mobility Data. **arXiv preprint arXiv:2005.03010**, 2020. Citado 1 vez on page 66.

IUCN. **The IUCN Red List of Threatened Species. Version 2020-1. ISSN 2307-8235**. [S.l.: s.n.], 2020. https://www.iucnredlist.org/. Citado 1 vez on page 60.

JOHNSON, Kaitlyn E et al. Cancer cell population growth kinetics at low densities deviate from the exponential growth model and suggest an Allee effect. **PLoS biology**, Public Library of Science, v. 17, n. 8, e3000399, 2019. Citado 2 vezes on pages 56, 62.

JOHNSON, N F et al. **Not sure? Handling hesitancy of COVID-19 vaccines**. [S.l.: s.n.], 2020. arXiv: 2009.08413. Citado 1 vez on page 82.

JOHNSON, Neil F et al. The online competition between pro-and anti-vaccination views. **Nature**, Nature Publishing Group, v. 582, p. 230–233, 2020. Citado 2 vezes on page 81.

JOHST, Karin; BRANDL, Roland; EBER, Sabine. Metapopulation persistence in dynamic landscapes: the role of dispersal distance. **Oikos**, v. 98, p. 263, 2002. Citado 1 vez on page 36.

JORNET, Marc. Modeling of Allee effect in biofilm formation via the stochastic bistable Allen–Cahn partial differential equation. **Stochastic Analysis and Applications**, Taylor & Francis, p. 1–11, 2020. Citado 1 vez on page 56.

JUHER, David; RIPOLL, Jordi; SALDAÑA, Joan. Analysis and Monte Carlo simulations of a model for the spread of infectious diseases in heterogeneous metapopulations. **Phys. Rev. E**, v. 80, p. 041920, 2009. Citado 1 vez on page 36.

JÚNIOR, Misael B.de Souza; F.FERREIRA, Fernando; OLIVEIRA, Viviane M.de. Effects of the spatial heterogeneity on the diversity of ecosystems with resource competitions. **Physica A**, v. 393, p. 312, 2014. Citado 1 vez on page 36.

KASPAR, F.; SCHUSTER, H. G. Easily calculable measure for the complexity of spatiotemporal patterns. **Phys. Rev. A**, American Physical Society, v. 36, p. 842–848, 2 July 1987. Citado 2 vezes on pages 59, 63.

KEELING, Matt et al. The mathematics of vaccination. **Math. Today**, v. 49, p. 40–43, 2013. Citado 1 vez on page 81.

KEITT, Timothy H; LEWIS, Mark A; HOLT, Robert D. Allee effects, invasion pinning, and species' borders. **The American Naturalist**, The University of Chicago Press, v. 157, n. 2, p. 203–216, 2001. Citado 1 vez on page 20.

KERMACK, William Ogilvy; MCKENDRICK, Anderson G. A contribution to the mathematical theory of epidemics. **Proceedings of the royal society of london. Series A, Containing papers of a mathematical and physical character**, The Royal Society London, v. 115, n. 772, p. 700–721, 1927. Citado 1 vez on page 14.

KHASIN, Michael et al. Minimizing the population extinction risk by migration. **Physical review letters**, APS, v. 109, n. 13, p. 138104, 2012. Citado 2 vezes on pages 33, 49.

KOROLEV, Kirill S. Evolution arrests invasions of cooperative populations. **Physical review letters**, APS, v. 115, n. 20, p. 208104, 2015. Citado 2 vezes on pages 33, 49.

KOROLEV, Kirill S; XAVIER, Joao B; GORE, Jeff. Turning ecology and evolution against cancer. **Nature Reviews Cancer**, Nature Publishing Group, v. 14, n. 5, p. 371–380, 2014. Citado 5 vezes on pages 19, 56, 62.

KRAEMER, Moritz UG et al. The effect of human mobility and control measures on the COVID-19 epidemic in China. **Science**, American Association for the Advancement of Science, v. 368, n. 6490, p. 493–497, 2020. Citado 1 vez on page 65.

KRAMER, Andrew M et al. The evidence for Allee effects. **Population Ecology**, Springer, v. 51, n. 3, p. 341, 2009. Citado 2 vezes on pages 18, 55.

LAHROUZ, Aadil et al. Complete global stability for an SIRS epidemic model with generalized non-linear incidence and vaccination. **Applied Mathematics and Computation**, Elsevier, v. 218, n. 11, p. 6519–6525, 2012. Citado 1 vez on page 85.

LAI, Alessia et al. Early phylogenetic estimate of the effective reproduction number of SARS-CoV-2. **Journal of medical virology**, Wiley Online Library, v. 92, n. 6, p. 675–679, 2020. Citado 1 vez on page 65.

LALLOUACHE, Mehdi et al. Opinion formation in kinetic exchange models: Spontaneous symmetry-breaking transition. **Phys. Rev. E**, American Physical Society, v. 82, p. 056112, 5 Nov. 2010. Citado 1 vez on page 84.

LAMPERT, Adam; HASTINGS, Alan. Synchronization-induced persistence versus selection for habitats in spatially coupled ecosystems. **Journal of The Royal Society Interface**, The Royal Society, v. 10, n. 87, p. 20130559, 2013. Citado 1 vez on page 33.

LEMPEL, Abraham; ZIV, Jacob. On the complexity of finite sequences. **IEEE Trans. Inf. Theory**, IEEE, v. 22, n. 1, p. 75–81, 1976. Citado 2 vezes on pages 59, 63.

LEUNG, Kathy et al. First-wave COVID-19 transmissibility and severity in China outside Hubei after control measures, and second-wave scenario planning: a modelling impact assessment. **The Lancet**, Elsevier, v. 395, p. 1382–1393, 2020. Citado 1 vez on page 72.

LEVIN, Simon. Ecosystems and the Biosphere as Complex Adaptive Systems. **Ecosystems**, v. 1, p. 431–436, 1998. Citado 1 vez on page 54.

LEVINS, Richard. Some demographic and genetic consequences of environmental heterogeneity for biological control. **American Entomologist**, Oxford University Press, v. 15, n. 3, p. 237–240, 1969. Citado 1 vez on page 13.

LI, Ruiyun et al. Substantial undocumented infection facilitates the rapid dissemination of novel coronavirus (SARS-CoV-2). **Science**, American Association for the Advancement of Science, v. 368, n. 6490, p. 489–493, 2020. Citado 1 vez on page 65.

LIU, Ying et al. The reproductive number of COVID-19 is higher compared to SARS coronavirus. **Journal of travel medicine**, v. 27, n. 2, 2020. Citado 1 vez on page 65.

LLOYD, S. Measures of complexity: a nonexhaustive list. **IEEE Control Systems Magazine**, IEEE, v. 21, n. 4, p. 7–8, 2001. Citado 1 vez on page 63.

LOMBARDO, Pierangelo; GAMBASSI, Andrea; DALL'ASTA, Luca. Nonmonotonic effects of migration in subdivided populations. **Physical review letters**, APS, v. 112, n. 14, p. 148101, 14 Apr. 2014. Citado 2 vezes on pages 33, 49.

LONGO, Giuseppe; MONTÉVIL, Maël. Randomness Increases Order in Biological Evolution. **Computation, Physics and Beyond**, v. 7160, p. 289–308, 2012. Citado 1 vez on page 53.

MACKEY, Michael C; MAINI, Philip K. What has mathematics done for biology? **Bulletin of mathematical biology**, Springer, v. 77, n. 5, p. 735–738, 2015. Citado 1 vez on page 13.

MAIER, Benjamin F.; BROCKMANN, Dirk. Effective containment explains subexponential growth in recent confirmed COVID-19 cases in China. **Science**, American Association for the Advancement of Science, v. 368, n. 6492, p. 742–746, 2020. Citado 1 vez on page 65.

MANCHEIN, Cesar et al. Strong correlations between power-law growth of COVID-19 in four continents and the inefficiency of soft quarantine strategies. **Chaos: An Interdisciplinary Journal of Nonlinear Science**, AIP Publishing LLC, v. 30, n. 4, p. 041102, 2020. Citado 1 vez on page 65.

MAP. **Our source code**. [S.l.: s.n.], 2019. https://github.com/PiresMA/optimal_diffusion_ecological_dynamics. Citado 1 vez on page 22.

MARRO, Joaquíln; DICKMAN, Ronald. **Nonequilibrium phase transitions in lattice models**. [S.l.]: Cambridge University Press, 2005. Citado 3 vezes on pages 54, 57, 60.

MCCANN, Kevin Shear. **Mathematical Ecology**. [S.l.]: Oxford University Press, 2012. Citado 3 vezes on page 13.

MEHTA, Rohan S; ROSENBERG, Noah A. Modelling anti-vaccine sentiment as a cultural pathogen. **Evolutionary Human Sciences**, Cambridge University Press, v. 2, 2020. Citado 1 vez on page 83.

MENON, Ashish et al. Modelling and simulation of COVID-19 propagation in a large population with specific reference to India. **medRxiv**, Cold Spring Harbor Laboratory Press, 2020. Citado 1 vez on page 72.

MERLIN, Francesca. **Chance and the sources of biological variation: a critical analysis of a multiplenotion**. [S.l.]: Ph.D. thesis, Institut d'Histoire et Philosophie des Sciences, Universit é Paris-1, Paris,France, 2009. Citado 1 vez on page 53.

MERON, Ehud. **Nonlinear physics of ecosystems**. [S.l.]: CRC Press, 2015. Citado 1 vez on page 97.

MONEIM, IA; GREENHALGH, D. Threshold and stability results for an SIRS epidemic model with a general periodic vaccination strategy. **Journal of biological systems**, World Scientific, v. 13, n. 02, p. 131–150, 2005. Citado 1 vez on page 85.

MUNIZ-RODRIGUEZ, Kamalich et al. Doubling Time of the COVID-19 Epidemic by Province, China. **Emerging Infectious Diseases**, v. 26, n. 8, 2020. Citado 1 vez on page 65.

NAGATANI, Takashi; ICHINOSE, Genki. Diffusively coupled Allee effect on heterogeneous and homogeneous graphs. **Physica A**, v. 521, p. 18, 19. Citado 1 vez on page 36.

NEEDELL, Jeffrey D. The Revolta contra Vacina of 1904: the revolt against modernization in Belle-Epoque Rio de Janeiro. **Hispanic American Historical Review**, Duke University Press, v. 67, n. 2, p. 233–269, 1987. Citado 1 vez on page 81.

NEMATZADEH, Azadeh; FERRARA, Emilio, et al. Optimal Network Modularity for Information Diffusion. **Phys. Rev. Lett.**, American Physical Society, v. 113, p. 088701, 8 Aug. 2014. Citado 2 vezes on pages 82, 93.

NEMATZADEH, Azadeh; RODRIGUEZ, Nathaniel, et al. Optimal modularity in complex contagion. In: COMPLEX spreading phenomena in social systems. [S.l.]: Springer, 2018. P. 97–107. Citado 1 vez on page 83.

NETO, Osmar Pinto et al. Compartmentalized mathematical model to predict future number of active cases and deaths of COVID-19. **researchgate preprint**, 2020. Citado 1 vez on page 72.

NEUFELD, Zoltan et al. The role of Allee effect in modelling post resection recurrence of glioblastoma. **PLoS computational biology**, Public Library of Science, v. 13, n. 11, e1005818, 2017. Citado 2 vezes on pages 56, 62.

O'GRADY, Julian J et al. What are the best correlates of predicted extinction risk? **Biological Conservation**, Elsevier, v. 118, n. 4, p. 513–520, 2004. Citado 1 vez on page 53.

OESTEREICH, André L.; PIRES, Marcelo A.; CROKIDAKIS, Nuno. Three-state opinion dynamics in modular networks. **Phys. Rev. E**, American Physical Society (APS), v. 100, n. 3, p. 032312, Sept. 2019. Citado 2 vezes on pages 10, 86.

OESTEREICH, André L; PIRES, Marcelo A.; QUEIRÓS, SM Duarte, et al. Hysteresis and disorder-induced order in continuous kinetic-like opinion dynamics in complex networks. **Chaos, Solitons & Fractals**, Elsevier, v. 137, p. 109893, 2020. Citado 2 vezes on pages 10, 97.

OLIVEIRA, Marcelo Martins de; DICKMAN, Ronald. The advantage of being slow: The quasi-neutral contact process. **PloS one**, Public Library of Science, v. 12, n. 8, 2017. Citado 2 vezes on pages 37, 38.

OLIVEIRA, MM de; FIORE, CE. Temporal disorder does not forbid discontinuous absorbing phase transitions in low-dimensional systems. **Physical Review E**, APS, v. 94, n. 5, p. 052138, 2016. Citado 2 vezes on pages 54, 62.

ORGANIZATION, International Labour. **Women and men in the informal economy: A statistical picture**. [S.l.], 2018. Citado 1 vez on page 67.

OWENS, Ian PF; BENNETT, Peter M. Ecological basis of extinction risk in birds: habitat loss versus human persecution and introduced predators. **Proceedings of the National Academy of Sciences**, National Acad Sciences, v. 97, n. 22, p. 12144–12148, 2000. Citado 1 vez on page 53.

PADILLA-VACA, Felipe; ANAYA-VELÁZQUEZ, Fernando; FRANCO, Bernardo. Synthetic biology: Novel approaches for microbiology. **Int. Microbiol**, v. 18, p. 71–84, 2015. Citado 3 vezes on pages 49, 63.

PAIXÃO, Balthazar et al. **Estimation of COVID-19 under-reporting in Brazilian States through SARI**. [S.l.: s.n.], 2020. arXiv: 2006.12759. Citado 1 vez on page 72.

PEDERSEN, Morten Gram; MENEGHINI, Matteo. A simple method to quantify country-specific effects of COVID-19 containment measures. **medRxiv**, Cold Spring Harbor Laboratory Press, 2020. Citado 1 vez on page 65.

_____. Quantifying undetected COVID-19 cases and effects of containment measures in Italy. **researchgate preprint**, 2020. Citado 1 vez on page 78.

PEDRO, Sansao A et al. Conditions for a second wave of COVID-19 due to interactions between disease dynamics and social processes. **medRxiv**, Cold Spring Harbor Laboratory Press, 2020. Citado 1 vez on page 72.

PELLIS, Lorenzo et al. Challenges in control of Covid-19: short doubling time and long delay to effect of interventions. **arXiv preprint arXiv:2004.00117**, 2020. Citado 1 vez on page 65.

PENG, Hao et al. Network modularity controls the speed of information diffusion. **Phys. Rev. E**, American Physical Society, v. 102, p. 052316, 5 Nov. 2020. Citado 1 vez on page 83.

PETROVSKII, Sergei; MOROZOV, Andrew; LI, Bai-Lian. Regimes of biological invasion in a predator-prey system with the Allee effect. **Bulletin of mathematical biology**, Springer, v. 67, n. 3, p. 637, 2005. Citado 1 vez on page 20.

PIGOLOTTI, Simone; BENZI, Roberto. Competition between fast-and slow-diffusing species in non-homogeneous environments. **Journal of theoretical biology**, Elsevier, v. 395, p. 204–210, 2016. Citado 3 vezes on page 37.

_____. Selective advantage of diffusing faster. **Physical review letters**, APS, v. 112, n. 18, p. 188102, 2014. Citado 1 vez on page 37.

PIMM, Stuart L; RAVEN, Peter. Extinction by numbers. **Nature**, Nature Publishing Group, v. 403, n. 6772, p. 843–845, 2000. Citado 1 vez on page 60.

PIRES, Marcelo A.; CROKIDAKIS, N; CAJUEIRO, DO, et al. What is the potential for a second peak in the evolution of SARS-CoV-2 in Brazil? Insights from a SIRASD model considering the informal economy. **arXiv preprint arXiv:2005.09019**, 2020. Citado 2 vezes on pages 10, 65.

PIRES, Marcelo A.; CROKIDAKIS, Nuno. Dynamics of epidemic spreading with vaccination: impact of social pressure and engagement. **Physica A**, Elsevier, v. 467, p. 167–179, 2017. Citado 3 vezes on pages 10, 84, 85.

PIRES, Marcelo A.; CROKIDAKIS, Nuno; QUEIRÓS, Sílvio Duarte. Randomness in Ecological evolution: the role of complexity on the Allee effect. **Authorea Preprints**, Authorea, 2020. Citado 2 vezes on pages 10, 51.

PIRES, Marcelo A.; CROKIDAKIS, Nuno; QUEIRÓS, Sílvio M. D. Diffusion plays an unusual role in ecological quasi-neutral competition in metapopulations. **Nonlinear Dynamics**, 2021. Citado 2 vezes on pages 11, 34.

PIRES, Marcelo A.; DI MOLFETTA, Giuseppe; QUEIRÓS, Sílvio M. D. Multiple transitions between normal and hyperballistic diffusion in quantum walks with time-dependent jumps. **Scientific Reports**, Nature Publishing Group, v. 9, n. 1, p. 1–8, 2019. Citado 1 vez on page 11.

PIRES, Marcelo A.; DIAS, Neylan D. Leal, et al. Modelagem das mudanças comportamentais durante a propagação do sars-cov-2: um estudo de caso considerando o atraso nos testes. **Research, Society and Development**, v. 9, n. 7, e780975475–e780975475, 2020. Citado 1 vez on page 11.

PIRES, Marcelo A.; QUEIRÓS, Sílvio M. D. Negative correlations can play a positive role in disordered quantum walks. **arXiv preprint arXiv:2008.08867**, 2020. Citado 1 vez on page 11.

_____. Optimal dispersal in ecological dynamics with Allee effect in metapopulations. **PloS one**, Public Library of Science, v. 14, n. 6, 2019. Citado 5 vezes on pages 10, 17, 36, 42, 61.

_____. Parrondo's paradox in quantum walks with time-dependent coin operators. **Phys. Rev. E**, American Physical Society, v. 102, p. 042124, 4 Oct. 2020. Citado 1 vez on page 11.

_____. Quantum walks with sequential aperiodic jumps. **Phys. Rev. E**, APS, v. 102, p. 012104, 1 July 2020. Citado 1 vez on page 11.

PIRES, Marcelo A.; RAISCHEL, Frank, et al. Modeling the functional network of primary intercellular Ca2+ wave propagation in astrocytes and its application to study drug effects. **Journal of Theoretical Biology**, Elsevier, v. 356, p. 201–212, 2014. Citado 1 vez on page 10.

PIRES, Marcelo A; OESTEREICH, André L; CROKIDAKIS, Nuno. Sudden transitions in coupled opinion and epidemic dynamics with vaccination. **J. Stat. Mech.**, IOP Publishing, v. 2018, n. 5, p. 053407, May 2018. Citado 6 vezes on pages 10, 57, 60, 84, 85.

PIRES, Marcelo A; OESTEREICH, Andre L; CROKIDAKIS, Nuno; QUEIRÓS, Sílvio M Duarte. The anti-vaxx movement and epidemic spreading in the era of social networks: nonmonotonic effects, bistability and network segregation. **arXiv preprint arXiv:2101.07869**, 2021. Citado 2 vezes on pages 11, 80.

PROCTOR, James D; LARSON, Brendon MH. Ecology, complexity, and metaphor. **BioScience**, American Institute of Biological Sciences, v. 55, n. 12, p. 1065–1068, 2005. Citado 1 vez on page 54.

PROULX, Raphaël. Ecological complexity for unifying ecological theory across scales: A field ecologist's perspective. **Ecological complexity**, Elsevier, v. 4, n. 3, p. 85–92, 2007. Citado 1 vez on page 54.

QUEIRÓS, Queirós M Duarte. On a comparative study between dependence scales determined by linear and non-linear measures. **Physica D**, Elsevier, v. 238, n. 7, p. 764–770, 2009. Citado 1 vez on page 61.

RAO, Feng; MANDAL, Partha S; KANG, Yun. Complicated endemics of an SIRS model with a generalized incidence under preventive vaccination and treatment controls. **Applied Mathematical Modelling**, Elsevier, v. 67, p. 38–61, 2019. Citado 1 vez on page 85.

REGOES, Roland R; EBERT, Dieter; BONHOEFFER, Sebastian. Dose–dependent infection rates of parasites produce the Allee effect in epidemiology. **Proceedings of the Royal Society of London. Series B: Biological Sciences**, The Royal Society, v. 269, n. 1488, p. 271–279, 2002. Citado 2 vezes on pages 19, 56.

REITER, Matthias; RULANDS, Steffen; FREY, Erwin. Range expansion of heterogeneous populations. **Physical review letters**, APS, v. 112, n. 14, p. 148103, 2014. Citado 1 vez on page 33.

ROBINET, Christelle et al. Dispersion in time and space affect mating success and Allee effects in invading gypsy moth populations. **Journal of Animal Ecology**, JSTOR, p. 966–973, 2008. Citado 1 vez on page 20.

ROCHA FILHO, Tarcisio M et al. Expected impact of COVID-19 outbreak in a major metropolitan area in Brazil. **medRxiv**, Cold Spring Harbor Laboratory Press, 2020. Citado 1 vez on page 65.

ROGERS, LCG. Ending the COVID-19 epidemic in the United Kingdom. **arXiv preprint arXiv:2004.12462**, 2020. Citado 1 vez on page 78.

ROSA, Laura Nuño de la; VILLEGAS, Cristina. Chances and propensities in evo-devo. **The British Journal for the Philosophy of Science**, 2019. Citado 1 vez on page 53.

ROSS, Ronald. **The prevention of malaria**. [S.l.]: John Murray, 1911. Citado 1 vez on page 13.

SAAD-ROY, Chadi M et al. Immune life history, vaccination, and the dynamics of SARS-CoV-2 over the next 5 years. **Science**, American Association for the Advancement of Science, v. 370, n. 6518, p. 811–818, 2020. Citado 2 vezes on pages 93, 97.

SALATHÉ, Marcel; BONHOEFFER, Sebastian. The effect of opinion clustering on disease outbreaks. **Journal of The Royal Society Interface**, The Royal Society London, v. 5, n. 29, p. 1505–1508, 2008. Citado 1 vez on page 93.

SEWALT, Lotte et al. Influences of Allee effects in the spreading of malignant tumours. **Journal of theoretical biology**, Elsevier, v. 394, p. 77–92, 2016. Citado 3 vezes on pages 19, 56, 62.

SHAW, Allison K; KOKKO, Hanna. Dispersal evolution in the presence of Allee effects can speed up or slow down invasions. **The American Naturalist**, University of Chicago Press Chicago, IL, v. 185, n. 5, p. 631–639, 2015. Citado 2 vezes on pages 33, 49.

SIMBERLOFF, Daniel. The ecology of extinction. **Acta Palaeontologica Polonica**, -, v. 38, n. 3-4, p. 159–174, 1993. Citado 1 vez on page 62.

SINGH, Sudhansu Sekhar; MOHAPATRA, Dinakrushna. Predictive Analysis for COVID-19 Spread in India by Adaptive Compartmental Model. **medRxiv**, Cold Spring Harbor Laboratory Press, 2020. Citado 1 vez on page 72.

SMALDINO, Paul E; JONES, James Holland. Coupled Dynamics of Behavior and Disease Contagion Among Antagonistic Groups.

bioRxiv, Cold Spring Harbor Laboratory, 2020. Citado 1 vez on page 84.

SMITH, Robert et al. Programmed Allee effect in bacteria causes a tradeoff between population spread and survival. **Proceedings of the National Academy of Sciences**, National Acad Sciences, v. 111, n. 5, p. 1969–1974, 2014. Citado 10 vezes on pages 17, 19, 21, 32, 33, 36, 49, 63.

SOLANO, CMD; OLIVEIRA, MM de; FIORE, CE. Comparing the influence of distinct kinds of temporal disorder in a low-dimensional absorbing transition model. **Physical Review E**, APS, v. 94, n. 4, p. 042123, 2016. Citado 1 vez on page 62.

SOUTH, AB; KENWARD, RE. Mate finding, dispersal distances and population growth in invading species: a spatially explicit model. **Oikos**, Wiley Online Library, v. 95, n. 1, p. 53–58, 2001. Citado 2 vezes on page 33.

SPAGNOLO, B; VALENTI, D; FIASCONARO, A. Noise in ecosystems: a short review. **Mathematical biosciences and engineering: MBE**, v. 1, n. 1, p. 185–211, 2004. Citado 1 vez on page 53.

SU, Ying; ZOU, Xingfu. Rich spatial–temporal dynamics in a diffusive population model for pioneer–climax species. **Nonlinear Dynamics**, Springer, v. 95, n. 3, p. 1731–1745, 2019. Citado 1 vez on page 37.

SU, Zhen; WANG, Wei, et al. Optimal community structure for social contagions. **New Journal of Physics**, IOP Publishing, v. 20, n. 5, p. 053053, 2018. Citado 1 vez on page 82.

SWEANOR, Linda L.; LOGAN, Kenneth A.; HORNOCKER, Maurice G. Cougar Dispersal Patterns, Metapopulation Dynamics, and Conservation. **Conservation Biology**, v. 14, p. 798, 2001. Citado 1 vez on page 36.

TAN, Zhi-Xuan; CHEONG, Kang Hao. Periodic habitat destruction and migration can paradoxically enable sustainable territorial expansion. **Nonlinear Dynamics**, v. 98, p. 1, 2019. Citado 1 vez on page 37.

TAN, Zhi-Xuan; KOH, Jin Ming, et al. Predator Dormancy is a Stable Adaptive Strategy due to Parrondo's Paradox. **Advanced Science**, v. 7, p. 1901559, 2020. Citado 1 vez on page 37.

TAYLOR, Caz M; HASTINGS, Alan. Allee effects in biological invasions. **Ecology Letters**, Wiley Online Library, v. 8, n. 8, p. 895–908, 2005. Citado 3 vezes on pages 19, 20, 56.

THOMPSON, John N. **Encyclopædia Britannica**. [S.l.]: Encyclopædia Britannica, inc., Nov. 2016. Citado 1 vez on page 36.

TSALLIS, Constantino; TIRNAKLI, Ugur. Predicting COVID-19 peaks around the world. **Frontiers in Physics**, Frontiers, v. 8, p. 217, 2020. Citado 1 vez on page 65.

TULJAPURKAR, Shripad. **Population Dynamics in Variable Environments**. [S.l.]: Springer, 1990. Citado 1 vez on page 53.

VAID, S et al. Risk of a second wave of Covid-19 infections: using artificial intelligence to investigate stringency of physical distancing policies in North America. **International Orthopaedics**, Springer, v. 44, p. 1581–1589, 2020. Citado 1 vez on page 72.

VALDEZ, Lucas D; BRAUNSTEIN, Lidia A; HAVLIN, Shlomo. Epidemic spreading on modular networks: The fear to declare a pandemic. **Physical Review E**, APS, v. 101, n. 3, p. 032309, 2020. Citado 1 vez on page 83.

VASCONCELOS, Giovani L et al. Modelling fatality curves of COVID-19 and the effectiveness of intervention strategies. **PeerJ**, v. 8, e9421, 2020. Citado 1 vez on page 65.

VEIT, Richard R; LEWIS, Mark A. Dispersal, population growth, and the Allee effect: dynamics of the house finch invasion of eastern North America. **The American Naturalist**, University of Chicago Press, v. 148, n. 2, p. 255–274, 1996. Citado 1 vez on page 20.

VINCENOT, Christian Ernest et al. Theoretical considerations on the combined use of system dynamics and individual-based modeling in ecology. **Ecological Modelling**, Elsevier, v. 222, n. 1, p. 210–218, 2011. Citado 2 vezes on pages 43, 61.

VOJTA, Thomas; HOYOS, José A. Infinite-noise criticality: Nonequilibrium phase transitions in fluctuating environments. **EPL (Europhysics Letters)**, IOP Publishing, v. 112, n. 3, p. 30002, 2015. Citado 1 vez on page 54.

VOLPATTO, Diego et al. **Assessing social distancing release strategies in Brazil and Rio de Janeiro state**. [S.l.]: SciELO Preprints, 2020. Citado 1 vez on page 72.

VUILLEUMIER, Séverine; POSSINGHAM, Hugh P. Does colonization asymmetry matter in metapopulations? **Proc. R. Soc. B.**, v. 273, p. 1637, 2006. Citado 1 vez on page 36.

WAGNER, Andreas. The role of randomness in Darwinian evolution. **Philosophy of Science**, University of Chicago Press Chicago, IL, v. 79, n. 1, p. 95–119, 2012. Citado 1 vez on page 53.

WANG, Le-Zhi et al. Build to understand: synthetic approaches to biology. **Integrative Biology**, Oxford University Press, v. 8, n. 4, p. 394–408, 2016. Citado 3 vezes on pages 49, 63.

WEBER, Albertine; IANELLI, Flavio; GONCALVES, Sebastian. Trend analysis of the COVID-19 pandemic in China and the rest of the world. **arXiv preprint arXiv:2003.09032**, 2020. Citado 1 vez on page 65.

WEISS, Howard Howie. The SIR model and the foundations of public health. **Materials matematics**, p. 0001–17, 2013. Citado 1 vez on page 14.

WINDUS, Alastair; JENSEN, Henrik Jeldtoft. Allee effects and extinction in a lattice model. **Theoretical population biology**, Elsevier, v. 72, n. 4, p. 459–467, 2007. Citado 5 vezes on pages 21, 30, 55.

WOLFRAM, Stephen. **A new kind of science**. [S.l.]: Wolfram Media, Inc., 2002. Citado 1 vez on page 53.

WU, Jiaocan et al. Optimal multi-community network modularity for information diffusion. **International Journal of Modern Physics C**, World Scientific, v. 27, n. 08, p. 1650092, 2016. Citado 1 vez on page 82.

XU, Shunqing; LI, Yuanyuan. Beware of the second wave of COVID-19. **The Lancet**, Elsevier, v. 395, n. 10233, p. 1321–1322, 2020. Citado 1 vez on page 72.

YANG, Kai-Cheng et al. Expansion of cooperatively growing populations: Optimal migration rates and habitat network structures. **Physical Review E**, APS, v. 95, n. 1, p. 012306, 2017. Citado 1 vez on page 33.

YÜKSEL, Yusuf et al. Nonequilibrium phase transitions and stationary-state solutions of a three-dimensional random-field Ising model under a time-dependent periodic external field. **Physical Review E**, APS, v. 85, n. 5, p. 051123, 2012. Citado 1 vez on page 54.

ZENG, Guang-Zhao; CHEN, Lan-Sun. Complexity and asymptotical behavior of a SIRS epidemic model with proportional impulsive vaccination. **Advances in Complex Systems**, World Scientific, v. 8, n. 04, p. 419–431, 2005. Citado 1 vez on page 85.

ZHAO, Shi; LIN, Qianyin, et al. Preliminary estimation of the basic reproduction number of novel coronavirus (2019-nCoV) in China, from 2019 to 2020: A data-driven analysis in the early phase of the outbreak. **International journal of infectious diseases**, Elsevier, v. 92, p. 214–217, 2020. Citado 1 vez on page 65.

ZHAO, Songnian; KUANG, Yan, et al. Risk perception and human behaviors in epidemics. **IISE Transactions on Healthcare Systems Engineering**, Taylor & Francis, v. 8, n. 4, p. 315–328, 2018. Citado 1 vez on page 83.

ZHOU, Shu-Rong; WANG, Gang. Allee-like effects in metapopulation dynamics. **Mathematical biosciences**, Elsevier, v. 189, n. 1, p. 103–113, 2004. Citado 1 vez on page 20.

_____. One large, several medium, or many small? **Ecological Modelling**, Elsevier, v. 191, n. 3-4, p. 513–520, 2006. Citado 2 vezes on pages 20, 31.

ZHOU, Tao; LIU, Quanhui, et al. Preliminary prediction of the basic reproduction number of the Wuhan novel coronavirus 2019-nCoV. **Journal of Evidence-Based Medicine**, Wiley Online Library, v. 13, n. 1, p. 3–7, 2020. Citado 1 vez on page 65.